
Final Report

November 2006

UF Project No. 00026900
Contract No. BD535

DEVELOPMENT OF A STANDARD ACCELERATED CORROSION TEST FOR ACCEPTANCE OF POST- TENSIONING GROUTS IN FLORIDA

Principal Investigators:

H. R. (Trey) Hamilton III
University of Florida
Andrea J. Schokker
The Pennsylvania State University

Graduate Research Assistants:

Enrique Vivas
University of Florida
Alexandre R. Pacheco
Melissa A. Brooks
Kunjan Shukla
Jeffrey Volz
The Pennsylvania State University

Project Manager:

Michael Bergin, P.E.

Department of Civil & Coastal Engineering
College of Engineering
University of Florida
Gainesville, Florida 32611
Engineering and Industrial Experiment Station



DISCLAIMER

The opinions, findings, and conclusions expressed in this publication are those of the authors and not necessarily those of the State of Florida Department of Transportation.

Technical Report Documentation Page

1. Report No.	2. Government Accession No.	3. Recipient's Catalog No.	
4. Title and Subtitle Development of a Standard Accelerated Corrosion Test for Acceptance of Post-Tensioning Grouts in Florida		5. Report Date November 2006	
		6. Performing Organization Code	
7. Author(s) Alexandre R. Pacheco, Andrea J. Schokker, and H. R. Hamilton III		8. Performing Organization Report No. 00026900	
9. Performing Organization Name and Address University of Florida Department of Civil & Coastal Engineering P.O. Box 116580 Gainesville, FL 32611-6580		10. Work Unit No. (TRAIS)	
		11. Contract or Grant No. BD535	
12. Sponsoring Agency Name and Address Florida Department of Transportation Research Management Center 605 Suwannee Street, MS 30 Tallahassee, FL 32301-8064		13. Type of Report and Period Covered Final Report	
		14. Sponsoring Agency Code	
15. Supplementary Notes			
<p>16. Abstract</p> <p>Recent corrosion problems found in Florida's post-tensioned bridges have shown how important quality grouting materials and proper grouting techniques can be to the longevity of State bridges. Portland cement grout is commonly used to fill the voids in post-tensioning ducts after the tendon is stressed. Portland cement grout provides a protective barrier, high alkaline environment, and bonds the tendon to the duct to allow higher tendon stresses to be developed in the tendon.</p> <p>Current FDOT specifications currently require that prepackaged grouts proposed for use in filling post-tensioning ducts must be tested using the accelerated corrosion test (ACT) method as outlined in Appendix B of the "Specification for Grouting of Post-Tensioning Structures" published by the Post-Tensioning Institute. The qualifying grout must show a shorter average time-to-corrosion than the control sample that is fabricated using 0.45 w/c. Furthermore, the time-to-corrosion must not exceed 1,000 hours. The ACT is an anodic polarization test of a "lollipop" specimen formed from a single strand and grout. Although already in use, the ACT is not fully developed and was in need of further development including studying the influence of using IR compensation during the ACT test because this phenomenon is likely to skew results for grouts of significantly different resistivities.</p> <p>Tests with four different types of grout (plain, with corrosion inhibitor, with silica fume, and with fly ash) at three different ages (7, 28, and 56 days) were conducted with and without IR compensation. On average, the increase in time-to-corrosion when IR compensation was not used was 11 to 46%, but reached values as high as 149%.</p> <p>Test specifications are presented for the ACT. The most significant of the recommendations is that the test results be compared to the results from a qualifying grout tested using the same equipment and strand. The current minimum 1,000 hour requirement should be eliminated.</p> <p>The ACT test can take several months to run for a good quality grout, so an alternate method was developed that can provide initial results immediately after the grout has cured. Linear Polarization Resistance provides a method by which the grout can be qualified more quickly than waiting for the time-to-corrosion results. A polarization resistance value of 700 kΩ-cm² is suggested until further LPR and ACT direct correlations are done. While a set limit would not be recommended as a single pass-fail criterion, in this case it provides a restrictive first level of testing so that the ACT can be avoided for some grouts. Grouts that do not meet this criterion, but then pass the ACT should not be penalized. The LPR method also is useful during new mix grout development as a quick evaluation technique.</p> <p>Bleed in grouts is also a significant problem and may lead to susceptibility of the prestressing strand to corrosion. A new method, the Wick Pressure test, was also developed in this study that combines the positive attributes of the other two test methods.</p>			
17. Key Word Grouts, post-tensioning, ACT, electrochemical, LPR, bleed, wick pressure test, Schupack test		18. Distribution Statement No restrictions. This document is available to the public through the National Technical Information Service, Springfield, VA, 22161	
19. Security Classif. (of this report) Unclassified	20. Security Classif. (of this page) Unclassified	21. No. of Pages 108	22. Price

ACKNOWLEDGMENTS

The authors would like to thank Florida Department of Transportation for their support of this research. In particular, we would like to thank Mr. Mario Paredes, for his insightful comments and assistance.

EXECUTIVE SUMMARY

Recent corrosion problems found in Florida's post-tensioned bridges have shown how important quality grouting materials and proper grouting techniques can be to the longevity of State bridges. Portland cement grout is commonly used to fill the voids in post-tensioning ducts after the tendon is stressed. Portland cement grout provides a protective barrier, high alkaline environment, and bonds the tendon to the duct to allow higher tendon stresses to be developed in the tendon.

Current FDOT specifications currently require that prepackaged grouts proposed for use in filling post-tensioning ducts must be tested using the accelerated corrosion test (ACT) method as outlined in Appendix B of the "Specification for Grouting of Post-Tensioning Structures" published by the Post-Tensioning Institute. The qualifying grout must show a shorter average time-to-corrosion than the control sample that is fabricated using 0.45 w/c. Furthermore, the time-to-corrosion must not exceed 1,000 hours. The ACT is an anodic polarization test of a "lollipop" specimen formed from a single strand and grout. Although already in use, the ACT is not fully developed and was in need of further development including studying the influence of using IR compensation during the ACT test because this phenomenon is likely to skew results for grouts of significantly different resistivities.

Tests with four different types of grout (plain, with corrosion inhibitor, with silica fume, and with fly ash) at three different ages (7, 28, and 56 days) were conducted with and without IR compensation. On average, the increase in time-to-corrosion when IR compensation was not used was 11 to 46%, but reached values as high as 149%.

Test specifications are presented for the ACT. The most significant of the recommendations is that the test results be compared to the results from a qualifying grout tested using the same equipment and strand. The current minimum 1,000 hour requirement should be eliminated.

The ACT test can take several months to run for a good quality grout, so an alternate method was developed that can provide initial results immediately after the grout has cured. Linear Polarization Resistance provides a method by which the grout can be qualified more quickly than waiting for the time-to-corrosion results. A polarization resistance value of 700 k Ω -cm² is suggested until further LPR and ACT direct correlations are done. While a set limit would not be recommended as a single pass-fail criterion, in this case it provides a restrictive first level of testing so that the ACT can be avoided for some grouts. Grouts that do not meet this criterion, but then pass the ACT should not be penalized. The LPR method also is useful during new mix grout development as a quick evaluation technique.

Bleed in grouts is also a significant problem and may lead to susceptibility of the prestressing strand to corrosion. A new method, the Wick Pressure test, was also developed in this study that combines the positive attributes of the other two test methods.

TABLE OF CONTENTS

1	INTRODUCTION.....	7
2	LITERATURE REVIEW.....	8
2.1	GENERAL BACKGROUND ON BLEED AND CORROSION CONCERNS	8
2.2	REVIEW OF ELECTROCHEMICAL THEORY	11
3	OBJECTIVES	21
4	PHASE I – EVALUATION OF ACT METHODOLOGY	22
4.1	VARIABLES.....	22
4.2	MATERIALS	24
4.3	TESTING SEQUENCE	25
4.4	TESTS AND MEASUREMENTS.....	27
4.5	SPECIMEN CONSTRUCTION	29
4.6	TEST EQUIPMENT AND PROCEDURES.....	34
4.7	RESULTS AND ANALYSES	38
4.8	RESULTS AND DISCUSSION	65
4.9	CONCLUSIONS AND RECOMMENDATIONS.....	73
5	PHASE II – FURTHER ACT TESTING.....	76
5.1	SILICA FUME GROUTS	77
5.2	PLAIN GROUTS.....	78
5.3	PREPACKAGED GROUTS.....	80
5.4	PHASE II SUMMARY AND CONCLUSIONS	80
5.5	PHASE II RECOMMENDATIONS	81
6	PHASE III – GROUT SEGREGATION TESTING.....	81
6.1	OBJECTIVES.....	81
6.2	REVIEW OF EXISTING BLEED TESTS	82
6.3	WICK PRESSURE TEST DEVELOPMENT	83
6.4	GENERAL TEST PROCEDURES.....	85
6.5	EXPERIMENTAL PROGRAM	87
6.6	RESULTS.....	87
6.7	CONCLUSIONS	90
6.8	RECOMMENDATIONS	91
7	REFERENCES.....	91
8	APPENDIX A: PROPOSED ACT STANDARD.....	95
9	APPENDIX B: CURRENT ACT SPECIFICATION (PTI 2003)	100
9.1	ACCELERATED CORROSION TESTING METHOD (ACTM)	100
10	APPENDIX C: PRESTRESSING STRAND REPORT.....	104
11	APPENDIX D: CEMENT MILL TEST REPORT	105
12	APPENDIX E: PHASE I EXPERIMENTAL DATA SUMMARY	106
13	APPENDIX F: BLEED TEST DATA	107

1 Introduction

Grout performance problems have usually been related to insufficient filling of the grout space due to low fluidity and inadequate bleed resistance. Observations made during the investigation of the Mid-Bay Bridge indicated that serious structural problems can result from poor grouting of the post-tensioning (PT) tendons (Corven Engineering 2001). In addition, FDOT (Alvarez and Hamilton 2004) has examined the performance of prepackaged grouts compared to that of plain grouts that are field formulated. Since then, FDOT requires the use of prequalified, prepackaged grouts on all PT bridge construction. Furthermore, corrosion testing conducted recently (Powers et al 2004) supports the field observation that voids in the grouted tendons combined with an aggressive environment can lead to significantly high corrosion rates and ultimately to tendon failure.

These recent corrosion problems have shown how important quality grouting materials and proper grouting techniques can be to the longevity of the State’s bridges. This issue is not restricted to Florida, but has captured national and even international attention due to problems encountered both here in Florida and abroad.

Portland cement grout has historically been used to fill the voids in post-tensioning ducts after the tendon is stressed. Portland cement grout provides a protective barrier, high alkaline environment, and bonds the tendon to the duct to allow higher tendon stresses to be developed.

The recently published Post-Tensioning Institute (PTI, 2003) guide specification for grouting of PT tendons represents a significant improvement over the previous specification, which was last revised in the 1970’s. The current specification requires that prepackaged grouts as well as grouts that are exposed to severe environments pass an accelerated corrosion test (ACT). The ACT is an anodic polarization test of a “lollipop” specimen formed from a single strand and grout (Figure 1). The test was originally developed as part of a FHWA research project on the durability of grouts (Thompson et al 1992). The method was further refined and modified by Hamilton et al 2000 and Schokker et al 1999.

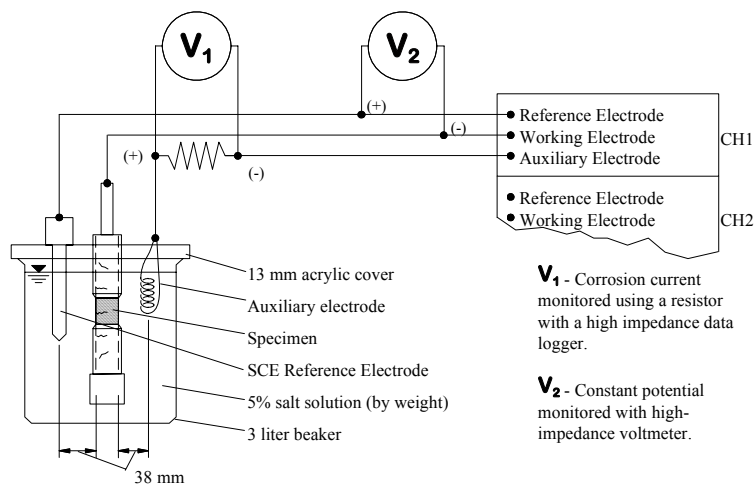


Figure 1 - Accelerated corrosion test setup

The PTI specifications (2003) indicate that the ACT has not been fully evaluated and does not represent a standardized test method. Yet, there is a need to have a relatively quick and effective method to evaluate new grouting materials for use in post-tensioned bridges. This is particularly true in Florida due to the required use of proprietary prepackaged grouts.

Another issue in the PTI specification is that of bleed. Bleed refers to the separation of the cement particles from water after injection of the duct and was a contributor to the tendon problems experienced on the Mid-Bay Bridge (Corven Engineering 2001). This phenomenon is exacerbated by the wicking effect of the strand bundle inside the PT duct. Voids and in some cases bleed water remain after grouting that can lead to corrosion of the strand. There are a number of commercially available products that can be used to control bleed. The current specifications require the use of the Schupack Pressure Bleed Test, which is used to evaluate the tendency of the grout to bleed. The test consists of placing a sample of fresh grout in a pressure filter. A set pressure is then applied to the sample to determine if water can be squeezed out of the sample. The quantity of bleed water is measured and compared to those given in the specifications.

2 Literature Review

2.1 GENERAL BACKGROUND ON BLEED AND CORROSION CONCERNS

The grouts used for post-tensioning systems are a mixture of ordinary portland cement and water, with some property-enhancing admixtures. Post-tensioning systems rely on the grout for corrosion protection and to provide bond between the tendon and concrete. Water is needed in the grout for hydration of cement. To ensure that grout has a sufficiently low viscosity to facilitate easy injection into the duct, however, more water is usually added than is required for hydration. This excess water causes the cement to flocculate (form lumps) and to settle (sedimentation) resulting in water rising and collecting at the top of the grout column. This process is known as “bleeding” and the excess accumulated water is referred to as “bleed” or “bleed lenses”.

Historically, the investigation of grout as a strategic component in the durability of post-tensioned tendons began with Schupack (1971), who evaluated varying grout mixes under adverse conditions such as high vertical rises and in ducts with sharp curvatures. The grouts that produced the best results in terms of void and bleed prevention were those using water-reducing and anti-bleed admixtures. Schupack (1974) again addressed grout problems related to bleeding and then developed a pressurized bleed resistance test (procedure given today in PTI 2003) to appropriately qualify grouts with respect to their bleed resistance. Corrosion of post-tensioning cables due to low-quality grout was not yet a major concern. Two decades later, however, the same author mainly addressed tendon corrosion occurrences, but correlating them to construction practices (Schupack 1994). In that work, it was found that an inspected 35-year-old bridge had an estimated loss of 2 to 3 wires in the tendons due to corrosion caused by chloride contamination of the post-tensioning grout. Dickson et al. (1993), also in field inspections, found moderate corrosion in a post-tensioned bridge after 34 years of its construction.

Lankard et al. (1993), in an experimental investigation, had seven different types of grout tested for bleed resistance using the Schupack pressure bleed test. While their control grout, a plain mixture of cement type II and water at a water-cementitious ratio of 0.44, had 38% of bleed, a plain grout with 5% of polysaccharide gum had only 1% of bleed. The most valuable

contribution of the work, however, was the creation of a method to test the corrosion protection capability of grouts: the ACT or accelerated corrosion test (procedures in PTI 2003). Specifically, the authors conceived a specimen that combined both grout and steel cable in a suitable manner that emulated a section of a post-tensioning tendon system, and used a well-known technique in electrochemistry, the potentiostatic polarization method (ASTM G 5 1999), to evaluate their grouts for corrosion protection. Also emulating a field situation, the authors used saltwater as electrolyte for the corrosion reactions. They reported that, based on preliminary investigations, 5% of sodium chloride by mass should be used for the electrolyte in order to simplify the test by avoiding tensioning the strands during the experiment. Upon testing their control and microsilica grouts, times to allow corrosion of 100 and 465 hours, respectively, were found. The authors briefly mentioned that the microsilica grout took more time to develop the same level of corrosion damage than the plain control grout. No details regarding possible shortcomings with the test, recommended number of specimens, or data scatter were addressed. A very similar experimental setup to the ACT was used by Hussain and Rasheeduzzafar (1994) to test concretes with improved corrosion characteristics due to cement replacements of 30% class F fly ash in their mixes. The times to corrosion, however, were found with polarization corrosion tests (half-cell measurements), instead of monitoring current levels. No comments regarding experimental difficulties were given, with the work focusing only on the fly ash's excellent performance.

The ACT data scatter was a major concern in the work by Hamilton (1995) and by Hamilton et al. (2000). Crack-controlled specimens were used to try to minimize this problem, having as a justification the fact that both grouts on stay cables and in post-tensioning ducts are prone to cracking (Hamilton 1998). They modified the original ACT specimen design to isolate one crack and control its width to a maximum value of 0.13 mm (0.005 in.). However, the variability of the results remained high, with coefficients of variation ranging from 14 to 69% (primarily in the 20 to 40% range). Outside of the variability due to the crack formation, the authors explain data discrepancies based on possible resistivity differences between the tested grouts. The discrepancies found would be associated with the voltage drop effect, a common source of error in electrochemical measurements that consists of a loss on the applied voltage due to the resistivity of the system being measured (usually in the electrolyte phase). Besides the significant variability, another problem observed by the authors was the result obtained for a grout with calcium nitrite, a widely used corrosion-inhibiting admixture in concrete that, in fact, reduced the corrosion performance of the grout mixtures tested. In addition to the regular result given by an ACT (the time-to-corrosion, t_{corr} , or the time in hours necessary for grouts to cease their corrosion protection under the test conditions), the authors investigated the trends of two other measurements: the open-circuit potential (E_{oc}) and the current density (i_{corr}) prior to the onset of corrosion. Weak or no signs of correlation were found between these variables and the ACT results. Another aspect of the ACT that could be confirmed is that even cracked specimens can take several days to corrode. For instance, a control grout took 272 hours (11 days) to allow corrosion.

Although fluidity and bleed resistance of grouts was the focus of the experimental study conducted by Schokker (1999) and by Schokker et al. (2002), the ACT had an important role in the development of high performance grouts for post-tensioning applications in those works. Five different grouts were tested for corrosion protection, with results ranging from 300 hours (13 days) to 1,000 hours (42 days). The authors incorporated in their version of the ACT method

several modifications proposed earlier by Koester (1995). In addition to redesigning the specimen dimensions, Koester proposed the reduction of the electrical potential applied on ACT specimens from 600 mV above the potential given by a saturated calomel electrode, i.e., +600 mV_{SCE}, to +200 mV_{SCE}, significantly reducing data scatter. However, a few grouts tested still showed high variability in the data and the time required to obtain an ACT result became more pronounced, as can be noticed from the number of hours aforementioned. Furthermore, these authors highlighted the necessity to compensate ACT experiments for the voltage drop effect, which may otherwise distort test results from grouts with pronounced resistivities, mainly when compared with more electrically conductive subjects. Schokker (1999) also found consistent variation in results when strand from two different sources were tested, and thus highlighted the need for use of consistent materials in testing.

The modeling of diffusion has been considered in several studies on cementitious materials because the ingress of chlorides and the attack of the steel reinforcement in structures can be directly related to service life estimations (induction period or initiation stage). Several approaches to determine structural service life based on the diffusion of chlorides have been considered by researchers. Examples of studies that applied experimental approaches to determine the chloride diffusion in concrete are the works by Hornain et al. (1995) and Li (2001). The experimental approach was defended by the latter by claiming that analytical approaches need to consider two restrictive boundary conditions that are difficult to be met in reality (e.g. homogeneous materials and semi-infinite planes). Andrade et al. (2003), reviewing analytical solutions, also make similar comments, saying that service life predictions have to consider numerous parameters and phenomena, and many are difficult to quantify. Peng et al. (2002) used a neural network analysis approach to model chloride diffusion in concrete, adapting to conditions that would be difficult to consider with other mathematical models (unsteady states of chloride profiles).

Probabilistic models, such as the one used by Kirkpatrick et al. (2002), are also adopted by researchers to predict service life of structures related to chloride-induced corrosion. Several analytical models try to determine the remaining service life of structures, i.e., after the onset of corrosion, which characterizes the propagation stage in structural service life. Ahmad (2003) reviewed models for prediction of the remaining service life of concrete structures and suggests an experimental approach for the determination of cracking and concrete spalling.

Studies regarding admixtures in cementitious materials are extensive. For instance, silica fume grouts had superior placement characteristics when compared to plain grouts in a work by Diederichs and Schutt (1989), mainly when the cement replaced by silica fume was 5%, suggesting an optimum content. Rasheedzafar et al. (1990) found that the cement alone influences corrosion behavior when testing type I cement, which performed significantly better in corrosion tests when compared with type V due likely to the higher C₃A content of the first type. Loretz and French (1995) found that the optimum silica fume content in concretes would tend to be a replacement of less than 9%. The optimum cement replacement in concretes was found by Idriss et al. (2001) as 8%, during linear polarization resistance (LPR) measurements in corrosion tests. Diamond (1997) found that, contrary to the good behavior observed in concretes, undispersed silica fume in grouts tend to produce alkali-silica reactions that can lead to distress and cracking of the grout matrix.

Corrosion inhibitors are discussed by Berke (1991), who highlights the importance of calcium nitrite for corrosion protection in concrete. Gu et al. (1997) ran LPR and electrochemical impedance spectroscopy (EIS) tests and found increased corrosion protection when inhibitors based on sodium nitrite and dinitrobenzoic acid were used in concrete samples. Hamilton found the opposite effect on grouts tested in the ACT (1995)

Electrochemical techniques have been used extensively in concrete testing with varying levels of success. Baweja et al. (1996), using potentiodynamic procedures, found that blended cement concretes have improved corrosion characteristics when compared with plain cement concretes. Montemor et al. (2000), using the EIS technique, found that a 30% cement replacement by type C fly ash significantly increased corrosion test performances in concretes with high water-cementitious ratios (0.57).

Rha (2001) showed with EIS measurements that mineral admixtures such as blast furnace slag and microsilica tend to modify the microstructure of mortars near the steel reinforcement surface, reducing porosity and pore size distribution at these sites. Montemor et al. (2003) reviewed electrochemical techniques for onsite applications, recommending half-cell tests as a first approach and then LPR measurements. They comment that EIS results are difficult to interpret and need to have their equivalent circuits reevaluated for every change in conditions. In addition, transient techniques such as the galvanostatic pulse may suffer deviations of results when non-activation behavior is expected. Andrade et al. (1990), Zivica (2001), and Millard et al. (2001) used LPR tests in reinforced concrete samples to find corrosion rates and, in the last two works, related them with levels of damage or with environmental conditions.

Baweja (1999) compared results from LPR, polarization corrosion, resistivity measurements, gravimetric mass loss, and EIS tests, obtaining satisfactory agreement between them. An important result regarding the ohmic drop effect in electrochemical tests in concrete samples was found by Berke et al. (1990), estimating that up to 27% overestimation of LPR readings can occur because of those effects and Escalante (1990) claims that the current interruption technique can eliminate 95% of the error related to them. Another important result for this work was given by Al-Tayyib and Khan (1988), affirming that LPR measurements do not significantly affect concrete samples exposed to 5% NaCl solutions and Tafel scans can be done afterwards. They also reported anodic Tafel constants varying from 400 to 500 mV/decade, while cathodic constants would be in range from 250 to 350 mV/decade.

The need for a corrosion resistant system combined with the information from the literature on previous studies in the area of electrochemical testing in concrete and grouts provide the basis for the development of this research. A detailed review of electrochemical theory is provided in the next section as background for Phase I and Phase II of this research program.

2.2 REVIEW OF ELECTROCHEMICAL THEORY

This section presents the theoretical background behind the aspects addressed during the research. It starts with an explanation on corrosion and pertinent analytical approaches. Then experimental aspects such as the ohmic or voltage drop effect and electrochemical techniques are presented. The Accelerated Corrosion Test (PTI, 2003) is also addressed.

2.2.1 Instrumentation

The separation into electrodes (the cathode and the anode) allows for instrumentation of the system using gauges to measure potential differences and currents. Since measured potential

differences between the electrodes would be a net result of anodic and cathodic reaction potentials, an auxiliary element, with an independent chemical reaction, has to be introduced in the cell in order to provide a baseline value for the measurements. In laboratory experiments, the SCE scale is typically used. This is illustrated in Figure 2.

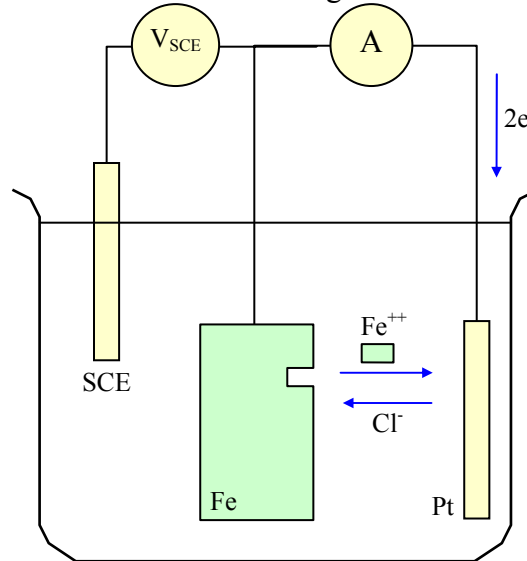


Figure 2 - Cell instrumentation

The SCE scale is given by the Saturated Calomel Electrode, which produces a baseline potential of 241 mV above the equilibrium potential for hydrogen evolution. Incidentally, this reaction would characterize another type of auxiliary electrode, the Standard Hydrogen Electrode (SHE). Half-cell measurements made in the field usually use a Copper-Copper Sulfate Electrode (CSE), which gives other values of potential for the same reactions. The transformation between all these scales (and any other) is straightforward and can be made as indicated in Figure 3.

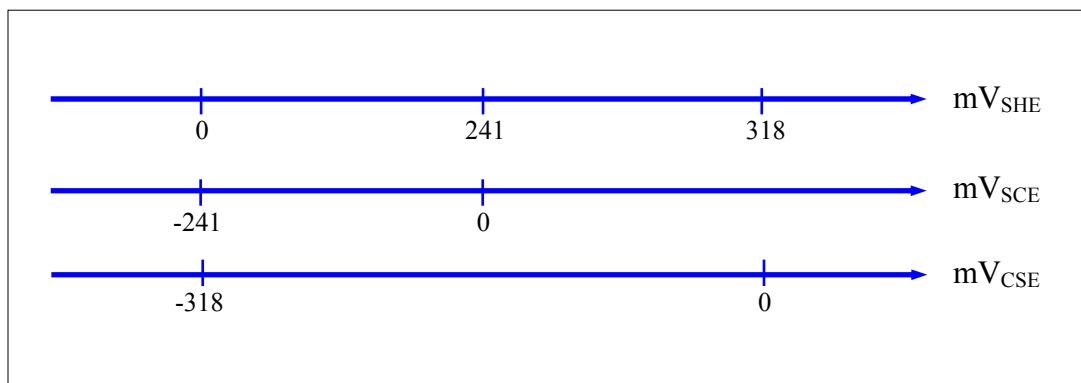


Figure 3 - Three scales given by different reference electrodes

In the figure, it can be seen that the saturated calomel electrode is 241 mV above the potential given by the hydrogen electrode and the copper-copper sulfate electrode is 318 mV above that potential. Thus, for instance, a potential of $-447 \text{ mV}_{\text{SHE}}$ is equivalent to $-688 \text{ mV}_{\text{SCE}}$ and to $-765 \text{ mV}_{\text{CSE}}$.

2.2.2 The Butler-Volmer Equation

In an electrochemical system, the relationship between potential difference (E) and electric current (I) is given by the well-known Ohm's law ($E = IR$), where R is the system's electrical resistance. The existence of a liquid phase in the corroding systems creates a more complex situation, where metal-electrolyte interfaces and ionic mass transport play important roles. Thus, in this case, and particularly at the interfaces, the relationship between potential and current is not linear, but exponential. This behavior is represented by the Butler-Volmer equation (see, for instance, Jones 1996 or Stansbury & Buchanan 2000):

$$i = i_0 \left(e^{\frac{2.3\eta}{\beta_a}} - e^{-\frac{2.3\eta}{\beta_c}} \right) \quad \text{Equation 2-1}$$

In Equation 2-1, the overpotential, η (given by $\eta = E - E_o$, where E is the applied potential and E_o is the reaction's equilibrium potential), is exponentially related to the current density, i (given by $i = I/A$, where I is the current and A is the exposed area to the electrolyte). The exchange current density, i_o , can be found in the literature (see, for instance, Jones 1996) and represents the current flow (per unit of area) between products and reactants when the reaction is at equilibrium. The constants β_a and β_c are called Tafel constants, named after the German physical chemist Julius Tafel.

The Butler-Volmer equation is the analytical representation of the anodic and cathodic responses of an element in electrochemical equilibrium (both reactions occur at the same time and rate). Figure 4 shows a plot of each term of the equation, as well as their summation. It is important to notice that, at a certain distance from the origin, one of the terms becomes insignificant in relation to the other one, and straight lines result when a semi-log scale is used. In this case, it is a common practice to plot the potentials in the linear ordinate axis, while the current densities are plotted in the logarithmic abscissa axis. The slopes of each branch give the values of the Tafel constants for the reaction. Another important aspect is that, in the linear plot, the behavior of the combined result (sum) is approximately a straight line when small values of potential are considered.

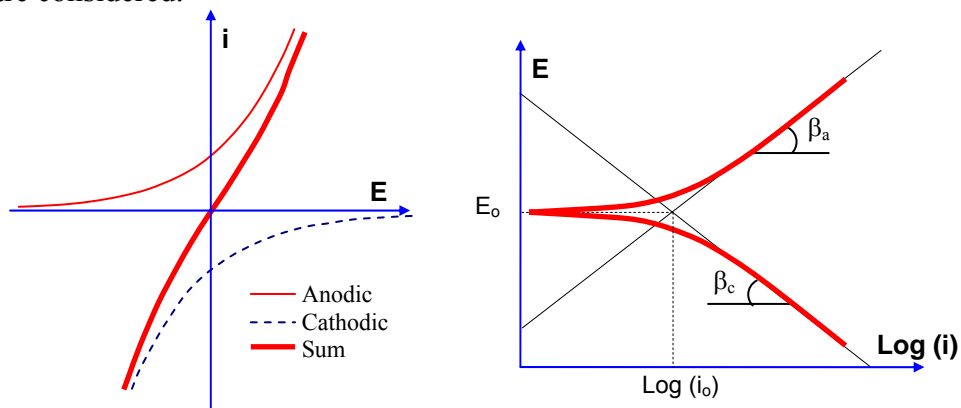


Figure 4 - Typical linear and semi-log plots of the Butler-Volmer equation

2.2.3 The Mixed Potential Theory

The corrosion process can be analytically represented using the Butler-Volmer equation for the corroding (oxidizing) species and the associated participating reducing reactions in the cell. The plots are then superimposed to obtain a final mixed result that now are described by a Butler-Volmer equation with i_0 and E_0 renamed as i_{corr} and E_{corr} , respectively, since they are a result of this superposition and represent the entire cell. An example of anodic and cathodic reaction superposition, producing a mixed plot, is given in Figure 5. The corrosion potential and corrosion current density can be found graphically from the mixed curve.

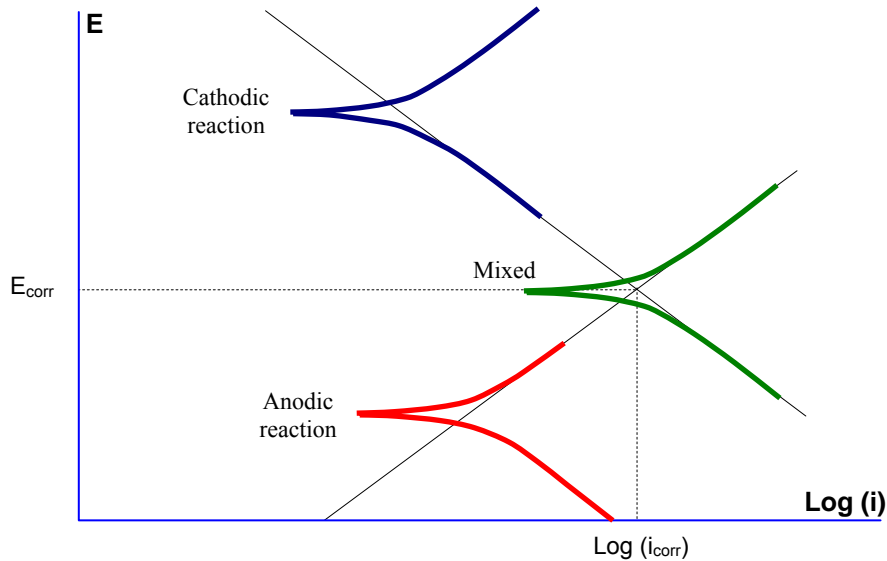


Figure 5 - The mixed-potential theory

An experimental result for a cell containing a segment of the prestressing strand used in this work in an electrolyte solution containing 1% by mass of CaO is given in Figure 6. As can be seen, unlike the theoretical curve, far from E_{corr} , passive response (i becomes independent of E) and transpassive behavior are present. A passive response can be expected in such a system because of the high pH (>12.5) of the electrolyte.

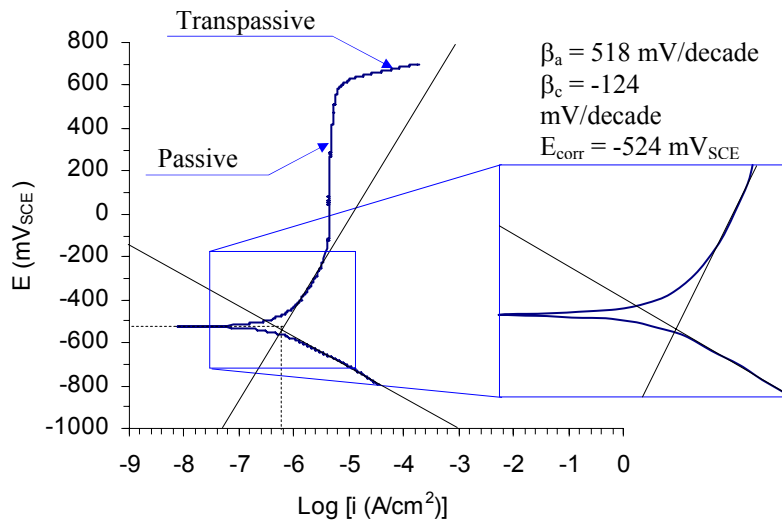


Figure 6 - Potentiodynamic behavior of steel in a 1% by mass CaO solution

From the potentiodynamic plot presented, additional considerations can be made. The first one is that, again differently from theoretical curves, the Tafel slopes do not meet at the $E_{\text{corr}}-i_{\text{corr}}$ point and adjustments have to be made. The second is related to the units that Tafel constants are given (mV per decade). It can be noticed that their units should be something such as mV/Log (A/cm²), since their calculation follows from $\Delta E/\Delta i$. However, that would be an awkward combination of units and it is usually preferred to report Tafel constants in variations of potentials in sets of ten units (or a decade) of the Log scale. Typically, for simplicity, even the “decade” is frequently omitted and only the “mV” is kept as a Tafel constant unit. Incidentally, authors mention (see, for instance Jones, 1996) the need for a development of at least “one decade” of the Tafel slopes in order to be satisfactorily determined. In the example given above (and commonly in grouted samples such as the ones tested in this work), the anodic Tafel slope does not meet this criterion.

2.2.4 The Nernst Equation and pH Effects

Dissolution of steel can be represented by the following anodic half-cell reaction:



This type of equation can be written in general form and in the cathodic direction as:



The equation that accounts for concentrations and activity of the elements involved in such reactions is given by the Nernst equation (see Stansbury & Buchanan 2000):

$$E = E_0 + 2.303 \frac{RT}{nF} \text{Log} \frac{(A)^a (H^{+})^m}{(B)^b (H_2O)^d} \quad \text{Equation 2-4}$$

where the parentheses indicate the activity of gases in atmospheres or a corrected value of concentration in gram equivalents per liter for solutions. R is the universal gas constant, T is the temperature in Kelvin, and F is the Faraday constant. E is the corrected value of potential and E_0 is the equilibrium potential of the reaction. When the appropriate values of the constants are used and the hydrogen evolution equation ($2H^+ + 2e^- = H_2$ or, when the solution is neutral or alkaline: $2H_2O + 2e^- = H_2 + 2OH^-$) is considered, the following version of Equation 2-4 can be found, where E is given in mV_{SHE} :

$$E = -59 pH \quad \text{Equation 2-5}$$

The same calculations can be made for the oxygen reduction reaction ($O_2 + 4H^+ + 4e^- = 2H_2O$ or, when the solution is neutral or alkaline, $O_2 + 2H_2O + 4e^- = 4OH^-$), which gives:

$$E = 1,229 - 59 pH \quad \text{Equation 2-6}$$

Upon plotting these two equations in a pH-potential or Pourbaix diagram, the graph shown in Figure 7 is found, which shows the conditions of stability for water according to values of potential and pH (detailed calculations can be found, for instance, in Jones 1996).

Similar constructions can be made for any other element, including corroding metals such as steel. These would show the conditions that the metals would have to have in order to corrode, be immune to corrosion, or even passivated.

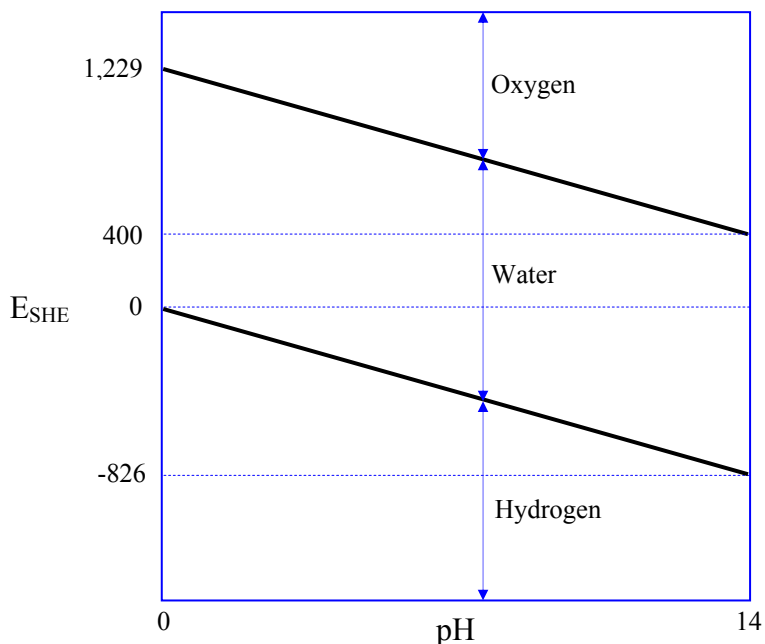


Figure 7 - Pourbaix diagram for water

2.2.5 The Voltage Drop Effect

Any electrochemical system inherently provides a certain degree of electrical resistance that is variable according to the characteristics of the system. This is true even for pure electronic circuits that do not involve any aqueous phases. Naturally, in these circuits, the amount of resistivity is usually negligible, since metallic phases are excellent electric conductors. In electrochemical circuits, however, the error generated in measurements because the voltage applied is reduced by a certain amount in the electrolyte can be important and has to be minimized or compensated accordingly.

One of the most commonly used methods to compensate for voltage drops is the Current Interruption Method (Escalante 1990). In this method, the current is interrupted at certain instants, with consequent drop of the potential being applied. Part of this potential has an instantaneous character because it is a result of the IR wasted in the electrolyte, i.e., the voltage drop error. Through extrapolation of the transient part of the potential that is tending to return to an equilibrium value, a very precise approximation of the instantaneous potential drop can be determined. With the amount of voltage drop due to the system resistivity determined, the error is compensated as the experiment is run. This process is illustrated in Figure 8.

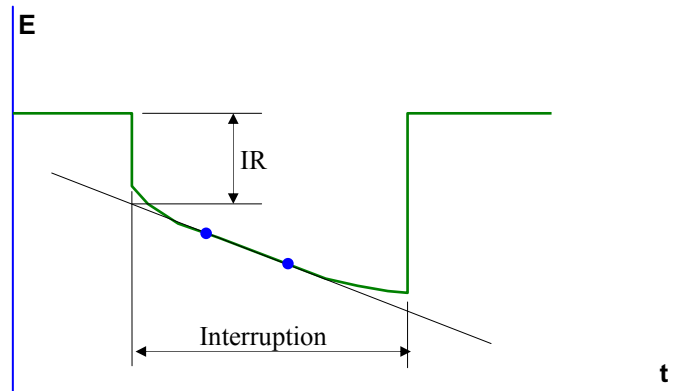


Figure 8 - IR compensation by current interruption

Another method used to compensate such errors is the Positive Feedback method (Berke 1990). This method consists of feeding a determined portion of the output potential back into the potentiostat. That portion redirected depends on the system being tested and is difficult to determine.

2.2.6 Experimental Techniques

Several techniques can be used to assess different aspects of materials and conditions of a given electrochemical system. They can be classified according to the nature of their electrical signal as DC (direct current) and AC (alternate current) techniques. DC methods are the ones most used in laboratory and field applications due to their relative simplicity in use and data interpretation. They involve an application of either current or voltage with respective measurement of voltage or current. On the other hand, while AC techniques measure the same variables, they need to be considered in a time frame. Consequently, the data analysis is typically processed in a frequency domain.

Examples of DC methods are Polarization Corrosion, Potentiostatic Polarization, Linear Polarization Resistance (LPR), and Potentiodynamic Polarization. Examples of AC techniques

are Electrochemical Impedance Spectroscopy (EIS) and Electrochemical Noise (for details on these methods, see, for instance, Jones 1996 or Stansbury & Buchanan 2000). DC techniques are the ones used for the methodology behind this work and are therefore detailed next.

2.2.7 The Polarization Corrosion Method

This method, also known as the Half-Cell Potential method, consists of the measurement of the equilibrium potential of corroding cells, E_{corr} . Although a regular voltmeter can be used for this task, one must consider the fact that corrosion potential measurements need time to reach a steady-state condition. The time necessary to obtain a stable measurement depends upon the corroding cell characteristics, and may vary from a few minutes to several hours.

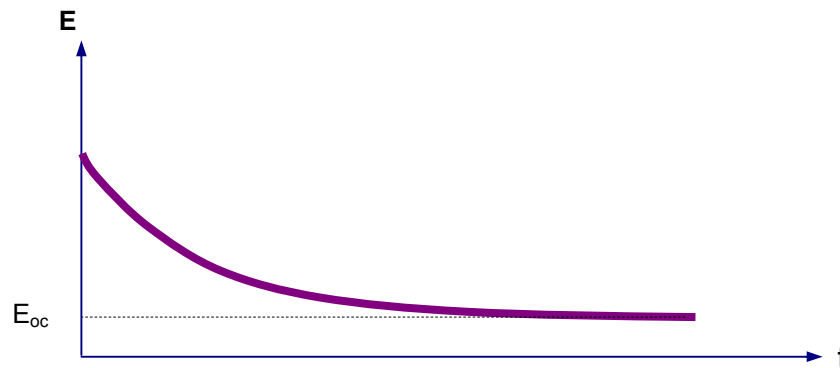


Figure 9 - Typical output plot from a polarization corrosion test

This method is widely used to monitor corrosion activity of reinforced concrete structures in the field. The values given in Table 1 indicate the probability of corrosion for different magnitudes of half-cell measurements (ASTM C876, 1999).

Table 1 - Probability of corrosion for different corrosion potentials

E_{corr} (mV _{CSE} *)	E_{corr} (mV _{SCE} **)	Probability
More positive than -200	More positive than -461	Higher than 90% that no corrosion is occurring
Between -200 and -350	Between -461 and -611	Corrosion is uncertain
More negative than -350	More negative than -611	Higher than 90% that corrosion is occurring

* The half-cell reaction is given by a copper-copper sulfate reference electrode.

** The half-cell reaction is given by a (standard) calomel reference electrode.

2.2.8 The Potentiodynamic Polarization Method

During a potentiodynamic polarization test, or polarization scan, a relatively large range of potentials (e.g., ± 250 mV or even ± 600 mV) is applied on the corroding metal and the corresponding current values are measured. The pair of values is typically plotted in a semi-log scale in order to allow the identification of the Tafel slopes (β_a and β_c). The intersection of lines

extrapolated from these slopes give the pair of values corresponding to the E_{corr} and i_{corr} of the ongoing electrochemical reaction.

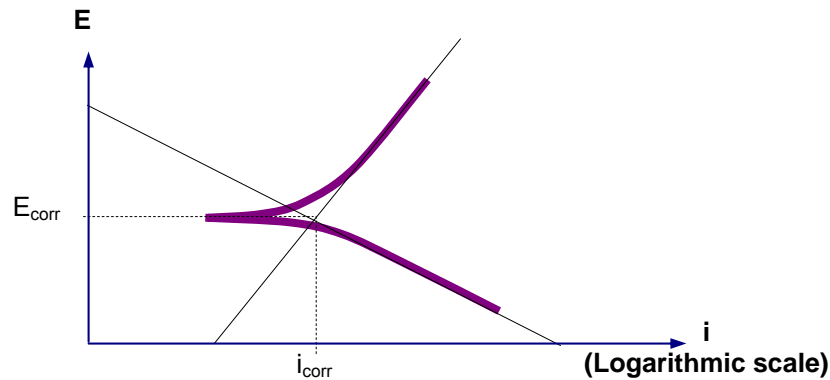


Figure 10 - Typical output plot from a potentiodynamic polarization test

This electrochemical method is very popular in corrosion investigations in the laboratory because it allows a complete description of the corrosion behavior of a system. Procedures for this method can be found in ASTM G 5 (1999) “Standard Reference Test Method for Making Potentiostatic and Potentiodynamic Anodic Polarization Measurements”.

2.2.9 The Linear Polarization Resistance Method (LPR)

The LPR method is another technique largely applied to reinforced concrete structures in the field due to simplicity in application and data interpretation. Although the procedure follows the same idea behind the Polarization Scan method, the range of potentials applied to the corroding metal is considerably smaller (typically ± 20 mV). This small range of potentials is used because only a short region around the inflection point between the anodic and cathodic responses can be approximated by a linear function. Example output from the LPR method is shown in Figure 11.

The information gathered from LPR readings is comprised of the system polarization resistance ($R_p = \Delta E / \Delta i$) calculated at zero current density, and by i_{corr} , which is also considered a measure of the system’s corrosion rate (ASTM G102 1999). The corrosion rate, however, should be carefully considered since it relates to the polarization resistance value through Tafel constants (β_a and β_c), which are typically assumed values for a certain system. For instance, LPR equipment used to assess concrete structures typically uses β_a and β_c ranging from 112 to 224 mV.

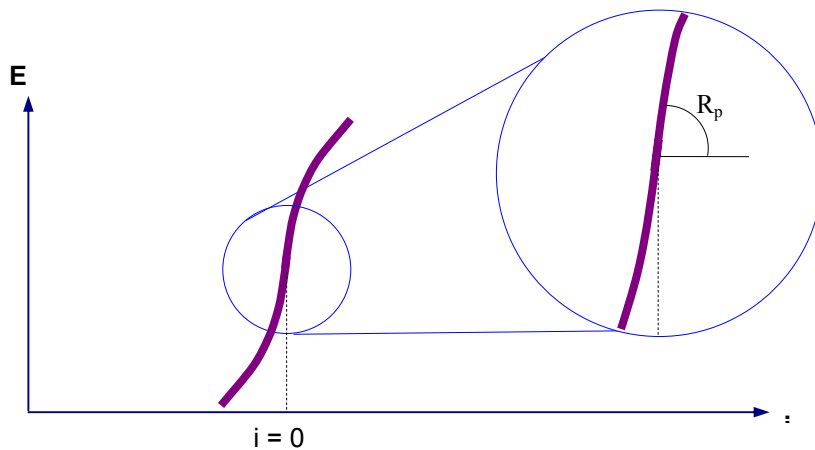


Figure 11 - Typical output plot from a LPR test

Procedures for this method can be found in ASTM G59 (1997) “Standard Test Method for Conducting Potentiodynamic Polarization Resistance Measurements”, where the relationship between Tafel constants, polarization resistance and corrosion rate is given by:

$$i_{corr} = \frac{\beta_a \beta_c}{2.303(\beta_a + \beta_c)} \frac{1}{R_p} \quad \text{Equation 2-7}$$

2.2.10 The Potentiostatic Polarization Method

The potentiostatic test is characterized by the application of steps of potential on the corroding metal in order to acquire correspondent current values. Although, similar plots to the ones resulting from a polarization scan can be obtained (ASTM G5 1999), it is the result gathered when only one potential step is used that is of particular interest for this research. A one-step potentiostatic procedure is the basis for the Accelerated Corrosion Test (ACT), which is used to assess grouts with respect to their degree of corrosion protection. The ACT is detailed in the next section.

2.2.11 The Accelerated Corrosion Test (ACT)

The ACT test is currently recommended by the Post-Tensioning Institute for assessment of the corrosion resistance of portland cement grouts for post-tensioning (PTI 2003). The ACT specimens are composed of segments of grouted post-tensioning strands exposed to a constant potential of +200 mV_{SCE}, while current values are monitored. The specimens are immersed in a saltwater solution of 5% NaCl by mass.

The test is finished when all specimens being tested fail due to intense corrosion development that is detected from an abrupt increase in the monitored electric current. This is illustrated in Figure 12. The average time required for each of the specimens to fail, t_{corr} , is then computed for characterization of the tested grout.

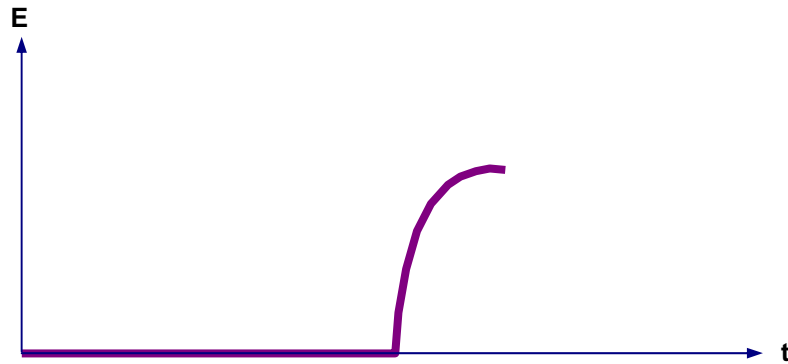


Figure 12 - Typical idealized output plot from ACT tests

Currently, PTI specifies that a given grout will satisfy an ACT test if its t_{corr} is greater than or equal to the t_{corr} obtained for a plain grout (only cement and water) at a water-cement ratio of 0.45. In addition, it is recommended by the Florida Departments of Transportation that t_{corr} values reach at least 1,000 hours (or 42 days of test duration) for final acceptance of grouts for post-tensioning applications based on the commentary discussion in the PTI specification (PTI 2003).

3 Objectives

This research contains several phases in which the work was divided between the University of Florida (UF) and The Pennsylvania State University (PSU). The objectives are defined as they fit into the phases of the research.

- *Phase I - Evaluation of the ACT methodology*
Evaluate the present ACT including the effect of IR compensation and recommend changes if needed.
Evaluate polarization resistance and dynamic polarization as alternate techniques to reduce the length of testing.
- *Phase II – Further ACT Testing*
Based on the data gathered in Phase I, complete further ACT testing to evaluate specific areas of concern.
- *Phase III – Grout Bleed Testing*
Develop an alternate bleed test that is more representative of the actual conditions under which grout will perform as compared to the Schupack pressure bleed test.

4 Phase I – Evaluation of ACT Methodology

4.1 VARIABLES

Five different grout groups were selected for Phase I: plain, plain with fly ash, plain with silica fume, plain with corrosion inhibitor, and prepackaged. Prepackaged grouts for post-tensioning tendons are typically proprietary, self-contained blends of portland cement and other cementitious materials along with admixtures designed to heighten the grout's performance. They are expected to give the best performance based on previous preliminary testing. The other grouts are mixes that contain portland cement along with the named pozzolan or admixture and were formulated and mixed by the researchers. Although prepackaged grouts are the only type of post-tensioning grout allowed by Florida DOT construction specifications, it was felt that these mixes would provide a wide range of performance levels, thus allowing the ACT test to be evaluated for a range of results. Grouts with fly ash in their mixture were also expected to perform well due to the increased resistivity typically conferred by fly ash (Schokker 1999). Their performance, however, was known to be sensitive to curing periods, since fly ash grouts tend to hydrate at lower rates when compared with cement. Silica fume grouts were expected to perform satisfactorily if the amount of cement replaced by the admixture was appropriate. Grouts with corrosion inhibitors in their mixture were selected since previous research showed mixed results in the ACT and new corrosion inhibitors are now available. Finally, a plain grout group was also tested to provide a lower bound control.

Two major variables were considered in addition to the grout formulation. Table 2 shows the grout formulation along with the curing period and IR compensation for grouts tested at PSU. The curing period was included to examine the effect of reduced and extended curing times. The IR compensation is a setting on the corrosion test equipment that allows for the resistance provided by the grout surrounding the strand. A third minor variable was that of the replacement amount of silica fume in grouts to determine the effect of the change on the results.

Table 2 - Combination of variables for the experimental program

Grout Group	Curing Period (days)	IR Compensation	Specimen Designations	Replicates
Plain grout	7, 14, 21, 28, 56	Yes and No (7, 28, 56)	PG 07Y; PG 14Y; PG 21Y PG 28Y; PG 56Y PG 07N; PG 28N; PG 56N	8
Fly ash grout (30% of Type F)	7, 28, 56	Yes and No	FA 7Y; FA 28Y; FA 56Y FA 7Y; FA 28N; FA 56Y	4
Silica fume grout (3, 5, and 7%)	7, 28, 56	Yes and No (28)	SF3 7Y; SF3 28Y; SF3 56Y SF5 7Y; SF5 28Y; SF5 56Y SF7 7Y; SF7 28Y; SF7 56Y SF3 28N; SF 28N; SF7 28N	4
3 corrosion inhibitor grouts	28	Yes and No	CI A 28Y; CI B 28Y; CI A 28N; CI B 28N;	4
			CI C 28Y, CI C 28N	8
5 prepackaged grouts	28	Yes	PP A 28Y; PP B 28Y; PP C 28Y PP D 28Y; PP E 28Y	8

The plain grout, which was the control group, was tested for five different curing periods (7, 14, 21, 28, and 56 days), in order to detail its gain in performance at early ages. All these ages were tested with IR compensation. In addition, three ages (7, 28, and 56 days) were tested without IR compensation to determine the overall effect of the various curing times. The same approach was considered for the fly ash grout group, but with no detailing of the gain in performance at early ages (14 and 21 days). For this group, a 30% replacement of the cement mass by fly ash was specified based on previous research (Schokker, 1999).

Three percentages of microsilica were chosen (3, 5, and 7%), considering that a low percentage should have been the optimum amount based on previous research on concrete and grouts. The percentages chosen were tested at three different ages (7, 28, and 56 days) with IR compensation, while only the age of 28 days was considered with no IR compensation.

Three corrosion inhibitors were chosen for testing. One was calcium nitrite, which had limited success in previous investigations of grout with the ACT (Hamilton 1995, Koester 1995, Schokker 1999). Another corrosion inhibitor was based on organic chemicals, while the third was a combination of organic and inorganic products. The three corrosion inhibitors were tested with and without IR compensation at 28 days of curing.

Five commercially available prepackaged grouts were selected for testing. These grouts were tested with IR compensation since the effects of various admixtures on IR compensation were established with the other tests in Table 2.

Table 2 also contains the naming convention for each test conducted. The two letters at the beginning of the test name indicate the grout group (PG: plain grout, PP: prepackaged, CI: corrosion inhibitor, FA: fly ash, and SF: silica fume). A third letter only occurs in the corrosion inhibitor group, in order to identify one of the three inhibitors used (A, B, or C). The following

two digits indicate the curing period of the grout (07, 14, 21, 28, or 56 days). The ending letter indicates whether the test was accomplished with IR compensation (Y), or without (N).

Only potentiostatic tests were conducted when no IR compensation was used. Hence, when results concerning other electrochemical tests are presented (potentiodynamic or LPR tests), many times the last letter of the test code is omitted, meaning that the parameters presented were obtained from tests that were accomplished under compensated conditions, even if their potentiostatic tests were run without compensation.

The number of specimens used in each of the experiments was determined based upon the number of stations available, a time limit of two years for testing, and previous ACT work.

4.2 MATERIALS

The cement used to obtain the four grouts produced in the laboratory was a Type II cement (cement mill test report is given in Appendix D). This type of cement was chosen because, due to lower amounts of C₃A in its formulation when compared with Type I, the curing process tended to generate less heat at a slower rate, which is likely to minimize distress and shrinkage cracking in the grouts. A Class F fly ash and densified silica fume were also used in testing.

Five prepackaged grouts available at the time of testing were chosen for the experimental program and are given generically in Table 3. The water-cementitious ratios shown are within the range of suggested values from the manufacturers.

Table 3 – Code and w/c ratio of the prepackaged grouts

Product Code	w/c
A	0.23
B	0.27
C	0.33
D	0.30
E	0.27

The corrosion inhibitors used are given generically in Table 4. The amount used for the inhibitor B was adapted, as a suggestion of the manufacturer, from 15 L per m³ of concrete (3 gal per yd³) to 55 L per m³ of grout (11.3 gal/yd³), while the amount for inhibitor C was recommended to remain at the same amount commonly used in concrete: 5 L/m³ (1 gal/yd³).

The recommended amount of inhibitor A in structural concrete is of 30 L per m³ of concrete (6 gal/yd³), as a maximum (higher amounts accelerate the setting time of concrete). Hamilton (1999) used 29 L/m³ in his work, with poor ACT results. Koester (1995), through contacts with the product manufacturer, increased the amount used to 80 L/m³ with still unsatisfactory ACT results. In this work, based on the amount of chlorides in the corrosion cells and extrapolation of the dosages given by the manufacturer together with the amount used by Koester, the amount of the inhibitor A was increased to 121 L/m³.

Table 4 - Code, denomination, and amounts used for the corrosion inhibitors

Code	Amount Used	Active Ingredients	Notes
A	121 L per m ³ of grout (24.44 gal/yd ³)	Calcium nitrite	1 L replaces 0.84 L (0.14 gal/lb); Added to water
B	55 L per m ³ of grout (11.3 gal/yd ³)	Organic and Inorganic	1L replaces 1 L (0.12 gal/lb); Added to grout.
C	5 L per m ³ of grout (1 gal/yd ³)	Organic	Added to water

4.3 TESTING SEQUENCE

The testing sequence is illustrated in Figure 13. This sequence was adopted initially to minimize the number of specimens to be cast for each grout condition (8 or 4) and was based on two assumptions. The first assumption was that defects such as air voids would occur in a maximum of two specimens (occurrence of 20 to 33% of defective specimens). It was felt that these specimens could still be used in potentiodynamic tests, since these tests take considerably less time to run and would not be affected by the penetration of the chlorides at the defect. The second assumption was that LPR measurements would not affect the results of subsequent potentiostatic tests, since LPR polarization potentials (± 20 mV vs. E_{oc}) are an order of magnitude less than the potential applied in the potentiostatic tests (+200 mV_{SCE} or, approximately, +440 mV vs. E_{oc}).

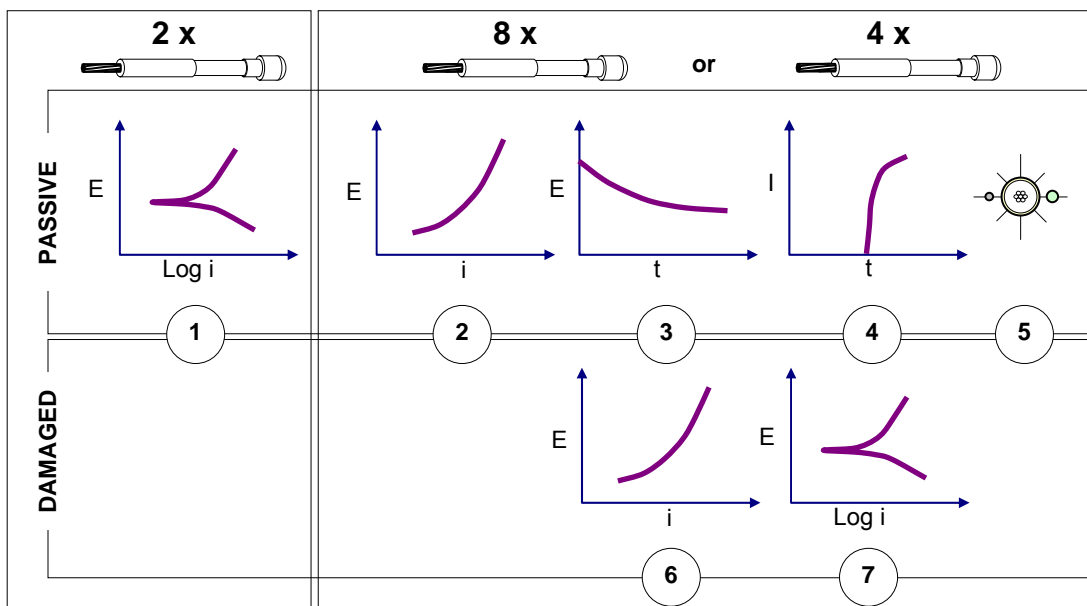


Figure 13 - Testing sequence for one grout condition

The first step in the sequence was to take two specimens (either with or without defects) per grout condition for potentiodynamic measurements to obtain the corrosion behavior of the specimens for passive (undamaged) conditions. Grouts that were going to be tested in uncompensated potentiostatic tests contributed two more specimens, doubling the number of results in this step for those grouts. The potentiodynamic curves obtained with this step allowed the determination of corrosion potentials (E_{corr}), corrosion rates (i_{corr}), and Tafel constants (β_a , β_c , and constant B). This test induces pitting rendering the samples unusable for further testing.

In the second step, eight remaining specimens (four in the cases specified in Table 2), free of defects, were used in LPR measurements. Again, grouts that were going to be tested in uncompensated potentiostatic tests contributed more specimens, doubling the number of results. The polarization resistances, R_p , for the passive conditions of the specimens were then determined.

As a third step in the sequence, the open circuit potentials, E_{oc} , were determined in polarization corrosion measurements. Eight (four in the cases specified in Table 2) results were determined for each grout condition. Once again, this number would double when considering the results for grouts intended for tests that did not have IR compensation.

The fourth step was the execution of the potentiostatic tests, which would take 16 ± 2 days, on average, to complete.

The fifth step was to identify the first spot of corrosion on each specimen. This is of interest to identify any bias due to placement of the electrodes in relationship to the specimen. In order to more easily identify the location of the first spot, the level of damaged imposed on the specimens should not be severe. Therefore, after the specimens experienced current not higher than 20 mA, the cable to the stations would be disconnected. The pictures shown in Figure 14 illustrate how difficult the identification of where the corrosion products first occurred may be for high levels of corrosion.



Figure 14 - Volume of corrosion products for low and high level of currents

After the corrosion of the specimens, the sixth and seventh steps were completed. The corroded specimens were allowed to depolarize from the ACT test and were then subjected to LPR tests and then to a potentiodynamic scan in order to determine the variables collected during

the first two steps for damaged conditions. In addition to this sequence of tests, samples of each grout were collected to determine their volume of permeable voids for grout characterization and potentiodynamic tests with steel samples not encased by grout were executed.

4.4 TESTS AND MEASUREMENTS

The experimental program was based upon a sequence of electrochemical tests that were executed for each grout condition specified previously. Additional observations and measurements were also accomplished to determine specific conditions that would occur on corrosion cells, and to characterize the subjects tested.

4.4.1 Electrochemical Tests

Four electrochemical test methods were chosen due to their simplicity and reliability: the corrosion potential test, the potentiostatic polarization test, the potentiodynamic polarization test, and the potentiodynamic linear polarization resistance (LPR) test.

The choice for the corrosion potential test was justified with the possibility that the open circuit potential, E_{oc} , the parameter obtained in that test, could work as an indicator of grout corrosion performance (Koester 1995), possibly in lieu of the more time consuming potentiostatic test.

The potentiostatic polarization test is the basis of the ACT method and therefore had to be considered in the experimental program. Its product, specifically the time-to-corrosion (t_{corr}) is associated with a grout's degree of corrosion protection, which is key information when considering IR drop implications on grout approval. The potentiostatic polarization test is going to be referred to in this work many times as "the potentiostatic test" and, since it was applied to ACT specimens, as "the ACT test" as well, mainly when limitations on grout approval are cited. The reference "ACT test or method" is also used to identify the method currently specified by the Post-Tensioning Institute for testing of grouts regarding their corrosion protection.

The other two tests were chosen because of their simplicity and classical role in electrochemistry. Moreover, they can be used to determine the corrosion rate (i_{corr}), which was likely to be associated with grouts' corrosion protection (Hamilton 1995, 2000). Selected grouts were chosen for this testing to evaluate the potential use of the method. The potentiodynamic linear polarization resistance test, which is going to be referred to in this work as "linear polarization resistance test", "polarization resistance test", or merely as "LPR", provides a measurement of resistance to the currents observed in a corrosion cell. Therefore, it is reasonable to infer that grouts producing higher polarization resistances would tend to protect post-tensioning strands for longer periods. The potentiodynamic polarization test, which is going to be addressed in this work as "the Tafel scan" or merely as "the potentiodynamic test", provides measures of several electrochemical parameters.

The settings initially used in each of the electrochemical tests mentioned above are presented in Table 5.

The potential used in the potentiostatic test (+200 mV_{SCE}) is the same potential specified by the PTI specifications (2003). Additionally, the potentials shown for the potentiodynamic tests were tentative and had to be adjusted several times as the work progressed in order to better define Tafel slopes (one-decade long slopes).

Table 5 - Settings for each electrochemical test

Test	Value
Corrosion Potential:	
Sample period (min)	0.2
Potentiostatic:	
Sample period (min)	30
Initial E (mV _{SCE})	+200
Potentiodynamic:	
Initial E (mV) vs. E _{oc}	-250
Final E (mV) vs. E _{oc}	+250
Scan rate (mV/s)	5
Sample period (s)	1
Linear Polarization Resistance:	
Initial E (mV) vs. E _{oc}	-20
Final E (mV) vs. E _{oc}	+20
Scan rate (mV/s)	0.5
Sample period (s)	0.2

4.4.2 Additional measurements

Preliminary potentiostatic tests in this work indicated that the failure of the grout protection generally occurred near the top of the specimen near the counter electrode. The cause of this probable concentration of current gradients at the top part of testing regions was assumed to be the short length of the counter electrodes adopted in those tests (8.5 cm or 3.3 in.). It was decided then, among the options considered (such as the adoption of more than one counter electrode in the cells, or even curving them around the specimens), to replace the counter electrodes being used with longer ones, which were 17 cm (6.7 in.) long, and to monitor the occurrence of the first spots of corrosion. Figure 15 shows the referential system used during this monitoring. Not only were the first signs of corrosion products registered along the testing region of specimens, but also around their periphery.

Additionally, in order to characterize the different grouts tested (each grout specimen resulting from a certain condition applied to a certain grout group), determinations of volume of permeable voids, which is considered in this work a measure of the grout's porosity, were accomplished according to ASTM C642 (1997) "Standard test Method for Density, Absorption, and Voids in Hardened Concrete". The characterization of each grout was important because their qualification with respect to porosity corroborated and explained their performances during the electrochemical tests.

The grouts were also characterized by the amount of electric charge that passed through their thickness during the potentiostatic tests. The values of charge were calculated considering the times-to-corrosion in each cell and the passing current values below 10 mA. Further details about this measurement are given in Section 4.7.1.2.

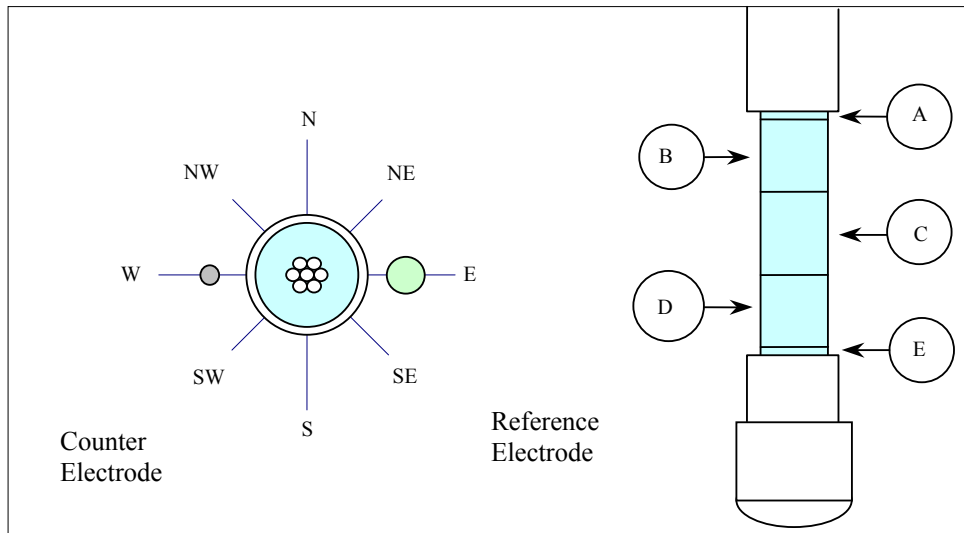
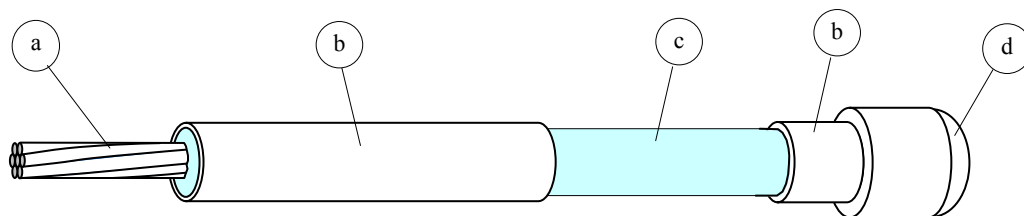


Figure 15 - Referential system used to locate first spots of corrosion on ACT specimens

4.5 SPECIMEN CONSTRUCTION

The ACT specimen was designed to expose a fixed amount of strand incased in grout to an aggressive media, an electrolyte, in which corrosion is facilitated (Figure 16).

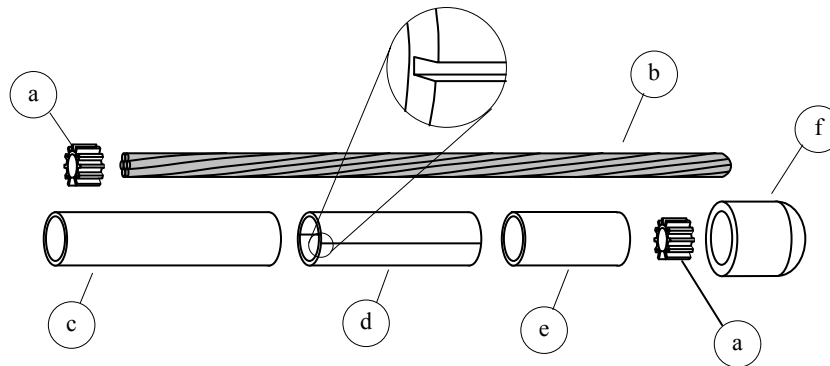
The critical part of the specimen is the testing region (*c*, in the figure). Prior to testing, careful visual examination of this region was necessary in order to check for defects such as cracks and voids left by air pockets or bubbles. These kinds of occurrences weakened the grouts' capability to protect the strand, skewing test results for short term testing.



- | | |
|--|---|
| a: Seven-wire post-tensioning steel strand. Length: 360 mm (14 in.). Diameter: 12.7 mm (0.5 in.) | c: Testing Region (exposed grout). Diameter: 25.4 mm (1 in.). Length: 90 mm (3.5 in.) |
| b: Clear plastic Tubing. Longer length: 150 mm (6 in.). Shorter length: 60 mm (2.4 in.) | d: 25.4 mm (1 in.) plastic cap. |

Figure 16 – Schematic of the specimens used

The fabrication of the specimens necessary for this study was comprised of four distinct steps. First, each part of the casing assemblage was prepared. Then, the parts were appropriately assembled to form the required number of casings. Finally, the specimens were cast and cured. This sequence is represented in Figure 17 and is detailed in the following sections.



- | | |
|---|---|
| <p>a: Plastic spacer with outer diameter that snugly fits inside casings</p> <p>b: Seven-wire prestressing steel strand.
Length: 360 mm (14 in.). Diameter: 12.7 mm (0.5 in.)</p> <p>c: Long plastic tubing. Internal diameter: 25.4 mm (1 in.). Length: 150 mm (6 in.)</p> | <p>d: Middle plastic tubing with two longitudinal slits (see detail). Internal diameter: 25.4 mm (1 in.). Length: 90 mm (3.5 in.)</p> <p>e: Short plastic tubing. Internal diameter: 25.4 mm (1 in.). Length: 60 mm (2.4 in.)</p> <p>f: 25.4 mm (1 in.) plastic end cap</p> |
|---|---|

Figure 17 - ACT specimen details (a) photo of parts with completed specimen (b) schematic details of construction.

4.5.1 Casing/Specimen Parts Preparation

Figure 17 specifies and gives the dimensions of the different parts in the ACT specimen assemblage. Plastic casings, a segment of prestressing strand and plastic spacers comprise these different parts and were prepared as described in the following sections. The PTI specification does not detail the specimen preparation and assembly. Because the ACT results were affected by inconsistencies in specimen quality, the following standardized preparation procedure was developed.

Clear rigid PVC tubing measuring 25.4 x 31.75 x 3.175 mm (1 x 1.25 x 1.125 in.) in internal diameter, external diameter, and thickness, respectively, was used to make the casing

segments. The use of clear, instead of opaque tubing, facilitated visual observation during the casting procedure. Figure 17 shows one of these tubes, measuring originally 183 cm (6 ft), ready to be cut with a bench saw to the required sizes of each casing segment, i.e., 15, 9, and 6 cm (6, 3.5, and 2.4 in.).

After cutting the casing segments, the parts were separated and the longitudinal diametrically opposed slits were made on the middle casing segment (shown previously in Figure 17). The slits were made so that only a thin wall (approximately 1 mm or 0.039 in.) would be left, facilitating the task of breaking them to remove the middle casing segments later on, when exposing the testing regions to the corrosion cell's electrolyte. The previous method used to expose testing regions (Koester 1995, Schokker 1999), which used grinding or cutting tools, often resulted in a damaged grout surface and may have led to significant scatter in results.

The casing parts were then cleaned with pressurized air and stored separately, as shown in Figure 18, which also shows some 25.4 mm (1 in.) end caps and plastic spacers. The spacers were cut from large round reinforcing bar spacers available for structural concrete construction. The final outside diameter of these spacers allowed a snug fit inside the casings.



Figure 18 - Casing parts ready for the assemblage procedure

The steel used for the specimens was a 12.7-mm diameter (0.5-in.) seven-wire prestressing strand that met ASTM A426 (2002) "Standard Specification for Steel Strand, Uncoated Seven-Wire for Prestressed Concrete". Details about the strand properties are given in Appendix C.

The strand was received in reels, which were then cut to the required size (360 cm or 14.2 in.) with an abrasive cut-off saw and had their extremities beveled afterwards in a bench grinder to facilitate insertion into the casing and spacer. Prior to the casting procedure, the strand segments were cleaned with acetone to remove impurities such as dust, spots of rust, and oil.

4.5.2 Casing Assembly

Alignment during assembly was aided with the use of metal pipes. These metal pipes allowed proper finishing at the junctions, reduced the possibility of casing defects, such as leakages and misalignments, and minimized the amount of caulking material needed to seal the junctions. Caulking was minimized to prevent accumulations inside of the casings, which reduced the grout cover and led to a premature failure. Pictures and details of the two auxiliary supports used in this step are shown in Figure 19.



Figure 19 – Auxiliary tubing supports used in the assemblage of the ACT casings

After caulking the junctions, the three sections of each casing were held together with duct tape and the end caps were cemented to the extremities that corresponded to their short plastic tubing sections. The specimens were left undisturbed for a minimum of one hour to allow the caulking to vulcanize before submitting the casings to a leakage test. The casings were filled with water, and any leakage was then identified and fixed. A set of assembled casings already caulked, taped, and leakage tested is shown in Figure 20.



Figure 20 - Set of assembled casings

The sets of assembled casings were then placed in a rack to keep them in an upright position. Their respective cleaned prestressing strands, with a spacer attached to their bottom end, were placed inside the casings. The assembled casings ready for grouting are pictured in Figure 21.



Figure 21 - Set of casings with placed strands ready for the casting procedure

With the sets of casings prepared, each casing already with its respective strand segment appropriately cleaned, and with a spacer attached at its bottom end, the preparation of the sets of specimens continued with the mixing and casting procedures. Firstly, however, quantities of grout mixing materials for each type of grout were measured. Cement and mineral admixtures (silica fume and fly ash) were weighed (mass determination), while chemical admixtures (corrosion inhibitors) were quantified by volume.



Figure 22 - Grout mixing and specimen casting ready to begin

The grout was mixed in a cylindrical container measuring 30 cm (11.8 in.) in diameter and 40 cm (15.7 in.) in height using a high-shear blade with a varying speed mixer (a 0-2,500

rpm drill). Figure 22 shows these and other utensils necessary for flow cone tests, which gives a measure of grouts' fluidity.

The same batching order was adopted throughout the mixes. The water was always placed in the mixing container first. Then, the cementitious materials were slowly added using low mixing speeds. The inhibitors A and C were added to the batch water, while B was added to the freshly mixed grouts, according to manufacturers' specifications. Each grout was mixed for approximately 4 minutes. After completion of mixing, the grouts were tested for fluidity in the flow cone. The flow cone test was executed according to the ASTM C939 "Standard Test Method for Flow of Grout for Pre Placed Aggregate Concrete" with modifications for thixotropic grouts as described in the PTI specifications (2003).

The specimens were then cast using the sequence of steps illustrated in Figure 23. The first step was to have each casing prepared for casting. One third of each casing volume was then filled with grout. To reduce voids and air bubbles, the strands were slowly moved and the casings tapped to induce moderate vibration on the casings. This procedure was repeated in the third and fourth steps. The last step, which completes the casting procedure, was the attachment of the second spacer to each strand at the top of the casings.

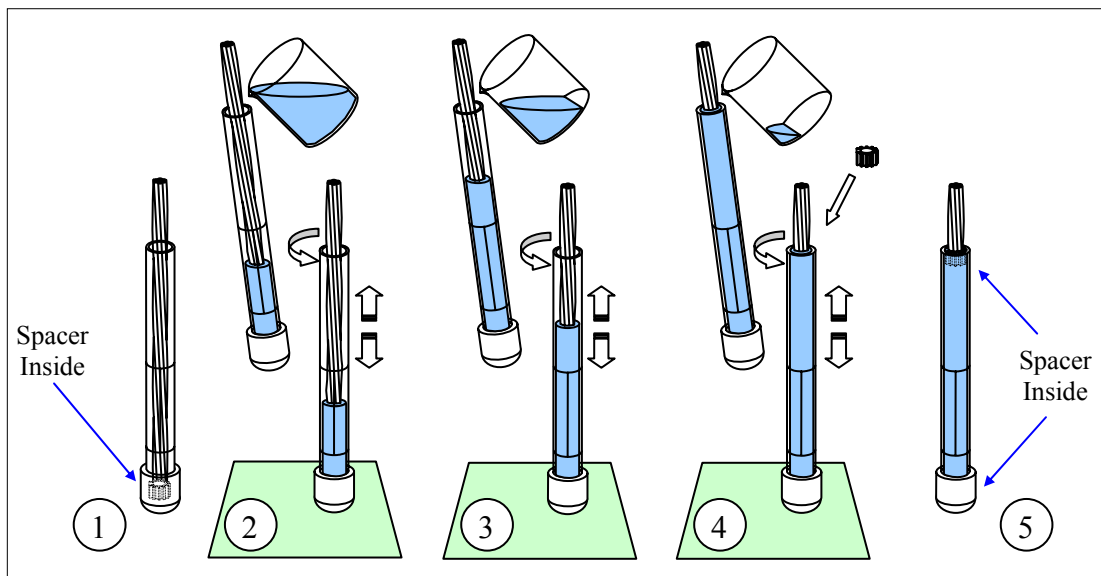


Figure 23 - Procedure used to cast the ACT specimens Specimen Curing

After completion of the casting step, each specimen received an identification label and the set of specimens was taken to the moist room for a specified curing period. Inside the chamber, the temperature and relative humidity was kept, respectively, at $23 \pm 1.7^\circ \text{C}$ (75.2°F) and at a minimum of 95%. While in the moist room, each specimen's protruding strand was protected against corrosion with a plastic cover.

4.6 TEST EQUIPMENT AND PROCEDURES

The ACT setup used in this research was composed of a potentiostat, a multiplexer, and the corrosion cells. The potentiostats were set to apply a voltage difference of 200 mV above the potential given by the saturated calomel reference electrodes. Multiplexers were used to connect

corrosion cells to potentiostats, allowing one potentiostat to control several cells. In this work, an eight-channel multiplexer was used to connect a maximum of eight stations to their respective potentiostat. The schematic presented in Figure 24 illustrates the test setup. A personal computer houses the potentiostats, facilitating operation and data collection.

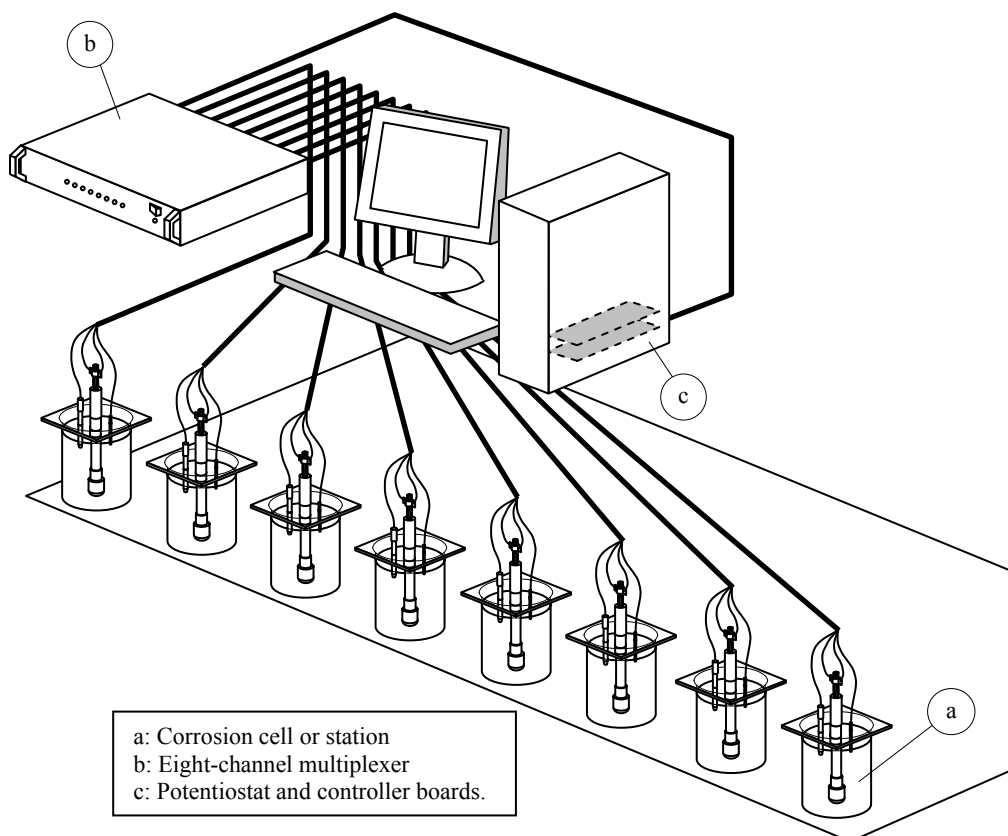


Figure 24 - Schematic of the ACT setups used

4.6.1 Electrochemical measurement system

The electrochemical measurement systems used in this work were manufactured by Gamry Instruments. The potentiostat, a PCI4/300, was capable of a current resolution of 1 fA ($f = 10^{-15}$), a voltage resolution of 2 μ V, and a maximum current output of 300 mA. The multiplexer, an ECM8, with eight channels, had a “local” potentiostat in each of its channels, being capable of polarizing the stations when they were not being polarized by the potentiostat. Figure 25 presents the three systems used in this work.



Figure 25 - Setups A (top left), B (top right), and C (bottom) were used in the tests

4.6.2 Corrosion Cell

Figure 26 presents schematics of the corrosion cells used in this work. They were assembled in 3 L beakers containing salt solution as electrolyte (5% NaCl by mass in distilled water). The water line was marked in every station to allow the addition of more water on a weekly basis to compensate for evaporation of the electrolyte in each cell.

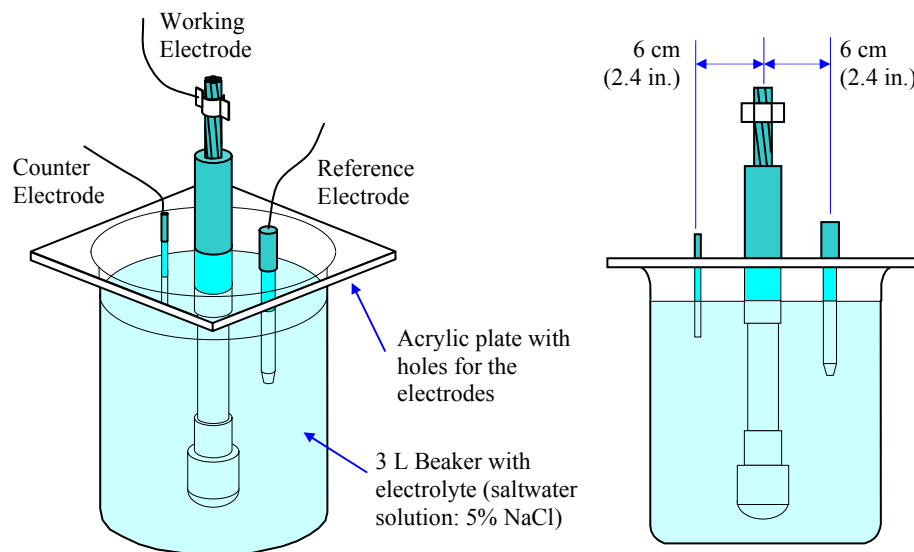


Figure 26 - Schematics of the corrosion cells (stations) used

Reference, counter (auxiliary), and working electrodes (ACT specimens) complete the necessary circuitry to measure the variables of interest. In addition, an acrylic plate with holes to suspend the electrodes completed the stations.

The reference electrode used in each corrosion cell was manufactured by Fisher Scientific. It was a plastic-bodied gel-filled Accumet™ saturated calomel electrode (SCE), which is commonly used in laboratory applications.

The counter electrodes were segments of platinum clad wires from Anomet Products Inc. Each segment, containing a double platinum thickness, 40% of niobium by cross-sectional area for increased mechanical and electrochemical protection of its copper core, measured 16.5 cm (6.5 in.) in length and 3.175 mm (0.125 in.) in diameter. The extremities of the counter electrodes were covered with a layer of silicone, to avoid corrosion of the copper core, and with a layer of epoxy for mechanical protection of the silicone layer. Both reference and counter electrodes are pictured in Figure 27.



Figure 27 - Reference and counter electrodes used

After curing, the middle plastic casing was removed to expose the grout over the test region. Immediately after the casing removal, each specimen was placed directly in its respective station to prevent drying shrinkage of the exposed section of grout, minimizing the possibility of cracking (the sequence of steps are illustrated in Figure 28). The use of a lathe or any other method to expose the testing region is likely to take too much time, facilitating the occurrence of cracking. In addition, even precise and careful cutting may damage the grout layer, increasing the tests' variability. With specimens in their stations, the corrosion cells were then complete and the electrochemical measurements were started.

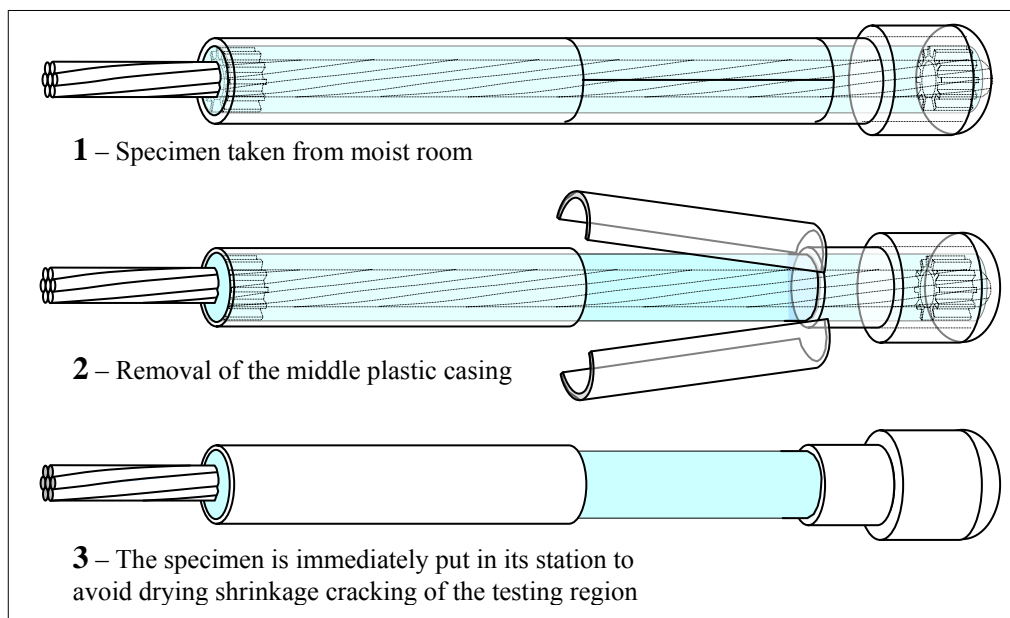


Figure 28 - ACT Specimens are working electrodes in the corrosion cells used

4.7 RESULTS AND ANALYSES

This chapter presents results from the experimental program and analyses conducted on the data to evaluate the test methods. Parameters affecting the ACT Test time-to-corrosion results are compared and discussed. The time-to-corrosion results are then compared to the current ACT limits. Finally, potentiodynamic polarization and linear polarization results are presented.

4.7.1 Factors Affecting Time-to-Corrosion

4.7.1.1 IR Compensation

Figure 29 shows the times-to-corrosion for selected grouts both with and without IR compensation. Typically the time-to-corrosion is reduced when IR compensation is used, which is expected since the compensation adjusts for the grout resistance ensuring that the selected polarization level is applied to the surface of the strand.

For instance, considering the tests run with IR compensation, the plain grout results, PG, increase from 282 hours at 7 days to 401 hours at 28 days (42% increase) and to 479 hours at 56 days (20% increase). For the same age intervals, the fly ash grout's t_{corr} , increased from 74 hours to 162 hours (118%) and finally to 435 hours (169%). This difference in behavior was expected since it is known that fly ash grouts take longer to develop their microstructure when compared to plain mixes.

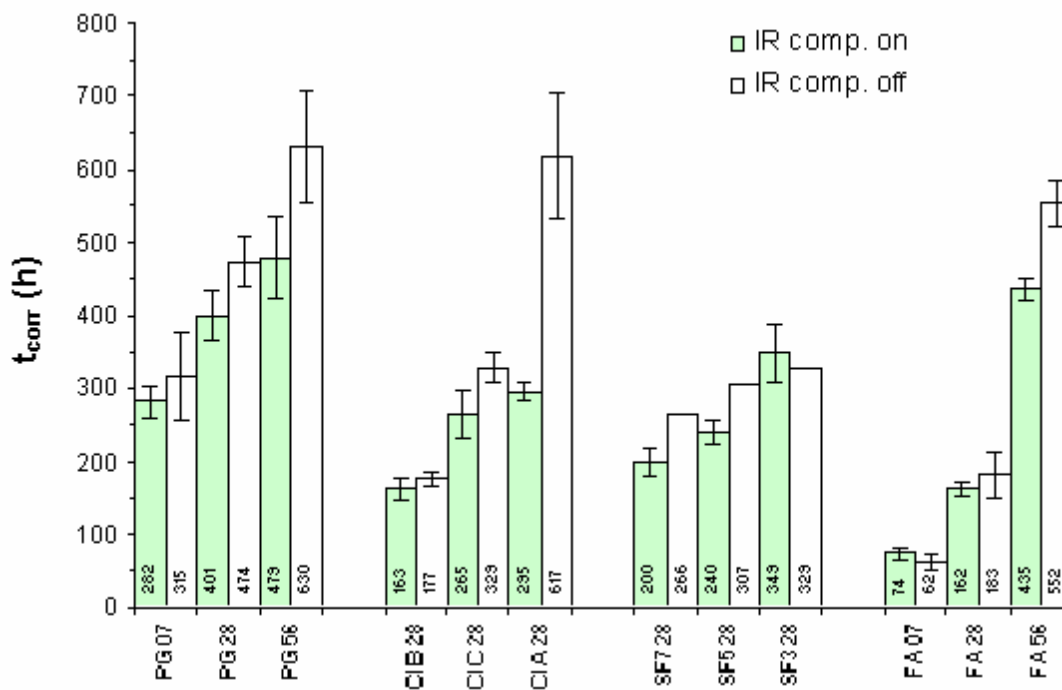


Figure 29 – Influence of IR compensation on ACTs for different grout groups

When the IR compensation option was not engaged, however, the value obtained for the fly ash grout at 56 days was only 27% higher than that for the compensated result. This difference should have been more significant since the control mix reached a 32% difference at the same age, and a more significant resistivity is typically expected from fly ash mixtures. This apparent lack of effect when the fly ash grout was tested with IR compensation may have been due to the higher variability in the plain grout data. Incidentally, it should be noted that the final compensated value obtained for the fly ash grout was only 9% higher than the result obtained for the control grout at 28 days.

Figure 30 shows the performance along the period of curing for the plain and fly ash grouts. In addition to the aspects mentioned above, the graph shows relatively constant development rates of t_{corr} for the plain mixture, but dramatic increases of the variable after 28 days for the mixture containing fly ash.

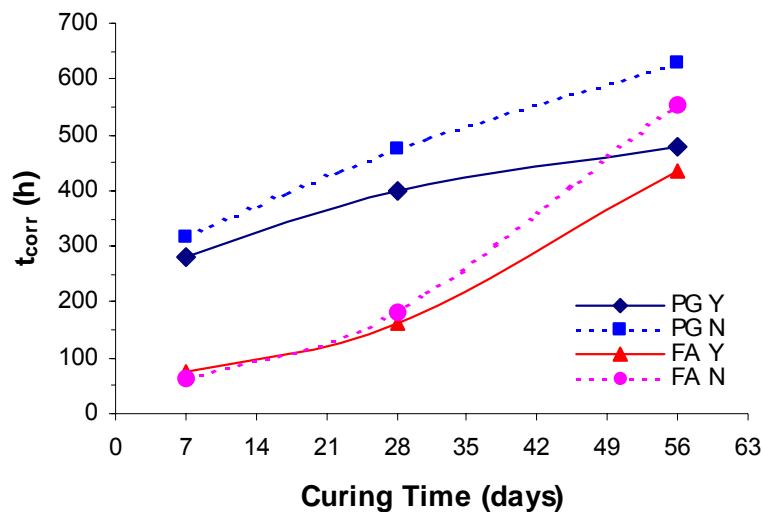


Figure 30 - Development of the time-to-corrosion for plain and fly ash grouts with the curing period

Regarding the other two groups, t_{corr} seems to be particularly sensitive to some types of corrosion inhibitor (corrosion inhibitor A is based on calcium nitrite, while the other two are based on organic and/or inorganic formulations), but little difference is observed among silica fume results. These effects are discussed in the following section.

4.7.1.2 Grout Constituents

Although improved performance was expected from the grouts with silica fume, Figure 29 shows that the specimens with silica fume had lower values of time-to-corrosion than the control. This apparent incongruence corroborates results found in previous tests (Schokker 1999) that show a tendency for grouts with silica fume to produce lower ACT results when compared to plain mixes. In addition, the silica fume grouts were influenced by IR compensation to a much lower degree.

Although silica fume additions are known to improve concrete durability, the absence of aggregates in grouts can undermine silica fume's effectiveness. The aggregates found in

concrete aid in the dispersion of the silica fume particles in the mix, leading to an improved microstructure. In grouts where no aggregates are present an interconnected net of undispersed silica fume agglomerates can form. These agglomerations of silica fume may have considerably facilitated the ingress of chloride ions through the grouts tested and contributed to the lack of IR compensation effect. This effect was investigated further in Phase II and is addressed in more detail later in the report. Moreover, the presence of silica fume agglomerations is also related to alkali-silica reactions (Diamond 1997) between the concentrated masses of microsilica with the alkaline cementitious products, generating expansion, internal stresses, cracking and, therefore, access of chlorides.

Figure 31 shows the complete series of microsilica grout results. The time-to-corrosion decreased as the amount of microsilica increased, probably due to agglomeration. Even considering the low result obtained for SF3 56Y, lesser amounts of silica fume consistently produced better results than higher proportions in all curing ages tested, with only SF5 07Y as an exception.

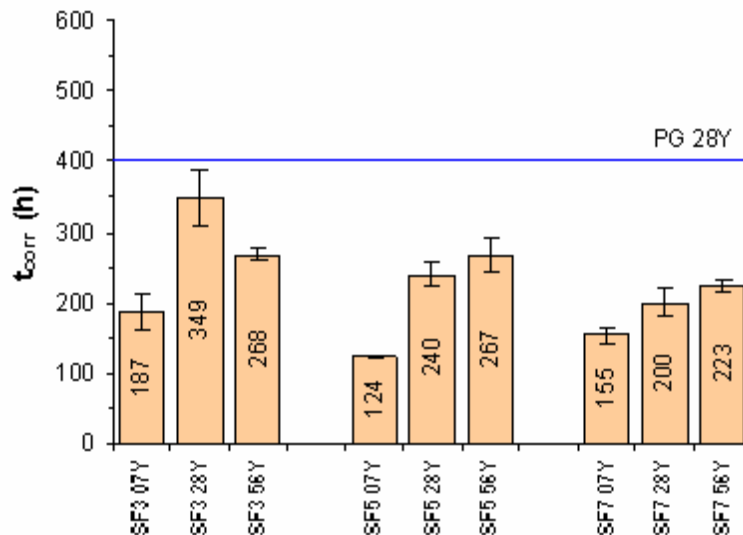


Figure 31 – Development of t_{corr} with curing period for three silica fume grouts

For the grouts tested with corrosion inhibitors in their mix, the only indication that may justify their low results is the fact that their measured resistances (from LPR tests) were probably at a lower level than that necessary to match the t_{corr} found for the plain grout. The three corrosion inhibitor grouts, A, B, and C, reached 193 ± 15 , 138 ± 21 , and 148 ± 6 $k\Omega cm^2$, respectively, while the control was at 325 ± 43 $k\Omega cm^2$ (all tested at 28-days). Therefore, it is possible that the addition of chemical admixtures reduced the resistivity of grouts with consequent low performances in ACT tests. In addition, the grouts with corrosion inhibitors B and C showed higher values of porosity (38 and 39%, respectively), while only the grout with corrosion inhibitor A showed the same level of permeable voids exhibited by the control mix (35%).

Another possibility is that proportions used were not appropriate for the voltage used in the ACT. This is supported by 109% higher time-to-corrosion from the uncompensated test. In addition, although the dosages used were approved by representatives of the products, the values

used are the same ones suggested in the specifications for concrete, not grout, and may need refinement.

4.7.1.3 Grout Age

Figure 32 presents the complete series of plain grouts obtained at various ages. The results show that grouts tested at 21 days had similar result to that obtained at 28 days. Although no statistical difference was seen between both results, it is still recommended to run control mixes at 28 days, when the cementitious matrix is closer to be fully mature.

Figure 33 shows the progression of results from the fly ash grout tests, which shows a significant increase in time-to-corrosion from 28 to 56 days. Consequently, when considering grouts with fly ash in their mixes, a curing period of 56 days will be required to fully develop the grout microstructure. This may, however, be impractical for mix development due to the long test time.

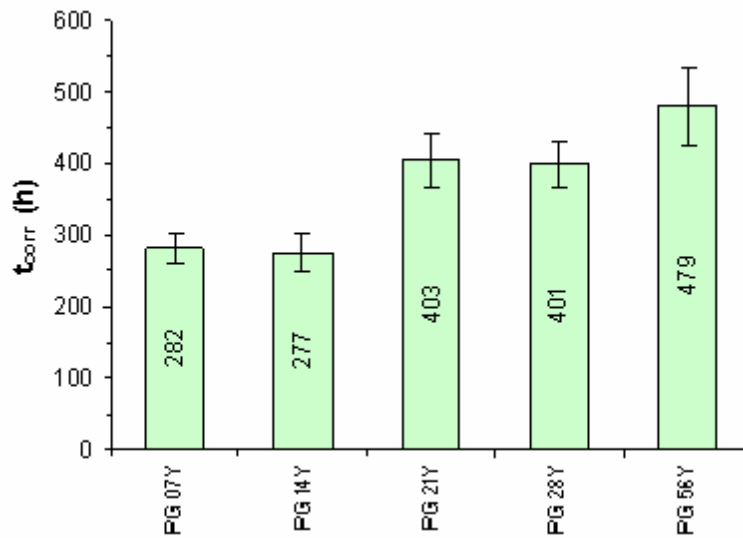


Figure 32 - Development of t_{corr} with curing period for a plain grout

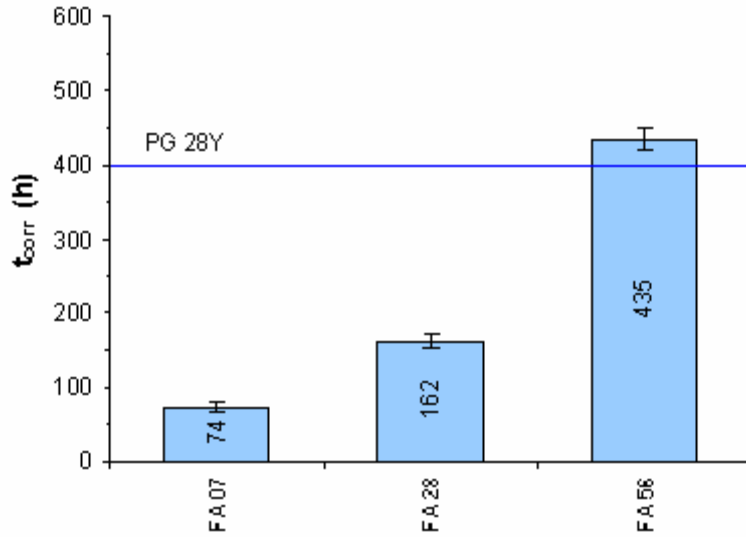


Figure 33 - Development of t_{corr} with curing period for a fly ash grout

4.7.1.4 Volume of Permeable Voids

Volume of permeable voids was determined for each grout using ASTM C642 (1999). The results for grouts tested at 28 days are presented in Figure 34. The porosities ranged in value from 28% to 41%. The prepackaged grouts had the lowest porosity of the grouts tested.

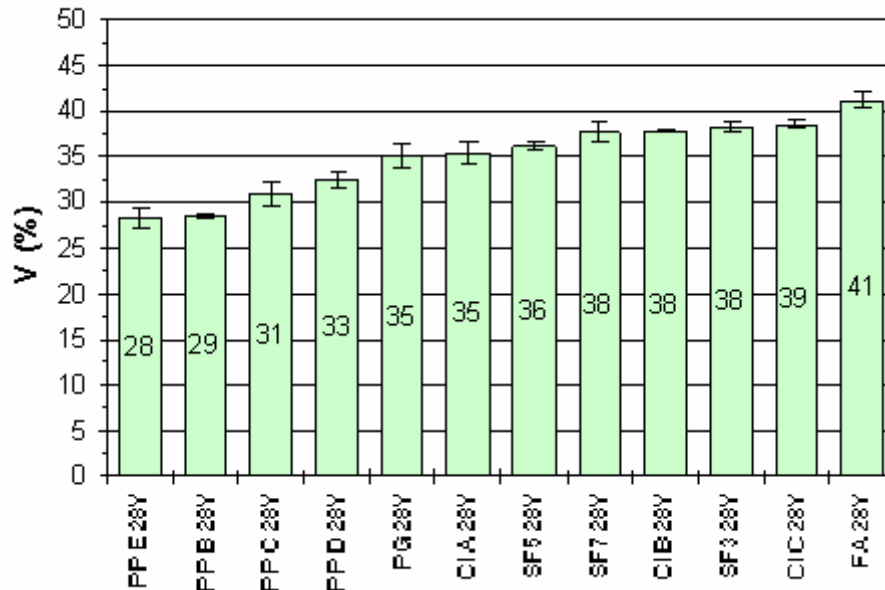


Figure 34 - Volume of permeable pores for different grout types at 28 days

In Figure 35 two distinct groups of grout can be identified: one with times-to-corrosion that were significantly high (above 600 h) and another with values that were significantly low (below 400 h). The figure indicates that other factors besides porosity were likely participating in the grouts' ACT performances and dictated a slightly different behavior between the two groups. The correlation between time-to-corrosion and the measure of porosity obtained (volume of permeable voids) is demonstrated in Figure 36.

The group with denser characteristics (grouts on the right of the graph) had a more direct effect on its t_{corr} values when variations were observed in the porosities. It is possible that the group with higher volume of permeable voids were more influenced by permeability and diffusivity, and less influence from variations on porosity. Nevertheless, even considering these aspects, the correlation between the variables V and t_{corr} is evident in Figure 36.

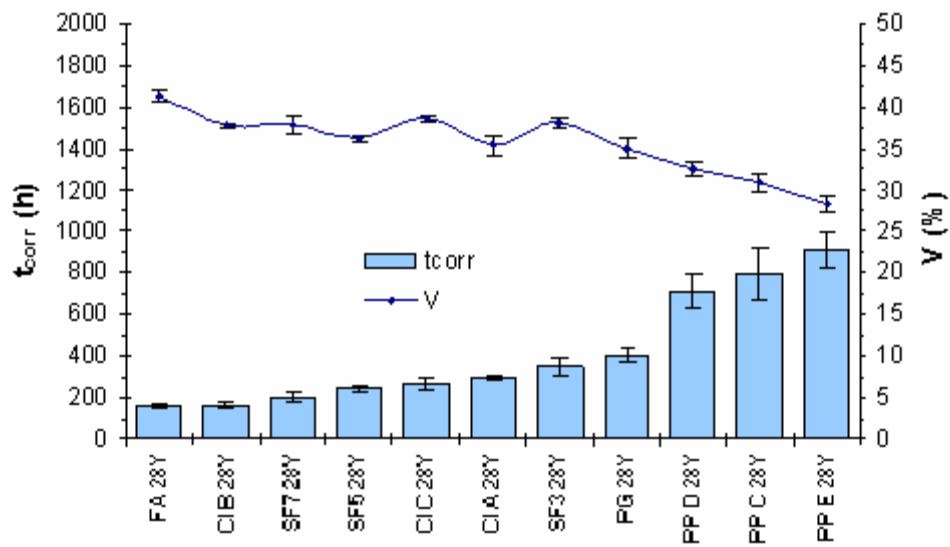


Figure 35 - Grout porosity trend with increase of the time-to-corrosion

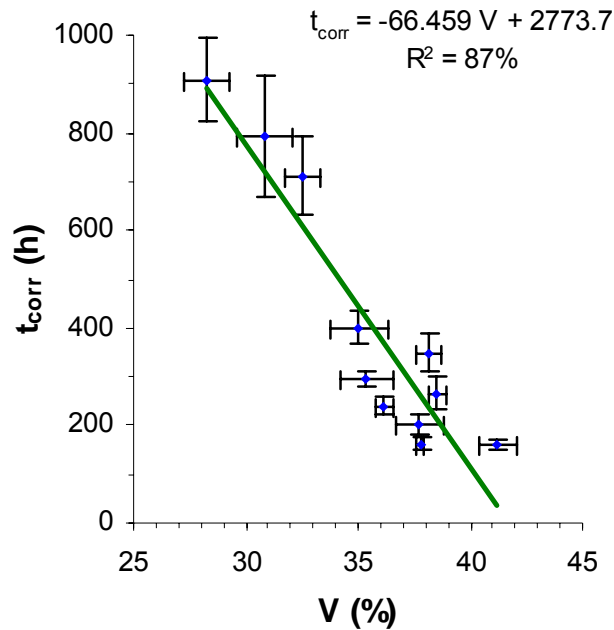


Figure 36 – Linear correlation between time-to-corrosion and volume of permeable pores

The expression that linearly correlates the variables V , given in percentage, and t_{corr} , in hours, is rewritten in Equation 4-1:

$$t_{corr} = -66.5V + 2774 \quad \text{Equation 4-1}$$

Although the linear fit presents good correlation in the interval considered, it is likely that an exponential fit would be more appropriate to represent the phenomenological interaction between the variables t_{corr} and V . Hence, V and t_{corr} limiting values should exist in a manner that an asymptotical behavior should be observed on their relationship, i.e., a very low V should reflect on an extremely high t_{corr} as well as a very high V should result on a practically null t_{corr} . In this way, assuming that the prepackaged grout B, which is characterized by 29% of permeable pores and was tested for 3,200 h, was near failure and would have allowed corrosion at, say, 3,400 hours, and also assuming that, say, 60% of porosity would lead to an almost instantaneous corrosion ($t_{corr} = 1$ h), the correlation in Figure 37 is found.

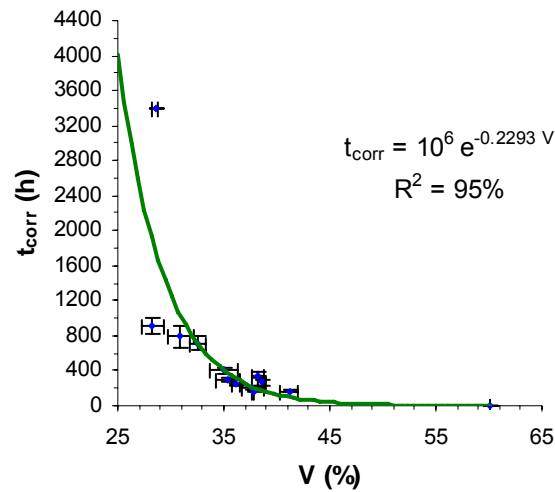


Figure 37 - Exponential correlation between time-to-corrosion and volume of permeable pores

The expression that exponentially correlates variable V, given in percentage, and t_{corr} , in hours, is rewritten in Equation 4-2:

$$t_{corr} = 10^6 e^{-0.23V} \quad \text{Equation 4-2}$$

The exponential correlation does not only fit the measured experimental points better, but it also describes in an appropriate phenomenological fashion the relationship between the two variables in consideration. Nevertheless, the two equations found should be valid only in the range of permeable voids investigated (28 – 41%), and extrapolations beyond this range should be considered carefully. In addition, despite the high correlation coefficient found on both cases, few points represent low porosity results and high porosity values do not completely define a well-behaved pattern.

Despite the reservations that one may have when considering the correlations obtained, two important aspects can still be drawn from the data. Firstly, the correlations highlight the strong influence that porosity certainly has on corrosion protection found in the ACT and, secondly, values of porosity as low as 33% correspond to good performance in the ACT. The linear and exponential expressions give t_{corr} values of 581 and 517 hours, respectively, for 33% permeable voids.

4.7.2 Correlation with Time-to-Corrosion

4.7.2.1 Electric Charge

Figure 38 presents ACT results for two specimens: one cast with a grout containing fly ash, which reaches 10 mA immediately after the onset of corrosion, and for another cast with a prepackaged grout, which reaches the same level of current after a much longer period of time. While the fly ash specimen generates a charge of 11 coulombs, the prepackaged one generates 2,939 coulombs, indicating a significant difference in behavior between the two grouts.

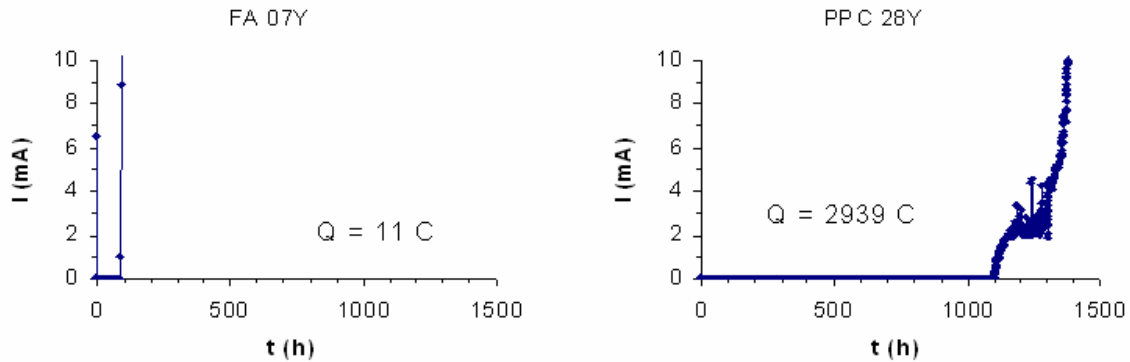


Figure 38 – Minimum and maximum electric charge values calculated from ACT results

Figure 39 presents calculated charge values for the grouts tested in this work that were allowed to reach electric currents higher than 10 mA in their ACT tests. The charge values were then calculated considering $t \geq t_{corr}$ and $I \leq 10$ mA as limits.

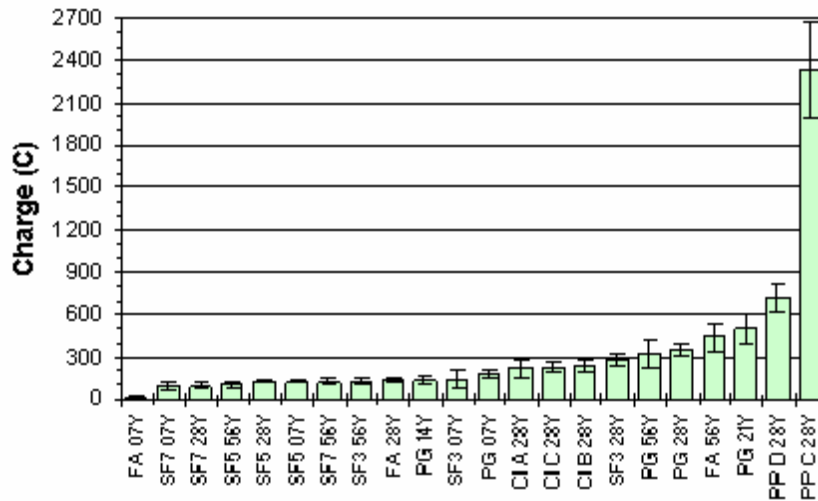


Figure 39 - Electric charge values calculated from ACT results

The charge values significantly increase along the grout series, being very sensitive and reaching significant amounts at the end of the series. This behavior is probably not only related to the porosity of the cementitious matrices, but also pore size, tortuosity, and permeability of the grouts. The most important aspect that can be drawn from the measurements taken, however, is that the prepackaged grouts have much higher accumulated charges than that of the grouts with pozzolans. The only exceptions were the 3% silica fume grout at 28 days and the fly ash grout at 56 days. The low silica fume content and the long curing period probably helped each one of these cases, respectively.

Electric charge generated are compared to the time-to-corrosion in Figure 40.

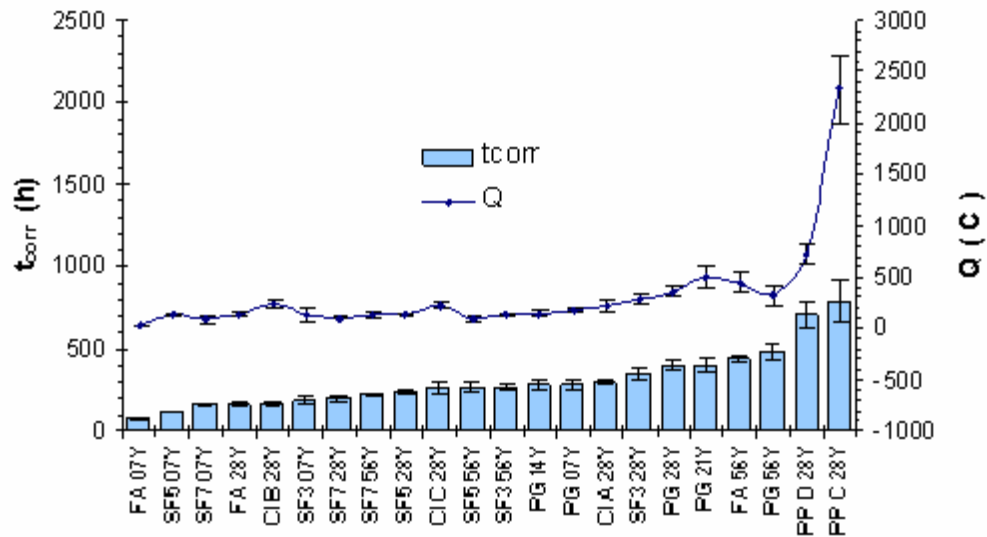


Figure 40 - Electric charge trend with increase of time-to-corrosion

It was also noted before that the electric charge, Q , would appropriately characterize grouts because the processes involved in the development of electric currents in an ACT would be intimately related to the properties of absorption, permeability, and diffusivity of the grout tested. Therefore, since these properties would strongly relate to porosity, an exponential relationship between Q and t_{corr} should also be expected, as apparently was the case when considering the correlation between the volume of permeable voids and t_{corr} . Figure 41 shows the result of the exponential correlation between Q and t_{corr} .

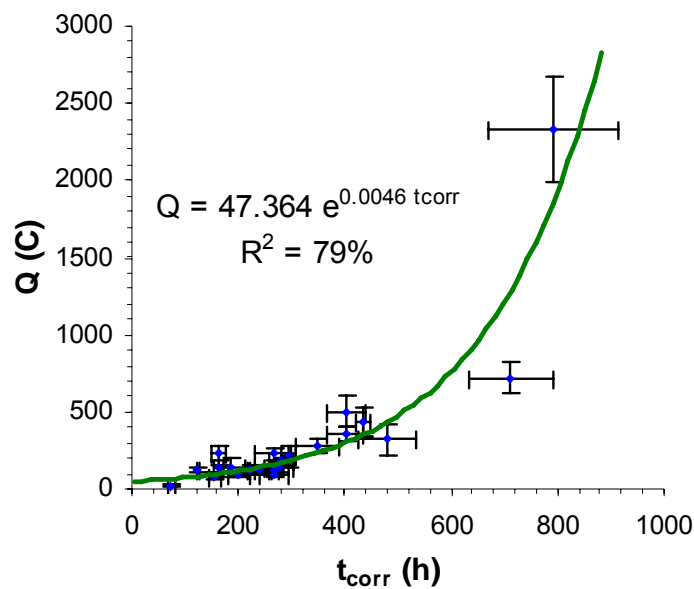


Figure 41 - Correlation between time-to-corrosion and electric charge

The expression that correlates Q , given in coulombs, and t_{corr} , in hours, is rewritten in Equation 4-3:

$$Q = 47e^{4.6 \times 10^{-3} t_{corr}} \quad \text{Equation 4-3}$$

This result, however, is of little importance as a direct alternative for grout testing, since ACT data must be available in order to determine the charge passed. Nevertheless, this result corroborates the exponential format assumed for the previous correlation between volumes of permeable voids and times-to-corrosion and indicates that grouts with times-to-corrosion below 400 hours produced values of charge below 300 C, while grouts with higher times-to-corrosion reached levels of charge as high as 2,500 C.

4.7.2.2 Open Circuit Potential

The open circuit potential, E_{oc} , for each grout type was determined prior to initiating the ACT test. In previous investigations (Hamilton 1995; Schokker 1999; Hamilton 2000), the correlation between these potentials and their respective times-to-corrosion were investigated, but little interaction was found between these variables. The researchers indicated that this may have been due to the small number of groups tested and lack of sophistication of equipment.

Figure 42 shows the open circuit potentials collected for Phase I grouts. The open circuit potential was relatively constant among the various grout mixes even though the times-to-corrosion varied significantly. This is in agreement with previous researchers findings.

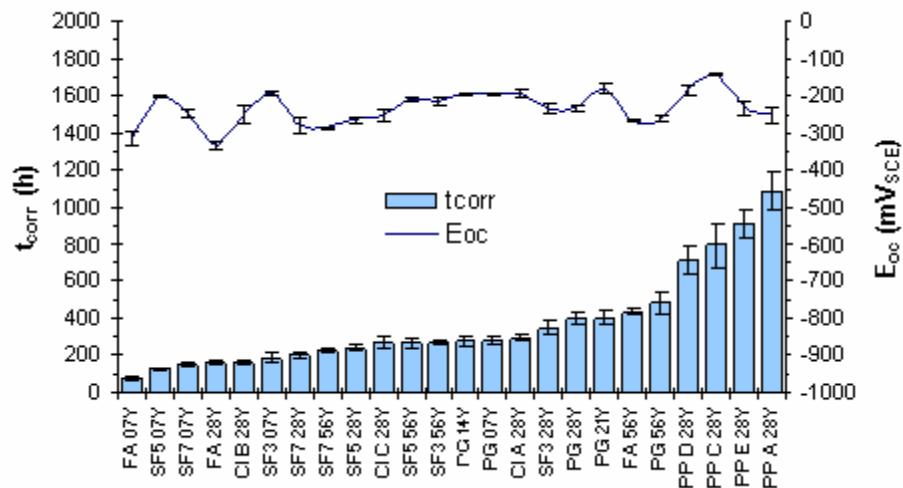


Figure 42 - Open circuit potentials obtained for grouts tested afterwards in compensated ACTs

4.7.3 ACT Limits Analysis

Figure 43 shows the average time required for corrosion to initiate under static polarization (t_{corr}). Only the results obtained with IR compensation are present in the graph. A vertical line at the top of each column represents the experimental standard error in the measurement (the standard deviation divided by the square root of the number of replicates tested). The grout represented by column PP B 28Y in the graph ran for 3,200 hours with no corrosion. Horizontal solid lines represent limits currently found in the PTI grouting

specification. Condition 1 represents the true *PTI Specification* recommendation of having a t_{corr} greater than a plain grout with water-cementitious ratio of 0.45. Condition 2 of 1,000 hours is mentioned in the commentary of the *PTI Specification* and is currently required in the FDOT specifications.

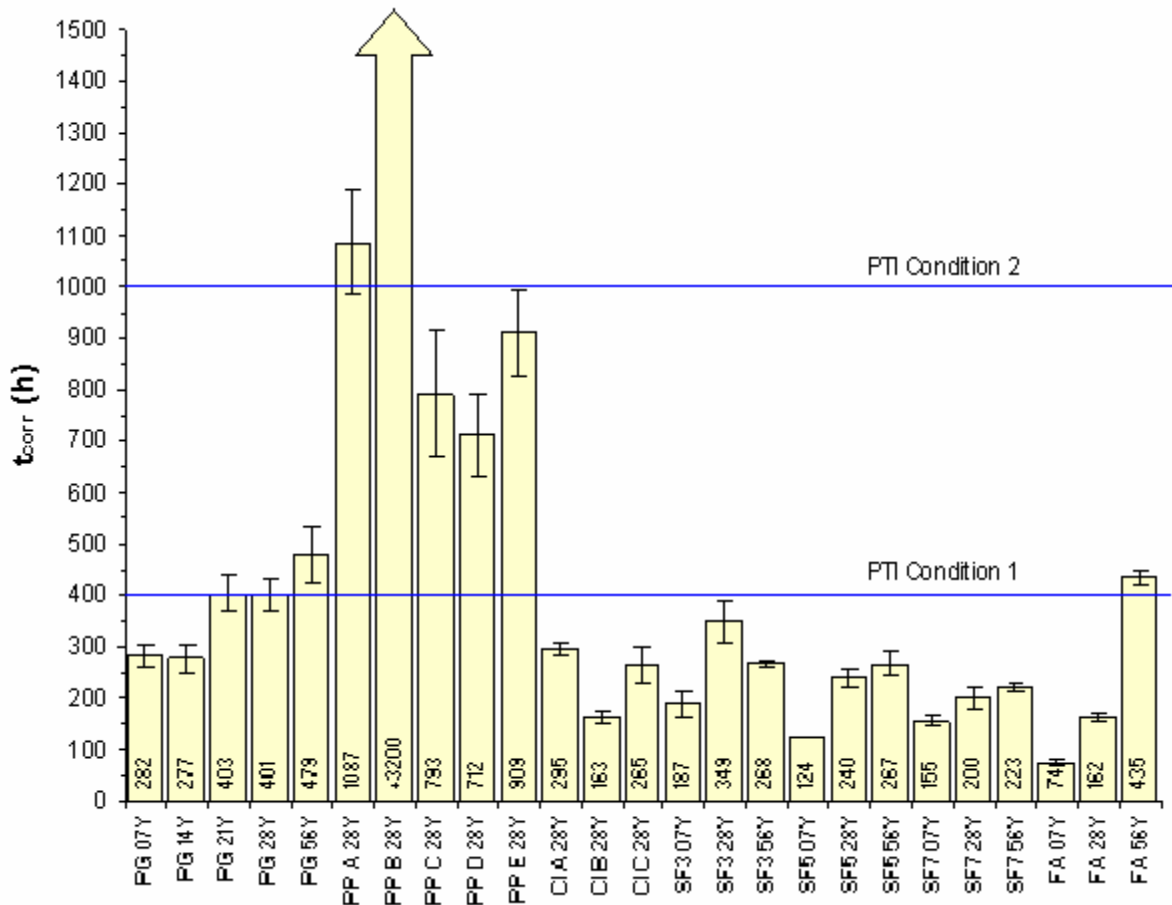


Figure 43 – Times-to-corrosion for different types of grout (IR comp on)

Measured times-to-corrosion ranged from as low as 74 hours to well beyond 1,000 hours indicating that the grout mix has a strong effect on the corrosion properties. All prepackaged grouts (PP) that were tested easily passed PTI Condition 1, i.e., their t_{corr} values were higher than the one measured for the control mix (plain grout at 28 days – PG 28Y). However, only two of them passed PTI Condition 2 (PP A 28Y and PP B 28Y), indicating, perhaps, an excessively stringent condition. The same grout may have a significantly different time-to-corrosion with different equipment, specimen preparation, or strand from a different reel (Schokker, 1999). Also, IR compensation was used in testing the prepackaged grouts. If a prepackaged grout did not reach 1000 hours in this testing, it does not necessarily mean that it is not capable of reaching this threshold under other conditions, but rather shows the drawback in using a set limit rather than a relative comparison.

With the exception of the prepackaged grouts, all grout types were also tested without IR compensation. The results of the two test conditions are compared in Table 6. When IR compensation was not used, the results had average standard errors ranging from 11% to 46%. It should be noticed, however, that one of the grouts presented a time-to-corrosion 149% above its respective compensated value.

Table 6 - Influence of IR drop on t_{corr}

Grout Test	t_{corr} found with IR compensation (h)	t_{corr} found with no IR compensation (h)	Difference Range (%)
PG 07	282 ± 23	315 ± 60	0 – 45
PG 28	401 ± 33	474 ± 35	1 – 38
PG 56	479 ± 55	630 ± 77	4 – 67
CI A 28	295 ± 13	617 ± 85	72 – 149
CI B 28	163 ± 14	177 ± 11	0 – 26
CI C 28	265 ± 34	329 ± 20	4 – 51
SF3 28	349 ± 40	329 ± 0	0 – 6
SF5 28	240 ± 17	307 ± 0	20 – 38
SF7 28	200 ± 20	266 ± 0	21 – 48
FA 07	74 ± 7	62 ± 12	0 – 10
FA 28	162 ± 9	183 ± 32	0 – 41
FA 56	435 ± 15	552 ± 32	16 – 39
		Mean (%)	11 – 46

The control grout produced a t_{corr} equal to 401 h when tested under IR compensation (characterizing Condition 1) and produced a t_{corr} equal to 474 h when no compensation was used. This difference amounts to 18%, but could have been 38%, considering the deviation as indicated in the table.

In order to illustrate the implication of these results, upon applying a 46% possible IR compensation change in t_{corr} to Condition 2 and 38% to Condition 1 in Figure 43, the horizontal lines shift to the positions shown in Figure 44. Under these altered conditions that provide an indication of the effect of the IR compensation, all the prepackaged grouts meet the new required minimum value. Moreover, at least seven other grouts, including early age ones (whose properties are knowingly not fully developed yet) meet or are close to meeting Condition 1.

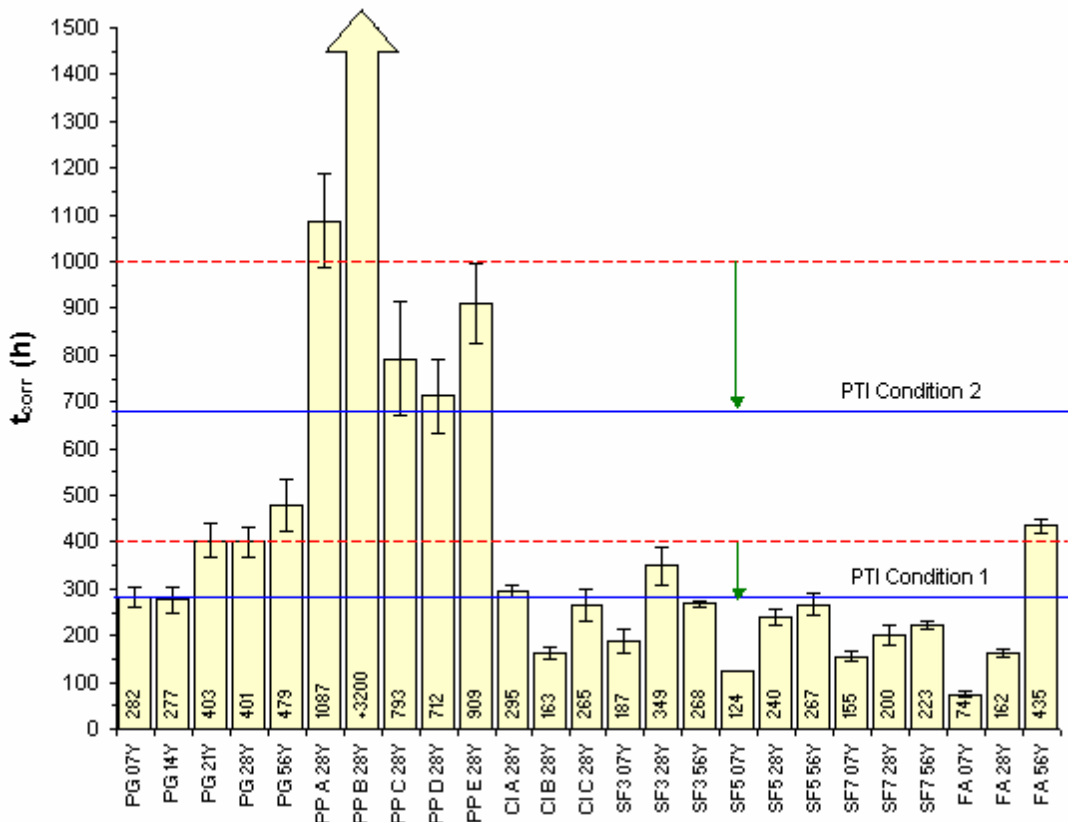


Figure 44 – Several grouts pass PTI conditions when effects due to IR drops are significant

Grouts with a high content of silica fume (above 5%) or with fly ash not fully matured fail even the modified Condition 1, indicating the importance of appropriate material proportioning and the necessity for extended curing periods, respectively. These aspects are specifically addressed in the next section.

In summary, corrosion requirements for post-tensioning grouts should explicitly express whether IR compensation is used in ACT testing. Another aspect to be considered, is that t_{corr} values can also vary significantly with equipment, user, strand lot, and other variables still not studied and a relative comparison such as that offered by PTI Condition 1 is, probably, a better approach, instead of adopting a fixed value for grout approval. If this condition is deemed too lax, a lower permeability qualifying grout may be used (such as 0.40 w/c rather than 0.45 w/c).

4.7.4 Potentiodynamic Polarization

In potentiodynamic polarization tests, the linear portions of the anodic and cathodic branches are identified when plotted in a semi-log format. These linear responses should develop for one order of magnitude (or decade) at a minimum, allowing the determination of their respective slopes, or Tafel constants, within an acceptable margin of error.

Since activation polarization is not a typical behavior of ACT specimens, as will be demonstrated in this section, the Tafel constants determined in these situations should be

regarded merely as tangents to “Tafel-like” slopes. Nevertheless, in this work, the terms Tafel and Tafel-like are used interchangeably.

4.7.4.1 Potentiodynamic Behavior

The grout surrounding the steel strand in an ACT specimen is a porous medium that creates a complex situation for electrochemical tests and especially potentiodynamic scans. Not only does the concentration of the different chemical species involved in the processes become a more difficult issue to analyze, but also the mass transport of ions from and towards the interface’s double layer is directly affected because of the physical barrier imposed by the grout.

In general, it was found during the experimental program that anodic responses are significantly affected by the type of grout used and, many times, have their Tafel-like behavior hindered, not allowing parameter determinations. The reasons for this behavior may be related to aspects such as the grout’s bulk density, specification of an appropriate range of potentials and the presence of the grout itself.

Figure 45 shows potentiodynamic polarization plots obtained for one ungrouted steel strand specimen in a 1% calcium oxide (CaO) solution by mass and for one grouted specimen in a 5% salt (NaCl) solution by mass. The data determined for the ungrouted steel was obtained after tests with strands containing different numbers of wires (one to seven) and characterize the corrosion behavior of the steel used in the ACT specimens (specifications given in the Appendices) when in a high pH environment (above 12.5). The data determined for the grouted specimen (control grout) was obtained from six replicates moist cured for 28 days.

Although the bulk electrolytes used in each of the two cases were different, it is reasonable to consider that, in the second situation, at a certain depth near the steel surface, a chloride-free zone does exist. Therefore, the significant differences observed between both plots are probably a consequence of the barrier imposed by the grout layer, which affects the ionic mass transport and the speed of the ongoing electrochemical reactions, thus modifying the output.

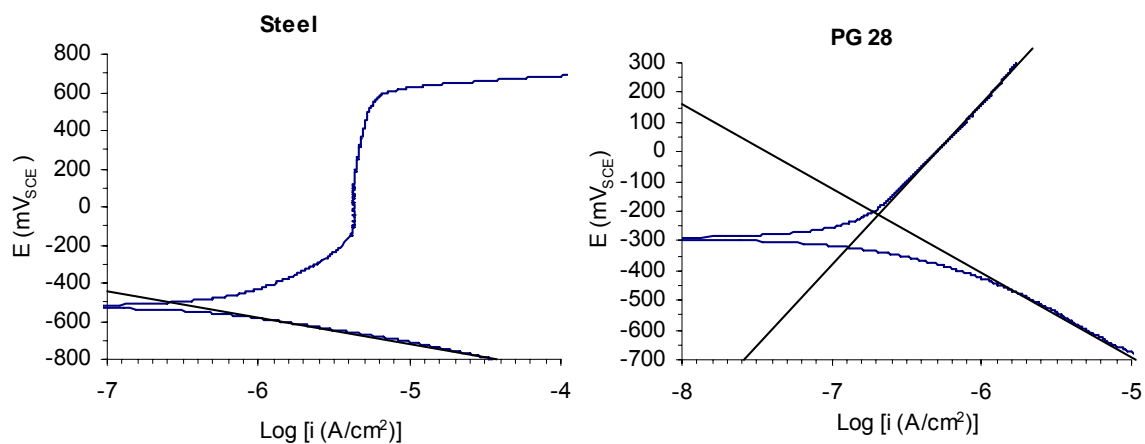


Figure 45 - Potentiodynamic plots for the steel used in the ACT specimens in a 1% CaO solution by mass and for a plain grout ACT specimen in a 5% NaCl solution by mass.

Data from the tests with ungrouted steel: $E_{\text{corr}} = -488 \pm 10 \text{ mV}_{\text{SCE}}$; $\beta_c = -127 \pm 1 \text{ mV}$; $i_{\text{corr}} = 0.30 \pm 0.03 \text{ } \mu\text{A}/\text{cm}^2$.
 Data from the PG 28 tests: $E_{\text{corr}} = -284 \pm 6 \text{ mV}_{\text{SCE}}$; $\beta_a = 549 \pm 36 \text{ mV}$; $\beta_c = -240 \pm 21 \text{ mV}$; $i_{\text{corr}} = 0.22 \pm 0.02 \text{ } \mu\text{A}/\text{cm}^2$

When compared to the second plot, the first shows a lower cathodic slope and no anodic constant can be promptly determined. In addition, a passivated state is clearly reached in the first graph, with an evident transpassive response afterwards.

The curve shape obtained in the second graph seems to be better behaved, with anodic and cathodic responses that could indicate a predominant activation polarization response. Nevertheless, further tests pictured in the next plots, revealed that the linearity observed on each curve branch was difficult to obtain and noise or signal instability was the typical pattern.

4.7.4.2 Tafel Constants

Twenty different types of grout were tested in potentiodynamic polarization tests and their plots, in general, allowed easy identification of the cathodic Tafel-like behavior. Nearly all of the cathodic curves developed a straight segment for approximately one decade at a minimum, allowing the calculation of cathodic Tafel constants. On the other hand, due to differences in quality of the anodic responses, the plots for each grout can be divided into three different categories that are presented next.

Figure 46 shows the first category, which is comprised of the only three cases that allowed clear identification of anodic linear branches. Grout FA 56, however, was tested four times and only one curve is satisfactory, but shows a quite different overall pattern where no cathodic Tafel-like behavior is present.

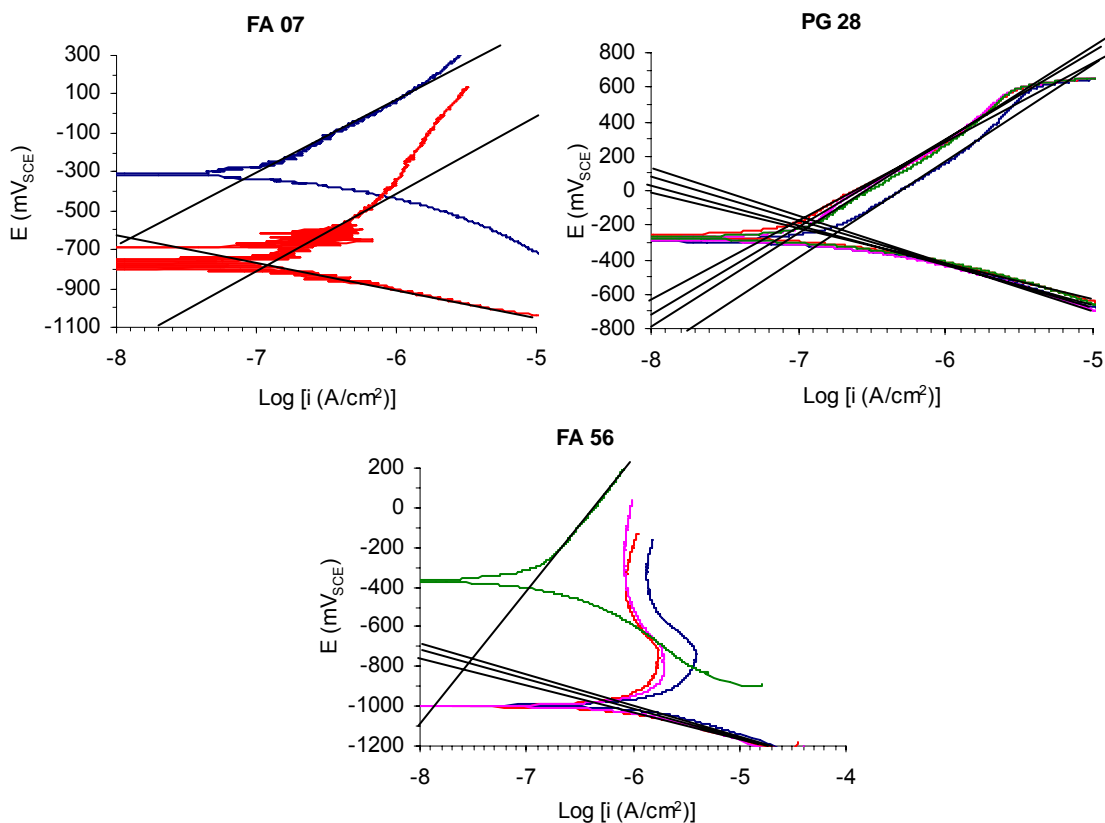


Figure 46 - Potentiodynamic plots showing satisfactory anodic and cathodic Tafel-like behaviors

The second category, shown in Figure 47, is composed of six cases that allowed limited identification of the anodic Tafel-like responses. Five cases generated limited responses probably because small ranges of potentials were used, while one case probably suffered with the grout's high porosity or with the high values of potentials applied, as speculated previously. The remaining eleven cases generated no anodic Tafel-like behavior and presented a varied pattern of anodic development length from grout to grout. Figure 48 and Figure 49 present these cases, which can be grouped in a third category of results. It should be noted from these figures that seven of the cases illustrated are results for silica fume grouts and that the problem regarding agglomeration of silica fume particles could have the same effect on the readings as high porosity would, perhaps confirming this problem.

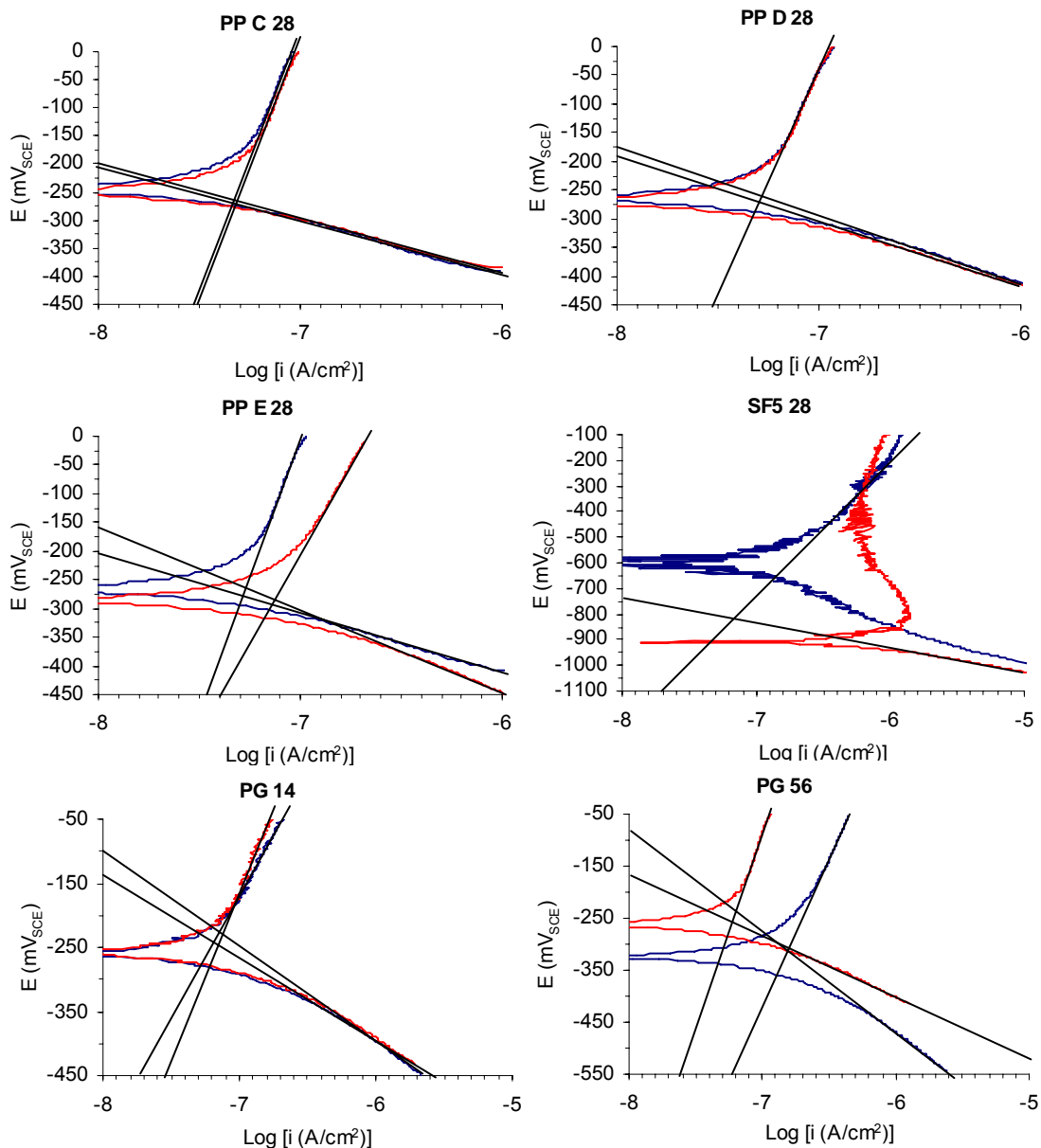


Figure 47 - Plots showing satisfactory cathodic and limited anodic Tafel-like behaviors

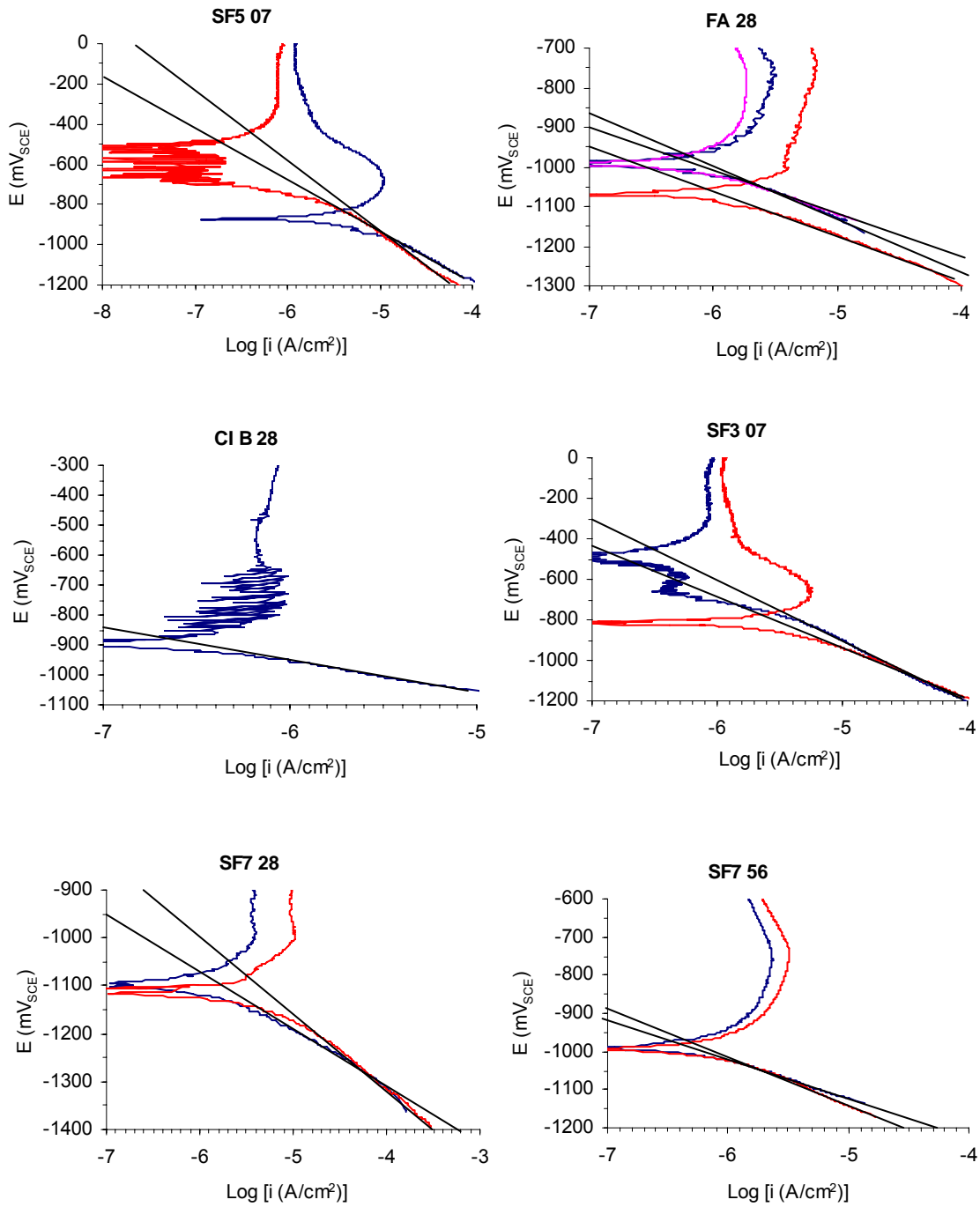


Figure 48 - Potentiodynamic plots showing only cathodic Tafel-like behaviors.

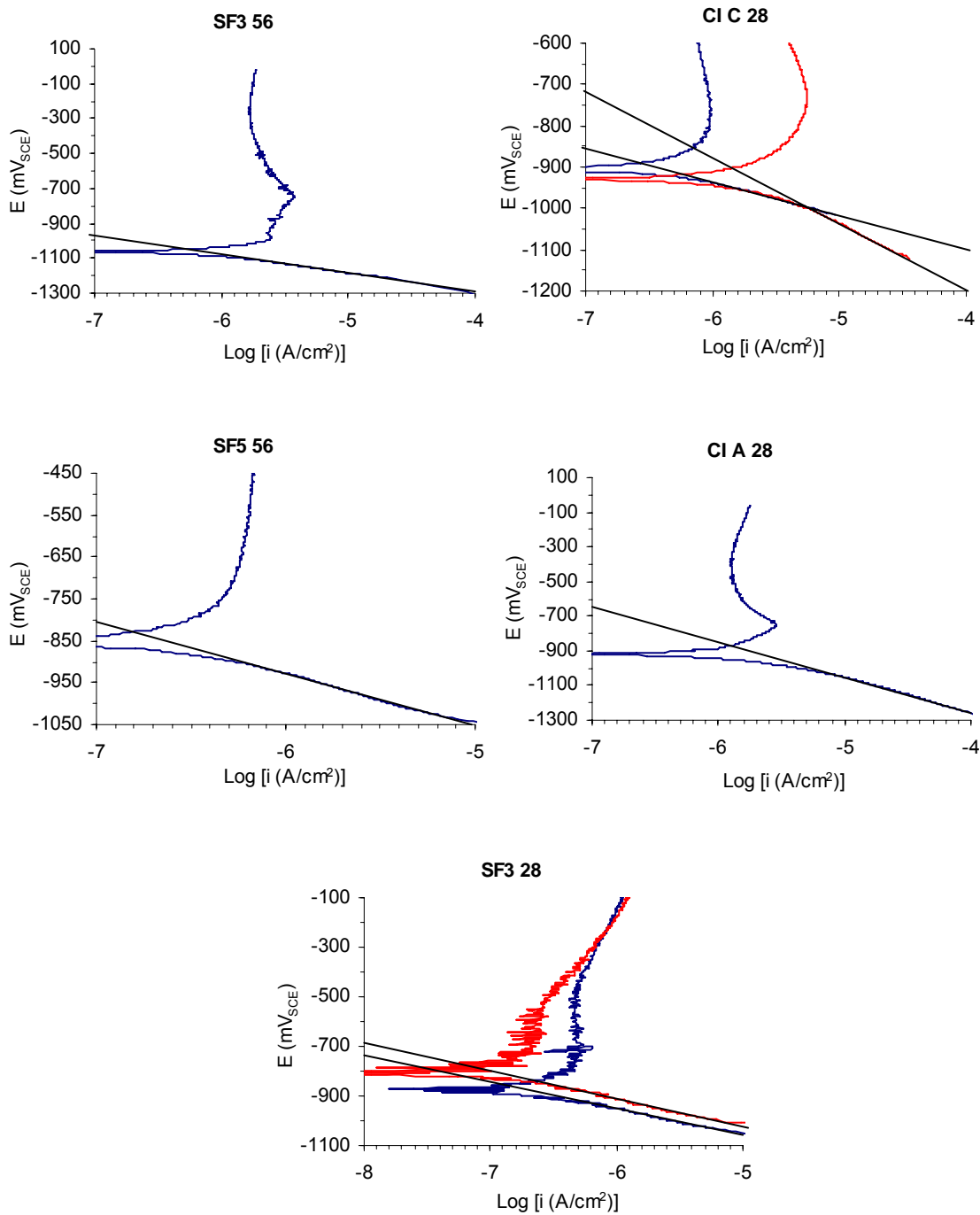


Figure 49 – Additional potentiodynamic scans showing only cathodic Tafel-like behaviors.

As can be seen, even when the anodic branches follow erratic paths, the cathodic Tafel-like curves can still be defined in most of the cases.

Figure 50 shows several different types of grout and their respective times-to-corrosion and cathodic Tafel constants. The significant increase in t_{corr} has little effect on β_c . The β_c values range from 91 to 287 mV, with an average of 157 ± 14 mV and no interaction is observed with the quality of the grouts tested regarding their corrosion protection. This result was expected, since the cathodic behavior, in this case, should reflect the responses for hydrogen or oxygen evolutions, being independent of grout characteristics.

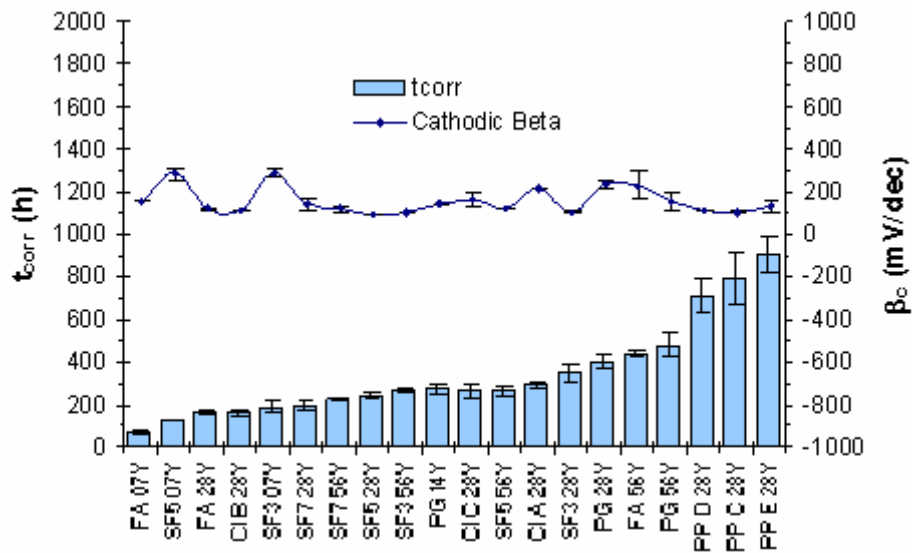


Figure 50 - Cathodic Tafel constant found for different types of grout (average: 157 ± 14 mV)

Figure 51 shows the trend obtained for anodic Tafel constants determined for grouts with increasing times-to-corrosion. β_a consistently increases with increasing times-to-corrosion. Upon plotting both variables, β_a and t_{corr} , as in Figure 52, their excellent agreement can be verified because of, firstly, the high adherence of the experimental points to the fitted curve and, secondly, because these points are fairly well distributed along the interval investigated.

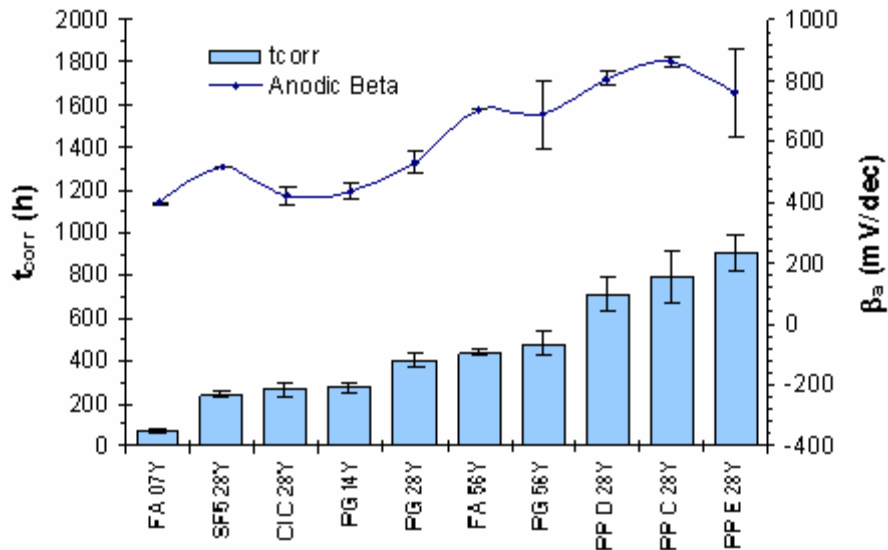


Figure 51 - Anodic Tafel constant found for different types of grout.

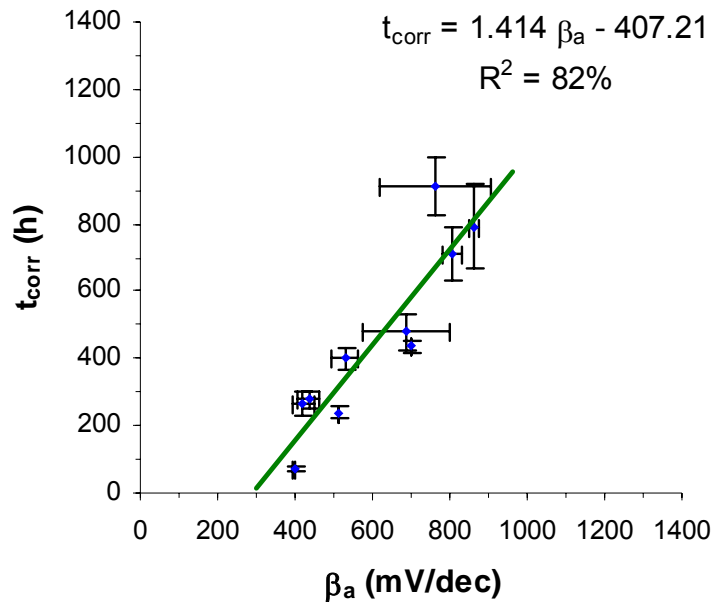


Figure 52 - Correlation between anodic Tafel constant and t_{corr}

The correlation equation given in the figure can be written, with no important precision loss, where t_{corr} is given in hours and β_a in mV, as:

$$t_{corr} = 1.4\beta_a - 400 \quad \text{Equation 4-4}$$

Although anodic Tafel constants provide a potential option for qualification of grouts regarding their corrosion protection degree, the use of β_a in this sense should be still considered with reservations. As commented before, approximately half of the potentiodynamic tests conducted provided appropriate corrosion behavior for determination of anodic slopes. In addition, only three out of twenty grouts produced an anodic Tafel-like length of at least one decade and one of these three grouts had to have four replicates tested to allow one satisfactory result. This result was still suspicious because its patterns varied significantly from the other three. Considering all of these points, it is remarkable that such a good correlation still could be found between β_a and t_{corr} . Additional data are necessary to corroborate the correlation found.

The results found for anodic Tafel constants, together with their cathodic counterparts allow the calculation of the constant B for the grouts tested according with Equation 4-5 (all variables given in mV per decade):

$$B = \frac{\beta_a \beta_c}{2.303(\beta_a + \beta_c)} \quad \text{Equation 4-5}$$

The results are presented in Figure 53. As can be seen, B seems neither to be influenced by the type of grout tested nor by the grout's performance in ACT tests.

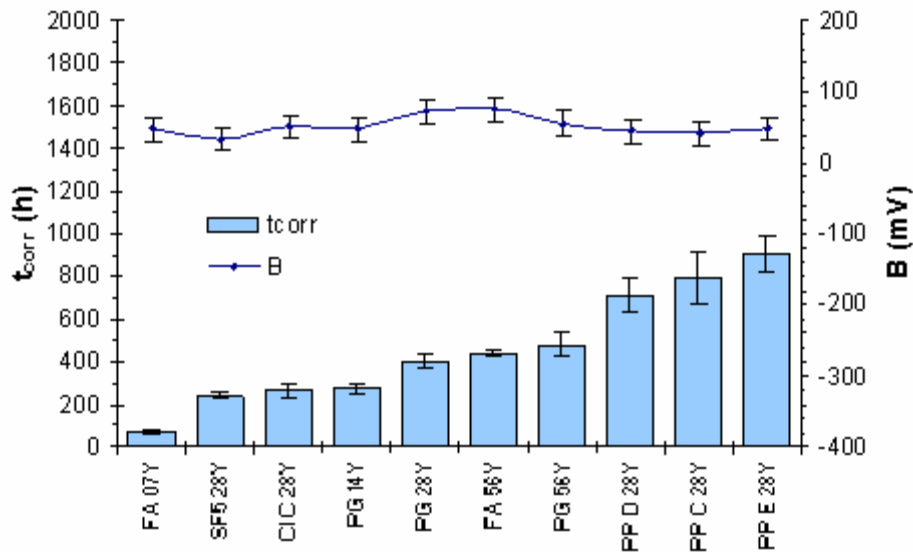


Figure 53 - Constant B found for nine types of grout (average: 52 ± 16 mV)

The minimum value observed for B is 34 mV and the maximum is 75 mV. These values are in the same order of magnitude than the values indicated in the literature for structural concrete: from 26 to 52 mV. The average found, 52 ± 16 mV, coincides with the upper limit, which is the value associated with passive conditions in structural concrete.

4.7.4.3 Corrosion Potential vs. Time-to-Corrosion

Corrosion potentials, E_{corr} , correspond to a steady-state condition between anodic and cathodic reactions in a similar way that equilibrium potentials, E_o , correspond to a redox balance

of a single substance, and similarly to the way that open circuit potentials, E_{oc} , characterize the mixed potential condition reached during a polarization corrosion test.

Although E_{corr} measurements do experience a considerable influence from the type of grout, they show little to no correlation with the t_{corr} from the ACT test. This is illustrated in Figure 54, where an erratic trend in E_{corr} measurements is observed while the time-to-corrosion significantly increases.

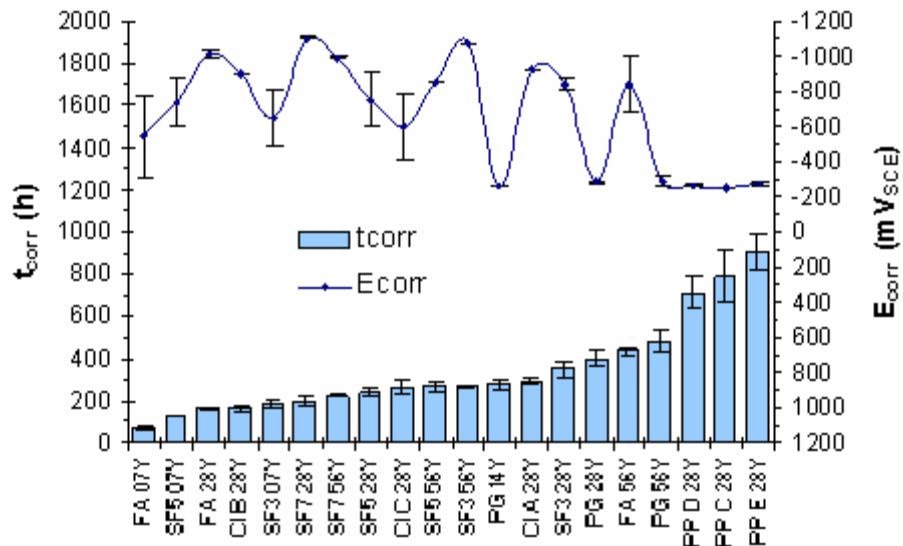


Figure 54 - Variation of corrosion potentials, E_{corr} , with times-to-corrosion.

The corrosion potentials, however, appear grouped in two distinct potential levels: one near -300 mV_{SCE} and another in the range from -600 to $-1,100$ mV_{SCE}. This can be more readily verified in Figure 55, where the two variables, E_{corr} and t_{corr} , are plotted in a Cartesian arrangement. Therefore, it is possible to infer that when E_{corr} is less negative (-271 ± 7 mV_{SCE}), nothing can be concluded in respect to the grout's corrosion protection, but when E_{corr} reaches highly negative values (-845 ± 46 mV_{SCE}), the grout's performance in an ACT is likely to be insufficient (t_{corr} equals to 232 ± 25 hours).

The fly ash grout results at 56 days reached a considerable value of E_{corr} (around -800 mV_{SCE}) but the grout performed, on average, better than the control grout during the ACT tests. Further testing in this area is needed to investigate these trends to arrive at more firm conclusions.

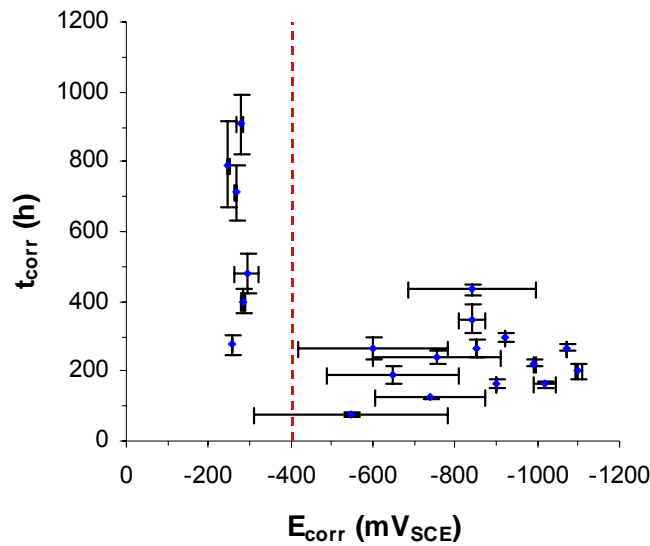


Figure 55 - High values of E_{corr} tend to correspond to low corrosion protection of grouts

4.7.4.4 Current Density vs. Time-to-Corrosion

The graph shown in Figure 56 illustrates the results of current density measurements for each grout tested.

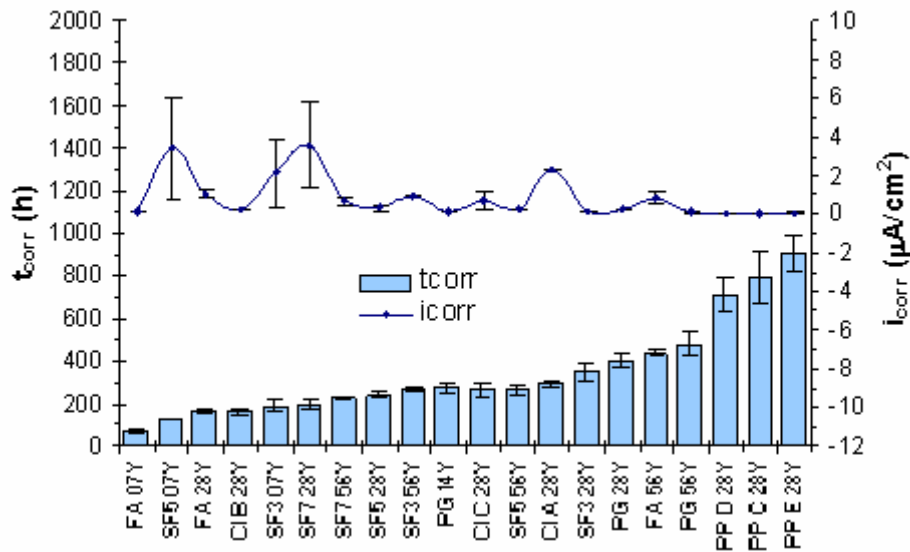


Figure 56 - Current density measurements for different types of grout

The current density (corrosion rate) measurements taken during the experimental program did not reflect any influence from the types of grout used in the tests. All mixes tested had low initial corrosion rates, varying from 0.03 to 5.2 $\mu\text{A}/\text{cm}^2$ (0.3 to 60 $\mu\text{m}/\text{yr}$). These values were obtained using the exposed surface area of the outer six wires of the strand. The averaged

corrosion rate, $0.87 \mu\text{A}/\text{cm}^2$ ($10 \mu\text{m}/\text{yr}$) would lead to the dissolution of 1 mm of steel by the end of 100 years, indicating a passivated state of the samples, independently of the grout type. This result was expected since the alkalinity of any of the mixes tested can be assumed as very high with little variation between them.

It is clear from the figure that the most variability occurs in the silica fume grouts. This may be due to the agglomeration of the silica fume.

4.7.5 Linear Polarization Resistance

The difficulties observed in potentiodynamic polarization measurements were not an issue during LPR readings. In fact, each LPR test runs faster and with considerably higher repeatability, when compared to other potentiodynamic scans. This is probably a consequence of the much lower range of potentials necessary to obtain the polarization resistances. Such range of potentials, which is on the order of 40 mV or, in other words, 10 to 20 times lower than the ranges required for regular potentiodynamic scans, would not condition the working electrode, preventing corrosion products or oxide layers to form between the strand surface and the encasing grout. Hence, no interaction of these products and layers in the grout's pores would occur, reducing any signal noise, distortion, and instability of the readings.

During the experimental program, however, some of the grouts were not tested in LPR tests and had to have their polarization resistance calculated from regular potentiodynamic scans. Figure 57 shows the variation of the polarization resistance, R_p , for each grout tested, showing also their degree of corrosion protection.

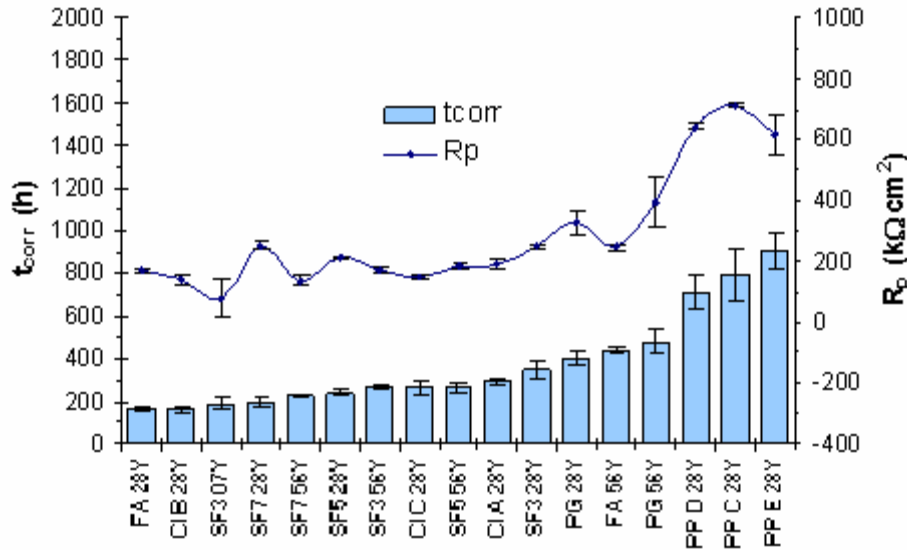


Figure 57 - Variation of the polarization resistance, R_p , for different types of grout

As shown in the figure, more variability is present on the experimental points for grouts SF3 7Y, PG 28Y, PG 56Y, and PP E 28Y. The polarization resistances for these tests, together with the values found for grouts PP C 28Y and PP D 28Y, were calculated with data collected from regular potentiodynamic scans, not LPR tests *per se*. These grouts are highlighted in Table 7, which presents again the list of grouts used in the previous graph and identifies those tests

whose R_p values were calculated from regular potentiodynamic data with much higher potential ranges, since this type of tests employ considerably higher values of potentials in order to define Tafel-like regions

In these cases, the polarization resistances were obtained through plotting of the potentiodynamic polarization data in a Cartesian or rectangular coordinate system, instead of a semi-log one. This procedure allowed the calculation of the desired polarization resistances, but probably led to the higher values of standard error observed.

Nevertheless, as can be seen from the data presented, R_p is a variable that is intensely affected by the quality of grouts' corrosion protection, reaching resistances that can be as high as $711 \text{ k}\Omega\text{cm}^2$ for extended values of times-to-corrosion or as low as $79 \text{ k}\Omega\text{cm}^2$ when the times-to-corrosion are deficient.

Table 7 - R_p and t_{corr} values obtained from LPR and regular potentiodynamic scans (highlighted)

Grout	R_p , ($\text{k}\Omega\text{cm}^2$)	t_{corr} , (h)	ΔE (mV)
FA 28Y	169 ± 6	162 ± 9	40
CI B 28Y	138 ± 21	163 ± 14	40
SF3 07Y*	79 ± 62	187 ± 25	2,100
SF7 28Y	251 ± 10	200 ± 20	40
SF7 56Y	136 ± 20	223 ± 8	40
SF5 28Y	211 ± 5	240 ± 17	40
SF3 56Y	172 ± 9	268 ± 8	40
CI C 28Y	148 ± 6	265 ± 34	40
SF5 56Y	183 ± 6	267 ± 25	40
CI A 28Y	193 ± 15	295 ± 13	40
SF3 28Y	249 ± 8	349 ± 40	40
PG 28Y*	325 ± 43	401 ± 33	500, 1600, 1800
FA 56Y	246 ± 13	435 ± 15	40
PG 56Y*	397 ± 82	479 ± 55	500
PP D 28Y*	641 ± 11	712 ± 78	500
PP C 28Y*	711 ± 9	793 ± 124	500
PP E 28Y*	618 ± 62	909 ± 85	500

* R_p values calculated from potentiodynamic scans

Therefore, in an attempt to find a correlation between t_{corr} and R_p , the plots pictured in Figure 58 are presented. The first one, (a), presents only results found in LPR tests, resulting in a weak correlation between the variables. Probably the main problem is the fact that the data are concentrated in a small range of times-to-corrosion, varying from 150 to 450 hours. However, in the second plot, (b), with the worst point removed (SF7 28), R^2 significantly increases from 29 to 62%, showing that the data were more consistent. Hence, in order to make more evident the correlation between the variables, the data for grouts SF3 56, SF5 28, and SF5 56 are removed in the third plot, (c), because they give, approximately, the same result that CI C 28 gives (times-to-corrosion of 240, 268, 267, and 265 hours, respectively). In addition, FA 28 (t_{corr} of 162 h) is

also removed from the plot, since CI B 28 (t_{corr} of 163 h) also gives, approximately, the same result. The correlation is even increased in the fourth plot, (d), where the remaining data obtained from grouts with mineral admixtures is removed (SF7 56 and SF3 28). It was expected that the data from these types of grout would be more difficult to fit in the correlations, mainly when the range of times-to-corrosion used is narrow, because, among all the types tested, they were the ones that shown more variability.

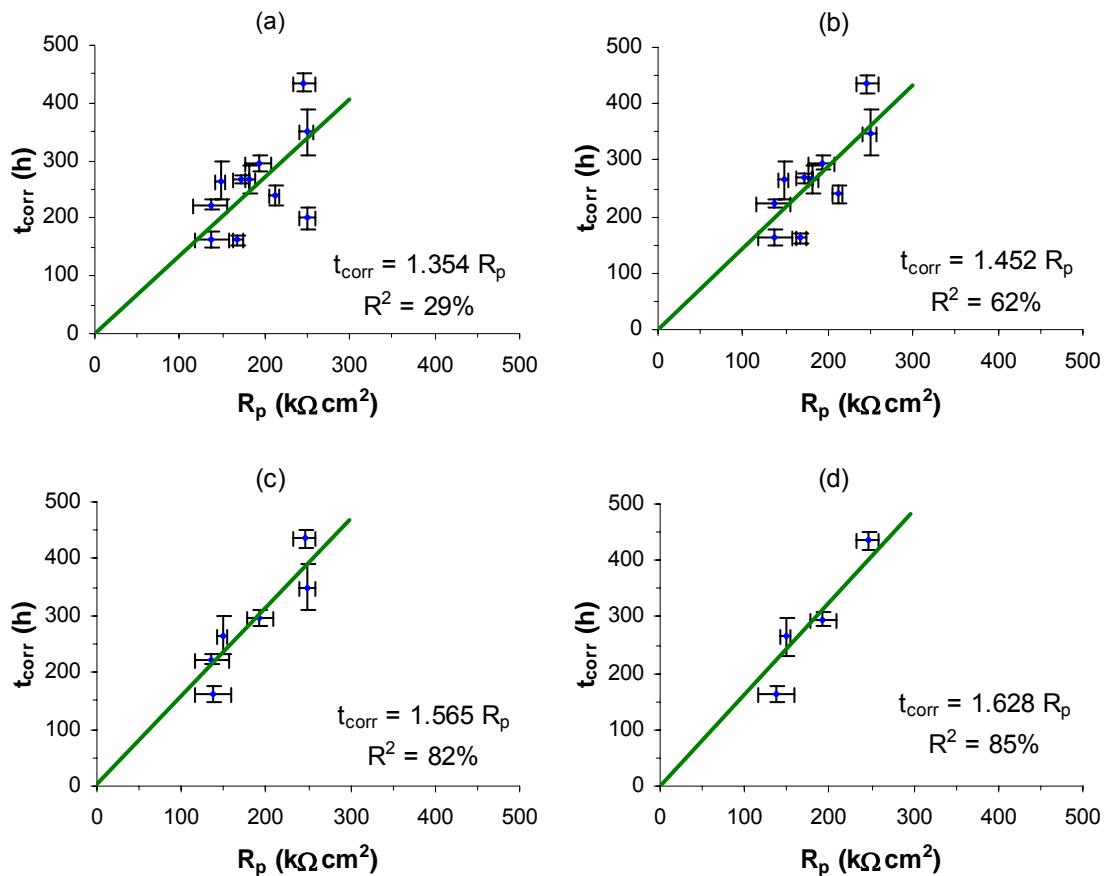


Figure 58 - Correlations between t_{corr} and R_p : (a) only data obtained from LPR tests are plotted; (b) the point SF7 28 is removed, significantly increasing R^2 ; (c) the points SF3 56, SF5 28, and SF5 56 are removed in order to obtain a distribution of fairly equidistant t_{corr} points; (d) only the grouts with no mineral admixtures are plotted

Even with the problems mentioned, regarding more variability of some types of grout (on t_{corr}) or even the fact that important data were found with inappropriate procedures (R_p values related to high values of t_{corr} found from regular potentiodynamic scans instead of LPR tests), a satisfactory correlation can still be found when all the information available is used.

Thus, upon plotting all of the values for polarization resistance against their respective ACT results, the linear correlation pictured in Figure 59 is found.

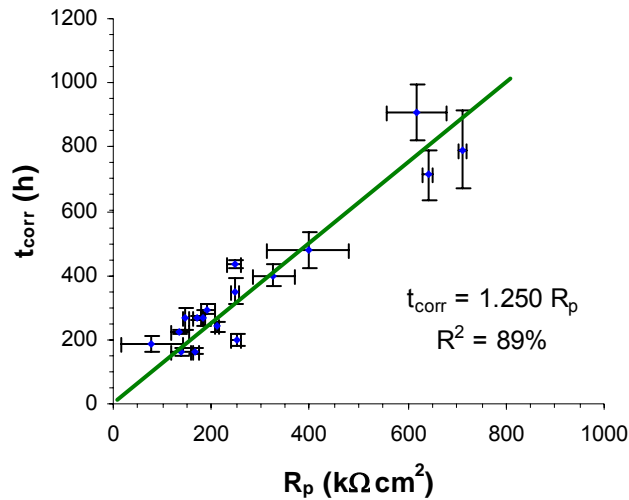


Figure 59 - Correlation between R_p and t_{corr}

The correlation between the two variables appears adequate, with values characterizing grouts of low and average corrosion protection appropriately adhering to the fit calculated. However, a small gap can be noticed between two apparent groups of values. In addition, few points representing grouts with high corrosion protection are available and more variability is present on their t_{corr} values.

The equation of correlation is highlighted, in Equation 4-6, where R_p is given in $k\Omega cm^2$ and t_{corr} in hours.

$$t_{corr} = 1.25R_p \quad \text{Equation 4-6}$$

Considering the satisfactory correlation between the two variables, the simplicity of LPR measurements, and their high repeatability, the method could be appropriately used as a prescreen for the current ACT procedures for estimation of grout's corrosion protection. A relative comparison to a base grout would still be preferable to a set limit of R_p . However, additional testing should be done focusing on the LPR method to establish this limit. Once this is done, the LPR method may also be considered as a replacement for the ACT. At this time, a logical approach would be to use the LPR method as a prescreen for very high quality grouts so that lengthy ACT testing is not necessary. For instance, a minimum polarization resistance value of $700 k\Omega cm^2$ may be a reasonable (but restrictive) approval limit, since it is likely to be measured on grouts that would produce a t_{corr} of 875 hours in an ACT test conducted with IR compensation. This limit also coincides with the break between the prepackaged grouts with good ACT performance and the remainder of the grouts tested (refer to Figure 59).

4.8 OBSERVATIONS AND DISCUSSION

This section complements the data presented in the previous section. It starts by discussing the results obtained for the prepackaged grout that did not corrode during the time frame of testing. Next, it shows the additional information obtained with the measurements

taken from the specimens after their passage from a passive state to a damaged condition. Then, considerations about the electric charge results obtained from the potentiostatic tests are discussed and, finally, it ends with a discussion of possible sources of error in the experimental program.

4.8.1 Parameters Measured for PP B 28Y

The prepackaged grout identified as PP B 28Y (moist cured for 28 days and tested in the potentiostatic test with compensation for voltage drops) could not be used in any of the correlation graphs shown in the previous sections because no t_{corr} value could be found for this grout. During its ACT test, as commented before, its specimens showed no indication of corrosion, even after more than 3,000 hours (more than 4 months) of continuous testing had elapsed and, for this reason, no time-to-corrosion could be determined.

Nevertheless, since this prepackaged grout was the best grout during the ACT tests, a question rises on how its properties would fit the trends set by the other grouts or whether PP B 28Y would corroborate the results. For instance, its value of porosity should be below 30% (28% was the lowest value found), its anodic Tafel constant should be around 2,558 mV (using Equation 4.2), and its polarization resistance should be around 2,560 $k\Omega cm^2$ (using Equation 4.6) or, at least, higher than 711 $k\Omega cm^2$ (the highest value found). These and other parameters are presented in Table 8.

Table 8 - Measured and expected parameters for grout PP B 28Y

Property	Measured	Expected
V (%)	28.6 ± 0.3	Less than 30
β_a (mV/decade)	$2,415 \pm 272$	2,558
R_p ($k\Omega cm^2$)	$1,011 \pm 226$	2,560 or higher than 711
E_{oc} (mV _{SCE})	-162 ± 11	From -334 to -144
E_{corr} (mV _{SCE})	-394 ± 39	More positive than -400
i_{corr} ($\mu A/cm^2$)	0.17 ± 0.07	From 0.07 to 0.86
β_c (mV/decade)	-462 ± 5	-157 ± 13
B (mV/decade)	168 ± 5	From 34 to 134

Indeed, regarding porosity, the prepackaged grout B presents a value right below the limit of 30% mentioned, with a volume of permeable voids of 28.6%. This porosity was reached with a water-bagged materials ratio of 0.27, according to the manufacturer's recommendations.

The grout was not tested in potentiodynamic tests prior to its ACT and, therefore, no anodic Tafel constants corresponding to a passive state can be determined. However, after completion of 3,200 hours of potentiostatic testing without signs of corrosion, potentiodynamic tests were then conducted, allowing the determination of an anodic Tafel constant for the grout of $2,383 \pm 293$ mV. Although this value was measured during an unknown intermediary condition of damage, it follows the trend found previously. In fact, the measured value is very close to the quantity determined with the correlation equation obtained when a t_{corr} of 3,200 hours is assumed (2,558 mV).

The value found for R_p of 1011 ± 226 $k\Omega cm^2$ is considerably high, but does not correspond to an estimated value using the correlation equation suggested previously, which

gives $2,560 \text{ k}\Omega\text{cm}^2$ for 3,200 hours. However, considering the conditions of the test conducted, the value measured can be considered as a reasonable one. In addition, it is higher than the highest value of polarization resistance found for the other grouts ($711 \pm 9 \text{ k}\Omega\text{cm}^2$). Another aspect to be considered is the likelihood of the linear correlation found not being valid for values of polarization resistance much higher than the interval studied and, in fact, an asymptotic behavior could be the correct trend. This aspect requires further investigation.

Figure 60 presents the curves from which the potentiodynamic parameters were calculated. The same data were used to calculate R_p .

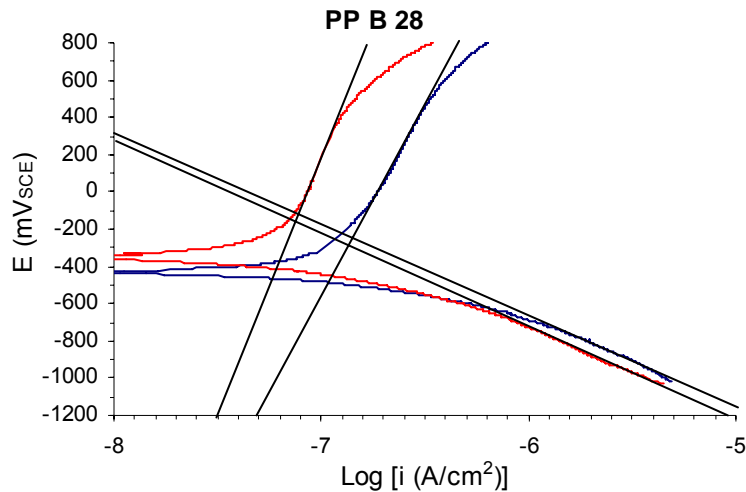


Figure 60 - Potentiodynamic curves obtained for prepackaged grout B after 3,200 hours of potentiostatic testing. The parameters calculated are: $E_{\text{corr}} = -394 \pm 39 \text{ mV}_{\text{SCE}}$; $i_{\text{corr}} = 0.17 \pm 0.07 \mu\text{A}/\text{cm}^2$; $\beta_a = 2,415 \pm 272 \text{ mV}$; and $\beta_c = -462 \pm 5 \text{ mV}$

Considering that the resulting E_{oc} from polarization corrosion tests was $-162 \pm 11 \text{ mV}_{\text{SCE}}$, the value is in the interval expected, but above the arithmetic mean obtained in those tests, which was $-235 \pm 9 \text{ mV}_{\text{SCE}}$. Regarding E_{corr} , it was commented before that grouts of high performances are more likely to have their corrosion potentials above the limit of $-400 \text{ mV}_{\text{SCE}}$, having an average result of $-271 \pm 7 \text{ mV}_{\text{SCE}}$. Thus, the value measured of -394 ± 39 is reasonable because it is above the mentioned limit, and since the specimens were ACT tested first, it is higher than the estimated average.

The value determined for i_{corr} , $0.17 \pm 0.07 \mu\text{A}/\text{cm}^2$, is between the estimated minimum and maximum limits for this variable in the tests conducted. The minimum limit is the average found for the four grouts with best performances, which reached significantly higher t_{corr} values. The maximum limit is the average of the remaining results (see section 4.6.3).

The value determined for $\beta_c = -462 \pm 5 \text{ mV}$ is significantly lower than the expected value of $-157 \pm 13 \text{ mV}$ and results in $B = 168 \pm 5 \text{ mV}$, which is outside the expected limits for this parameter (between 34 and 134 mV).

In addition to the fact that the potentiodynamic measurements were taken after many hours of ACT testing, high range of potentials were also used (a range of 1800 mV), which may

explain the minor discrepancies observed for this prepackaged grout. Overall, the results corroborate the trends observed.

4.8.2 Charge Level With and Without Compensation

Figure 61 presents calculated electric charges developed in ACT tests with and without compensation for voltage drops. As commented previously, all the charge values were calculated considering time values larger or equal to each specimen's individual t_{corr} and currents lower or equal to 10 mA. This allows a direct comparison between values.

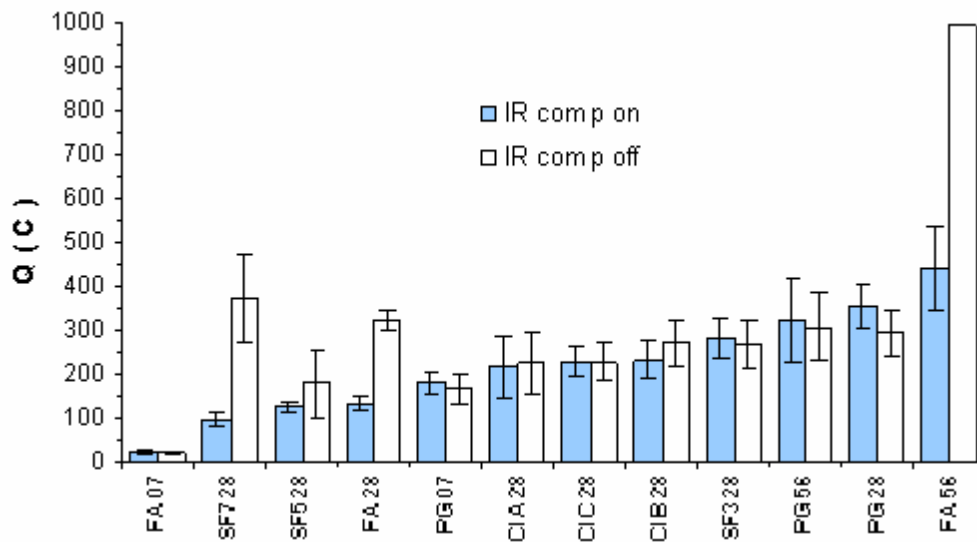


Figure 61 - Electric charges in compensated and uncompensated ACTs

As can be seen, the calculated charges tend to reach the same levels either whether the option for compensation of voltage drops is engaged or not. Only three cases shown in the figure are significantly higher during the tests conducted without compensation. Therefore, confirming the hypothesis outlined earlier regarding the electric charge as a parameter for grout characterization, no significant increase in the level of charge can be expected when the polarization voltage drops. The direct effect of this drop is clearly the increase in the grout's t_{corr} , but, once the corrosion is onset, the physical characteristics of the grout are the factors that will dictate the escalation of the measured current and, consequently, the level of the generated charge.

4.8.3 Error Sources

Although many measures were taken to reduce error in the ACT testing as described in previous sections, several factors are likely to have negatively influenced the responses obtained from each of the electrochemical tests. These factors are discussed in this section.

4.8.3.1 Number of Specimens

The number of specimens used in each of the experiments was determined based upon previous ACT work, the number of stations available, and a time limit of two years.

When the experiments were initiated, only eight stations were available (one setup). Five months later, a new setup was acquired and the number of stations doubled to sixteen. The third setup, however, was only available after the second year of experiments had been initiated, bringing the number of stations to a total of twenty-four. Since thirty-seven different ACTs had to be completed, several grouts were run in pairs in the same setup, reducing the number of specimens in these cases from eight to four. This reduction in the number of specimens happened for all grouts with silica fume, fly ash, and with two different corrosion inhibitors (A and B) in their mixes as detailed in Table 8, resulting in 22 tests out of 37 with a reduced number of specimens.

Table 9 - Number of specimens required and adopted in each test type

Test	Number of Specimens
	Adopted
Potentiostatic:	
All grout types together	8 and 4
Plain grout	8
Prepackaged	8
Corrosion inhibitor	4
Silica fume	4
Fly ash	4
Polarization Corrosion	8 and 4
Potentiodynamic	2
LPR	8 and 4
Grout characterization:	
Volume of permeable pores	4 and 2
Electric charge	8 and 4

Due to smaller standard deviations, when the grout types (plain, prepackaged, corrosion inhibitor, silica fume, and fly ash) are considered alone, the number of specimens adopted is adequate, even when only four replicates are considered. The only exception concerns silica fume grouts, whose results are typically low and, therefore, close to each other. The number of specimens adopted for the polarization corrosion, potentiodynamic, LPR, and characterization tests can be also considered adequate.

4.8.3.2 Counter Electrode Configuration

The first four grout tests, namely, PP A 28Y, PP B 28Y, PG 28Y, and PG 07Y, were conducted with the use of short counter electrodes measuring only 8.5 cm (3.3 in.) in length. These electrodes were later replaced by electrodes 17 cm (6.7 in.) long, which were able to completely span the testing region of ACT specimens. This is illustrated in Figure 62.

Figure 63 shows the incidence of the first spot of corrosion on the specimens when both lengths of counter electrodes were used. Since the tests for prepackaged grouts A and B were not verified for first spot occurrences, only results for 16 specimens were available for the shorter electrode length, while 206 specimens were accounted for the tests with the longer length of electrode.

As can be seen, when the electrode length was too short (result on the right), the distribution of occurrences was uneven, with 43.8% of the cases (18.8% plus 25%) being located on the west side of the specimens (nearest the counter electrode), while only 25% occurred on the off side.

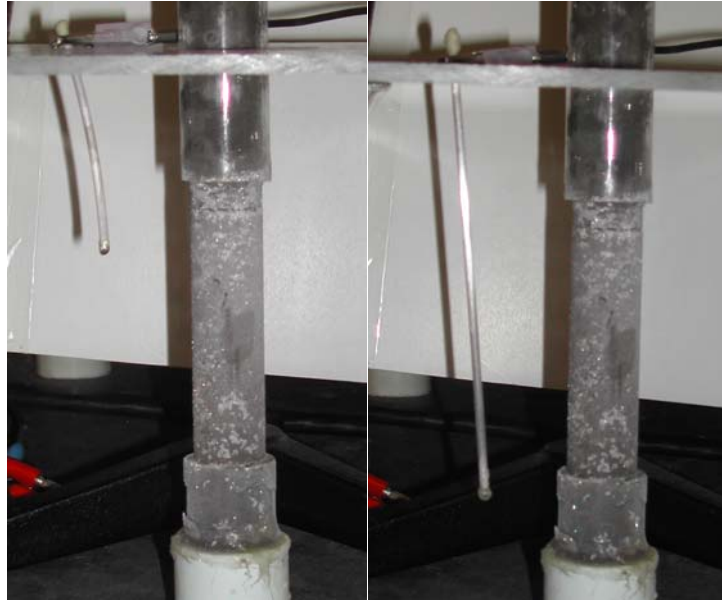


Figure 62 - The two counter electrode lengths used

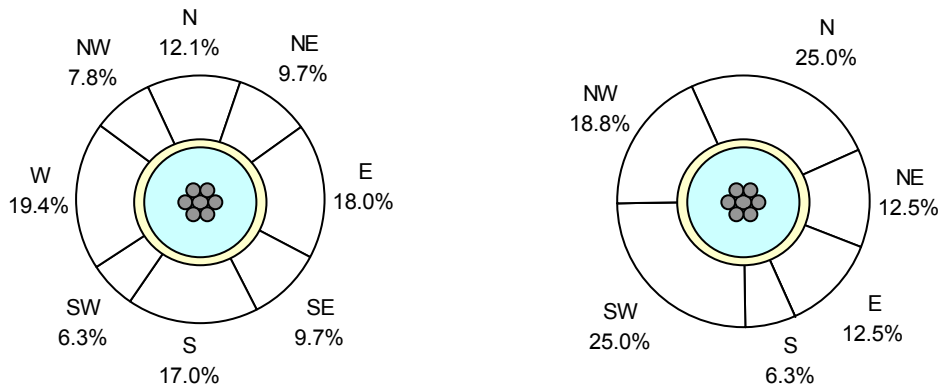


Figure 63 – Cross-sections of ACT specimens showing the incidence of occurrences of the first spot of corrosion when the counter electrode is 170 mm long (left figure) and 85 mm long (right figure). The counter electrode is on the west side.

On the other hand, when the counter electrode extended past the exposed grout region, the incidence of occurrences was fairly well distributed, with 33.5% of the first visible corrosion

products on the counter electrode side, while 37.4% occurred on the other side. In addition, 29.6% of the occurrences faced the north side of the specimens, while 33% occurred on the opposite face. These numbers show that, when an appropriate length of counter electrode is used, there is neither necessity for additional counter electrodes in the corrosion cells nor the need for counter electrodes with complicated shapes in order to better distribute the cells' electric current flow.

Figure 64 corroborates the previous result, showing that a short counter electrode (ending in the exposed grout region) may induce a concentration of the electric flow at a certain location of the ACT specimen.

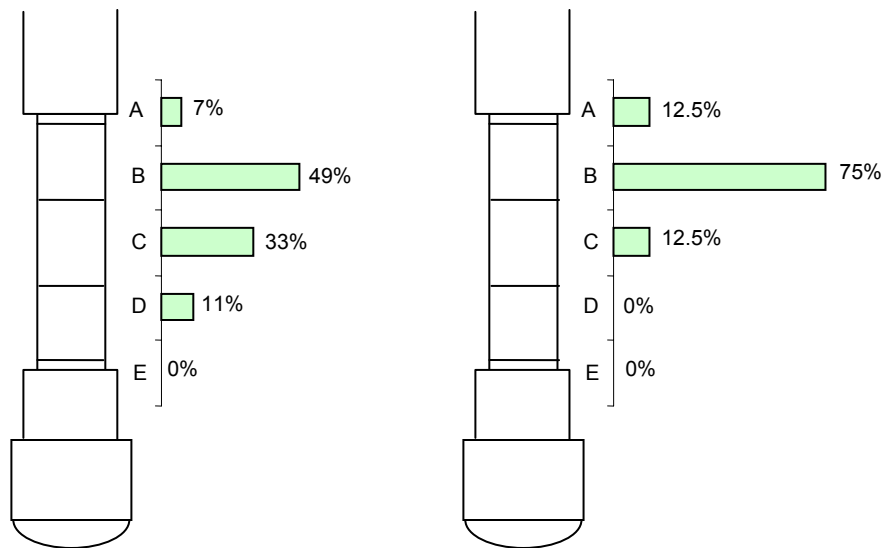


Figure 64 - Occurrence distribution of the first sign of corrosion when the counter electrode spans the testing region (left figure) and when it is too short (right figure)

The result found for the longer electrode indicates that the tendency toward a preferred location still exists, although to a lower degree. It is possible that an even longer counter electrode would reduce this problem to some degree. In all cases it is important to utilize a plastic spacer to centralize the strand to provide as consistent a grout cover as possible.

Another way that the counter electrodes used in this research could have influenced the ACT readings is through their own corrosion during the tests. Their core, which is made of copper, can corrode if no preventive measures are taken. If their extremities are not appropriately covered with a sealant, the copper core will be attacked by the salt solution. This phenomenon was observed in some of the tests conducted because only a layer of adhesive, which turned out later to be too porous, was used to caulk the counter electrode's extremities, and green corrosion products could be noticed after some time. This was remedied for the remainder of testing.

4.8.3.3 Working Electrode Configuration

The first design of an ACT specimen (by Lankard et al. 1993) had the prestressing strand in the testing region delimited by a coating layer of coal tar epoxy. All designs that followed, including the one used in this work, did not include this step in order to simplify the

manufacturing procedure. In addition to complicating the manufacture of specimens, the epoxy coating of the prestressing strand is not a foolproof measure because, due to its shape, with coiled wires, it is very difficult to completely cover the strand's external surface area, especially the portions between wires.

The second design (by Hamilton 1995) had the grout layer increased and introduced the use of clear tubing. The author also tried, without adopting it, the use of split sections of tubing for easy exposure of the test region. This procedure is then adopted in this work, as an attempt to reduce cracking and data spread. The next designs included dimensions augmented in order to expose more grout to the electrolyte since the applied potential in the ACTs was significantly lowered (from +600 mV_{SCE} to +200 mV_{SCE}). This brief history is illustrated in Figure 65.

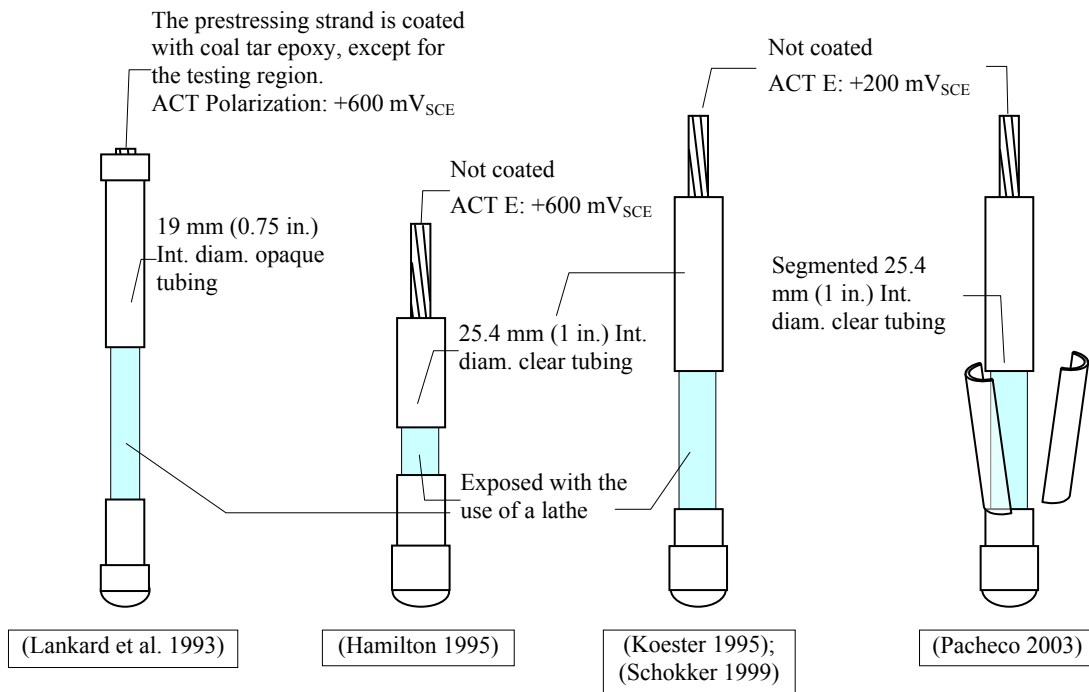


Figure 65 - Different ACT specimen designs adopted in different investigations (scale: 1:5)

The absence of a delimited prestressing strand surface may present inconsistencies in potentiodynamic testing since it does not allow a fixed amount of anodic area to form. Figure 66 illustrates this problem with a sequence of events that represents an electrolyte front reaching the center of a specimen and, eventually, expanding beyond its testing region.

Without a delimitation of the amount of steel surface area to be exposed to the testing conditions, significant differences in potentiodynamic and some difference in potentiostatic tests between samples may occur. In a potentiodynamic test the situation is more serious because, with unknown and inconsistent areas being exposed to electrolyte from specimen to specimen, comparative results are likely to be distorted.

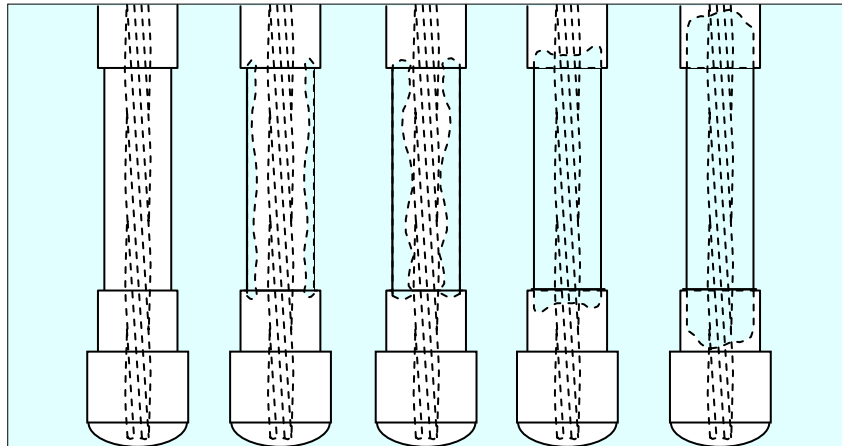


Figure 66 - Sequence showing an electrolyte front moving beyond a testing region

4.9 CONCLUSIONS AND RECOMMENDATIONS –PHASE I

In Phase I a series of ACT tests were conducted on grouts with various admixtures including mineral and corrosion inhibiting. Supplemental testing was conducting on these specimens to gain a better understanding of the corrosion behavior under the potentiostatic polarization test. The following are significant conclusions that can be drawn from Phase I:

- The results of volume of permeable voids test and electric charge passed (during ACT) were compared. The two characterization tests showed that the prepackaged grouts had lower porosity levels and higher charges passed when tested at 28 days (28 to 31%). Mixes containing silica fume, fly ash at early ages (7 and 28 days), and corrosion inhibitors B and C, had higher porosity values between 36 and 41%. Charge passed results were the lowest for the silica fume grouts (less than 150 C). Fly ash grout had a 3-fold increase in charge passed from the 28-day test to the 56 day test compared to a negligible increase in charge passed for the plain grout
- Correlation equations derived for voids and charge passed indicated that porosities higher than 33% will lead to (IR compensated) times-to-corrosion above 500 hours and electric charges as high as 2,500 C.
- Tests with four different types of grout (plain, with corrosion inhibitor, with silica fume, and with fly ash) at three different ages (7, 28, and 56 days) were conducted with and without IR compensation. On average, the increase in time-to-corrosion when IR compensation was not used was 11 to 46%, but reached values as high as 149%.
- Grouts containing corrosion inhibitors showed reduced times-to-corrosion when compared with the control mix. A dramatic difference, however, was observed between the compensated and uncompensated results found for the grout with corrosion inhibitor A (calcium nitrite), amounting to 109%. This significant difference may be indicative of inappropriate dosages for the product despite attempts to solve the dosage problem found in previous testing.

- Grouts with silica fume in their formulation showed reduced times-to-corrosion when compared with the control mix. This was likely due to the absence of aggregates in their mixes hindering the proper dispersion of the silica fume particles.

Potentiodynamic tests:

- Grouts with silica fume in their formulation showed reduced times-to-corrosion when compared with the control mix. This was likely due to the absence of aggregates in their mixes hindering the proper dispersion of the silica fume particles.
- For potentiodynamic testing it was found that an appropriate potential range was from –700 to +200 mV. Narrower ranges did not allow development of the anodic branches. Wider ranges resulted in signal distortion. It was also noted that the grout itself and its porosity may also increase signal noise and instability of the curves.
- Although the anodic constant is apparently influenced by t_{corr} , this did not affect the constant B. The minimum and maximum values observed for B were 34 mV and 75 mV, respectively, which agree with the literature. When corroded (damaged), the specimens were tested again and the constant B was, on average, 86 ± 6 mV. This increase observed was likely a result of the significant volume of corrosion products accumulated around the strands.
- Although a portion of the data was not obtained with a traditional LPR scan with low potentials, a strong correlation was found between the variables t_{corr} and R_p . The expression that correlates the two variables is highlighted, in Equation 4.6 where R_p is given in $k\Omega cm^2$ and t_{corr} in hours.

4.9.1 Revisions to the ACT Method

A standard method for evaluation of the degree of corrosion protection of post-tensioning grouts is presented in Appendix A in the form of an ASTM Standard test method. This standard method uses the main conclusions drawn from this research, listed above, in a way that post-tensioning grouts may be evaluated in a more appropriate and potentially faster method. The proposed standard also accommodates grouts with slower maturity rates (such as grouts containing fly ash). The following improvements were made:

- The current FDOT specifications require that a grout should be approved if its degree of corrosion protection, measured in an ACT test, is higher than the protection given by a 0.45 water-cementitious ratio neat grout. Furthermore, the time-to-corrosion must also be above 1,000 hours. The results found in this work indicate that the 1,000 hours should be an appropriate value only for ACT conducted without IR compensation. In addition, the result found in this work for the neat grout ($t_{corr} = 401$ h) is considerably lower than 1000 hours. This difference between the two guidelines creates confusion. Due to the many potential variances in testing as discussed previously, a fixed hour limit is inappropriate for qualifying a grout in the ACT. A qualifying grout such as the 0.45 water-cement ratio currently used or a lower 0.40 water-cement ratio can be used for more aggressive environments.
- Based on their simplicity and repeatability, the proposed standard allows the use of LPR as a method to prescreen the grout specimens. This provides a method by which the

grout can be qualified more quickly than waiting for the time-to-corrosion results. A polarization resistance value of $700 \text{ k}\Omega\text{-cm}^2$ is suggested until further LPR and ACT direct correlations are done. While a large number of grouts were tested in this program, the R_p values were not all found from the LPR method. While a set limit would not be recommended as single pass-fail criterion, in this case it provides a restrictive first level of testing so that the ACT can be avoided for some grouts. Grouts that do not meet this criterion, but then pass the ACT should not be penalized. The LPR method also is useful during new mix grout development as a quick evaluation technique.

4.9.2 Recommendations for Phase II

Based on the findings in Phase I, Phase II work focused on three key areas:

- Confirm the problem observed in silica fume grouts regarding formation of agglomerations that cause very low time-to-corrosion values.
- Investigate whether the current ACT control mixture (plain 0.45 water-cementitious ratio neat grout) and the proposed one for severe field conditions (plain 0.40 water-cementitious ratio neat grout) are appropriate.
- Confirm the relationship between potentiodynamic scans and t_{corr} by evaluating grouts in regions of the correlation curve where test data are sparse.

5 Phase II – Further ACT Testing

Phase II testing focused on answering remaining questions from Phase I and filling in gaps in data to confirm the relationships between the ACT t_{corr} value and potentiodynamic scans (both β_a and R_p values) developed in Phase I. Phase II objectives were as follows:

- Investigate the agglomeration problem in silica fume grouts and consider interground silica fume cement as a potential alternative.
- Investigate whether the current ACT control mixture (plain 0.45 water-cementitious ratio neat grout) and the proposed control mix for severe field conditions (plain 0.40 water-cementitious ratio neat grout) are appropriate.
- Confirm the relationship between potentiodynamic scans and t_{corr} by evaluating grouts whose results are in regions of the correlation curve where test data are limited. Also investigate the R_p versus t_{corr} relationship developed in Phase I for these grouts.
- Provide t_{corr} values for the three additional prepackaged grout formulations that became available after Phase I testing was complete

The grouts considered in Phase II are shown in Table 10 and grouped by type. All grouts were cured 28 days and IR compensation was used in the ACT testing with 8 specimens. Potentiodynamic scans were run on selected grouts (2 specimens per test) to acquire both β_a and R_p values to confirm the relationship of these variables to t_{corr} developed in Phase II. The prepackaged grouts tested were fabricated at UF and two were sent to PSU for testing where additional equipment was available. Grouts tested in this phase used strand from a different reel than that in Phase I because the Phase I strand supply was depleted prior to Phase II.

Table 10 – Phase II grouts

Grout Group	Specimen Designations	w/cm*	Casting Location	Testing Location
Silica Fume	SF8 28Y	0.45	PSU	PSU
Interground Silica Fume	SF8-IG 28Y	0.45	PSU	PSU
Plain	PG 28Y-0.40	0.40	PSU	PSU
	PG 28Y-0.45	0.45		
	PG 28Y-0.50	0.50		
	PG 28Y-0.60	0.60		
Prepackaged	PP F 28Y	Per manufacturer?	UF	PSU
	PP G 28Y	Per manufacturer?		UF
	PP H 28Y	Per manufacturer?		PSU

*water-cementitious materials ratio (water-bagged materials for prepackaged grouts)

5.1 SILICA FUME GROUTS

The potential for agglomeration in silica fume grouts was discussed in the previous section under Phase I testing. Microscopic evaluations showed evidence of this problem that is likely to lead to the short t_{corr} values seen in many silica fume grouts in past research. Figure 67 shows a comparison of a grout with silica fume added as a cement replacement and a grout with an interground silica fume cement from Lafarge at the same replacement percentage (8%). Intergrind indicates that the silica fume was added at the clinker stage in the cement production so that they are ground together. The agglomeration is clearly visible in the standard silica fume grout on the left, but not in the interground silica fume cement grout on the right. These two grouts were tested in the ACT and their t_{corr} values are given in Figure 73 in comparison to a standard water-cement grout at 0.45 w/c. Since a different reel of strand was used in Phase II, results are expected to differ for the 0.45 w/c plain grout tested in this phase. In this case, the plain grout t_{corr} was lowered considerably (from 401 hours to 244 hours), again pointing out the need for a relative comparison in the ACT rather than a set hour limit. The standard silica fume grout in this case performed slightly better than the control grout, but the interground silica fume grout gave a significantly higher t_{corr} value. When the agglomeration issue was alleviated (in this case by an interground silica fume cement), the t_{corr} value nearly doubled.

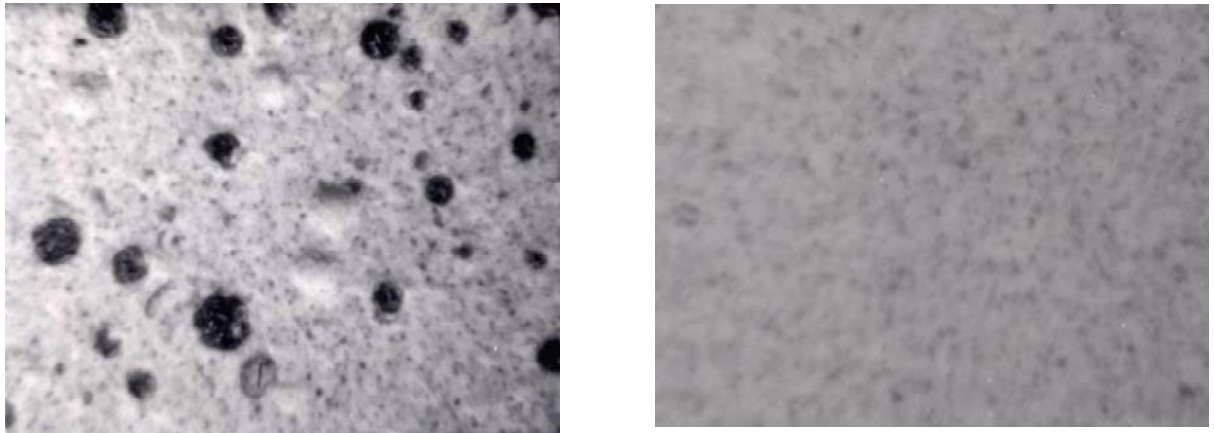


Figure 67 – Agglomeration in standard silica fume grout (left) versus more uniform dispersion in an interground silica fume grout (right); 10x magnification

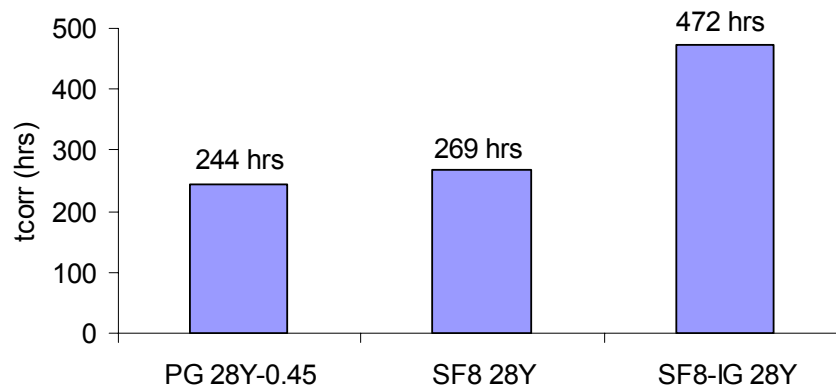


Figure 68 – Comparison of silica fume grouts and plain grout at 0.45 w/c

5.2 PLAIN GROUTS

5.2.1 Correlations to t_{corr}

Three additional plain grouts (0.40 w/c, 0.50 w/c, and 0.60 w/c) were tested in both the ACT and in potentiodynamic tests in Phase II to fill in data at the lower end of the t_{corr} correlations. A summary of critical values is given in Table 11. The data for each critical parameter follows the expected trend of higher values with lowered w/c. These data points are incorporated into the Phase I correlation plots for β_a versus t_{corr} in Figure 69. The Phase II values are distinguished by the square data points in the figure. Each point follows the trend from Phase I closely. A new trendline has been superimposed on the data that incorporates the Phase II points. The R^2 value increases 3% with the new data. The general equation (Equation 4.4) of the trendline remains approximately the same within the accuracy of the testing.

R_p versus t_{corr} values are plotted in Figure 70 with the additional Phase II data points. In this case, the 0.40 w/c grout follows the Phase I data very well, but the higher w/c grouts fall well away from the anticipated values. An adjusted trendline to incorporate these values lowers the R^2 value to 75% from 89%. It should be noted that the R_p values were estimated from potentiodynamic scans, so that error may be increased. In addition the error in the t_{corr} value can be significant for very poor grouts.

Table 11 – Phase II correlation data (plain grouts)

Grout	t_{corr} (hrs)	β_a (mV)	R_p ($k\Omega cm^2$)
PG 28Y-0.40	413±86	432	393
PG 28Y-0.50	115±8	372	333
PG 28Y-0.60	76±30	362	275

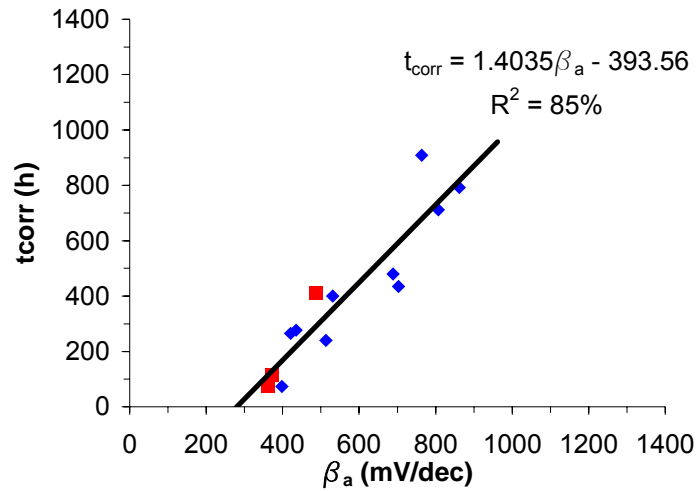


Figure 69 – Correlation of t_{corr} with β_a

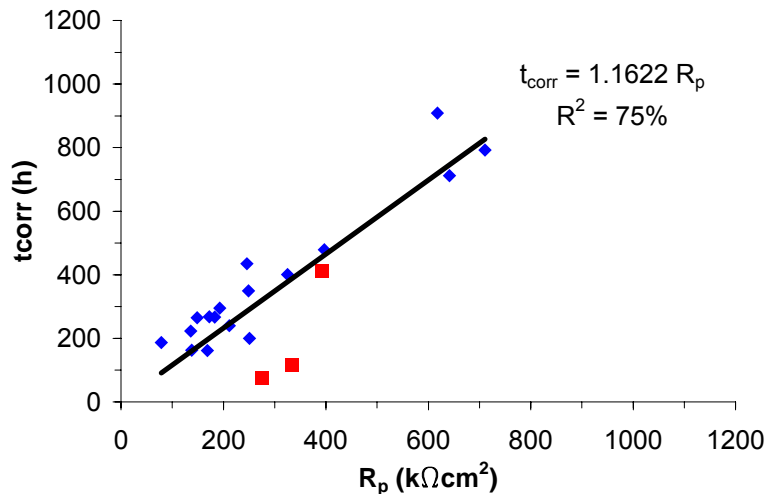


Figure 70 – Correlation of t_{corr} with R_p

5.2.2 Qualifying Grouts

Phase I recommendations indicate that the use of a qualifying grout is preferable to a set time limit due to the variations in strand and cement as well as the natural variation in results between labs. As discussed in Phase I recommendations, the use of a 0.40 w/c plain grout to set the time-to-corrosion limit may be preferable to a 0.45 w/c grout if additional corrosion protection is required. A change of strand in this testing resulted in a 39% reduction in the value of t_{corr} . For the Phase II testing, both a 0.45 w/c grout ($t_{\text{corr}} = 244$ hours) and 0.40 w/c grout ($t_{\text{corr}} = 413$ hours) were tested. The 0.40 w/c grout provided a significant reduction in the time-to-

corrosion indicating an improvement in corrosion protection. A 0.40 w/c plain grout mix has sufficient water that it can be cast without having to use superplasticizers.

5.3 PREPACKAGED GROUTS

Three additional prepackaged grouts were available for testing after Phase I was complete. These grouts were tested under Phase II in the ACT test to acquire a t_{corr} value. The prepackaged grout specimens tested in Phase II were fabricated at the University of Florida. Figure 71 summarizes the ACT results for these grouts. PP 28Y G had one specimen out of 8 that did not corrode at 3500 hours, so the specimen was stopped at that point. The t_{corr} value incorporates the 3500 hour time into the average. All three grouts performed significantly better than the control grout. Two surpassed 1000 hours, although the standard deviation was high in both cases.

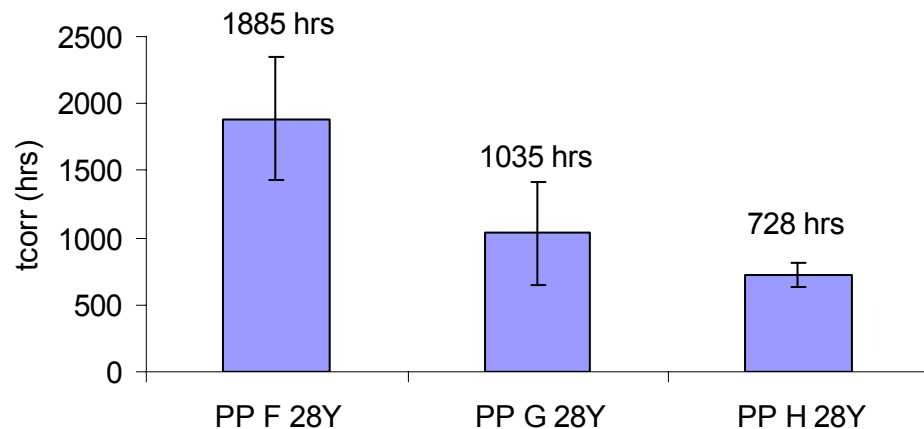


Figure 71 – Additional prepackaged grout results

5.4 PHASE II SUMMARY AND CONCLUSIONS

Phase II testing focused on areas of interest from Phase I. These included silica fume agglomeration, comparison of control grouts, and confirmation of the t_{corr} relationships developed in Phase I. The following conclusions can be drawn from this testing phase:

- Interground silica fume cements can be used to avoid agglomeration. These grouts performed well in ACT testing (almost doubling the t_{corr} value found with the standard silica fume grout).
- The additional data from Phase II testing fits well with the correlations between β_a versus t_{corr} and supports the relationship found in Phase I.
- R_p versus t_{corr} values for very poor grouts did not fit the trendline established in Phase I, while the 0.40 w/c grout followed the trendline very well.
- Increasing water-cement ratios provide reduced the times-to-corrosion as expected. A 0.40 w/c grout provides a better quality reference grout (as reflected in the reduced

time-to-corrosion) while still being workable enough to cast ACT specimens without the addition of chemical admixtures.

- The additional prepackaged grouts tested in this phase performed significantly better than the control grout.

5.5 PHASE II RECOMMENDATIONS

- If silica fume is used in grouts, care must be taken to avoid agglomeration. One method that was shown successful in this research is the use of an interground silica fume cement.
- The relationships in Equation 4-4 and Equation 4-6 provide a link between short-term electrochemical tests and the longer-term ACT test. The LPR method used to develop Equation 4-6 provides the quickest and most direct approach and is recommended for use as a tool for prequalifying grouts as detailed in Appendix A.

$$t_{corr} = 1.4\beta_a - 400 \quad \text{Equation 4-4}$$

$$t_{corr} = 1.25R_p \quad \text{Equation 4-6}$$

- For aggressive environments or where additional corrosion protection is needed, the qualifying grout for qualification testing in the ACT should be lowered from 0.45 w/c to 0.40 w/c. A set hour value should not be used due to variability between labs and with use of different materials.

6 Phase III – Grout Segregation Testing

Under actual field conditions a grout may be subjected to high gravity pressure heads when the tendon profile has significant changes in elevation such as found in stay cables, piers, or very deep flexural members. The existing benchtop tests for bleed resistance (Schupack and standard wick tests) lack the capability of replicating the combined effects of pressure head and strand filtering effects seen in an actual tendon. The test developed in this phase more closely simulates the actual conditions during grouting and provides information about the performance of the Schupack Pressure Test with respect to the newly developed test.

6.1 OBJECTIVES

The objective of this phase of testing was to develop a test for evaluation of bleed-resistance in grouts that combines both the pressure effects and strand-wicking effects. The test should simulate these effects in a way that represents the actual condition in a tendon as closely as possible.

This objective is met through the following tasks:

- Devise the apparatus for the proposed bleed test which simulates actual on-site conditions, including the pressure effect and wicking action of strands. The apparatus should be readily available, quick to set up, reusable and suitable for use under both field and laboratory conditions.
- Develop a testing procedure for the new pressure bleed test.
- Develop a relationship between pressures applied to the grout and the grout bleed for predicting expected bleed volume from a grout under a specified pressure. This relation is then used to make recommendations about the suitability of a grout for a particular application.
- Develop a guideline for allowable bleed limits under various pressures similar to those for the Schupack pressure test in the Post –Tensioning Institute’s (PTI) Grouting Specification (2003).

6.2 REVIEW OF EXISTING BLEED TESTS

ASTM C940: This test involves placing freshly mixed grout in a graduated cylinder and taking readings of the accumulated bleed every 15 minutes for the first 60 minutes and then at hourly intervals until two successive readings show no further bleeding. The bleed volume is measured to the nearest 0.01 fl. oz and is expressed as a ratio of the initial volume of grout. This test does not include wicking effects from the strand and only incorporates a very small vertical rise. This test is not sufficient for evaluating post-tensioning grouts and is not recommended in the PTI specifications (2003).

Modified ASTM C940 (standard wick test): A modification of the ASTM C940 test (2002) has been outlined in the PTI specifications (2003). For this modified approach a single strand is introduced into the graduated cylinder containing grout. The introduction of the strand simulates the wicking action (filtering effects), but does not induce a significant pressure head on the grout. The Florida DOT specifications and PTI specifications require 0% bleed in the Wick Test. The test is adequate for applications with very little pressure head, but is inadequate for the majority of bridge grouting applications.

Schupack Pressure Filter Test: The Schupack pressure filter test is used to directly measure the bleed resistance under pressure. It has been successfully demonstrated that the Schupack pressure filter test replicates the pressure head and some of the filtering effects in the post-tensioned tendons (Schokker et al. 2002). The results of the pressure filter test compared favorably with early experience in grouting of a number of high vertical strand tendons in major structures. This test may be used in both laboratory and field conditions.

The test apparatus for the Schupack test consists of a commercially available and standardized stainless filtration funnel (a Gelman filtration funnel produced by Fischer-Scientific), stand, pressure supply with gauge and valve and a bleed water collection container (Figure 72). The Gelman filtration funnel consists of a steel cylinder with a top and bottom end cap. The top cap connects to the pressure supply while the bottom cap contains a stainless steel screen and filter paper as well as the bleed exit tube. The filter at the bottom of the Gelman funnel is used to simulate the filtering effects of the strands. Freshly mixed grout is placed into

the filtration funnel. The funnel is held in an upright position and its top end is connected to a pressure supply (commonly compressed air or Nitrogen). The grout is allowed to rest in the funnel for 10 minutes before pressure is applied from the top end of the funnel. The pressure is increased to the desired level and the grout is subjected to this pressure for 5 minutes. The resulting bleed is measured to the nearest 0.01 fl. oz. at the end of the hold time. The bleed is expressed as percentage of sample volume. The PTI specification (2003) gives required maximum bleed values for various applications.

The Schupack pressure test accounts for high pressures exerted by a high vertical column of grout. The bleed behavior from the test also includes the filtering action by using the fiber glass filter. Since the filter paper provides only a simulation of the anticipated filtering effect of the strands, it is desirable to compare the Schupack test to a test with actual strand for filtration.

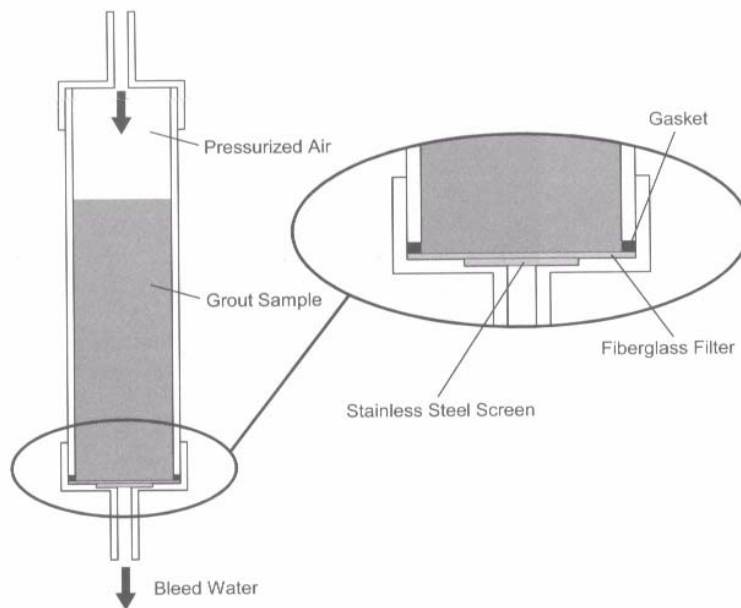


Figure 72 – Schupack pressure filter test schematic (PTI, 2003)

6.3 WICK PRESSURE TEST DEVELOPMENT

Ideally, to simulate field conditions, the test system should have the grout placed under high pressure in combination with the filtering provided by a strand bundle. The Schupack pressure test incorporates the higher pressures, but filtering is provided by the filter paper. Conversely, the modified ASTM C940 (standard wick test) incorporates strand, but the grout is not pressurized. The Wick Pressure Test (WPT) developed in this phase of the research combines the key attributes of both tests into a compact yet effective pressure test system that includes a strand for wicking. Figure 73 shows the schematic and photo of the apparatus. The apparatus is composed of a pressure chamber constructed of clear PVC that holds the grout during testing. At the bottom of the chamber is a single strand that passes through a cleanout plug drilled to the appropriate diameter and fitted to the strand. The test is conducted by placing grout in the chamber and pressurizing the grout from above. Bleed from the strand is then monitored during the pressurization period. A detailed description of the components follow.

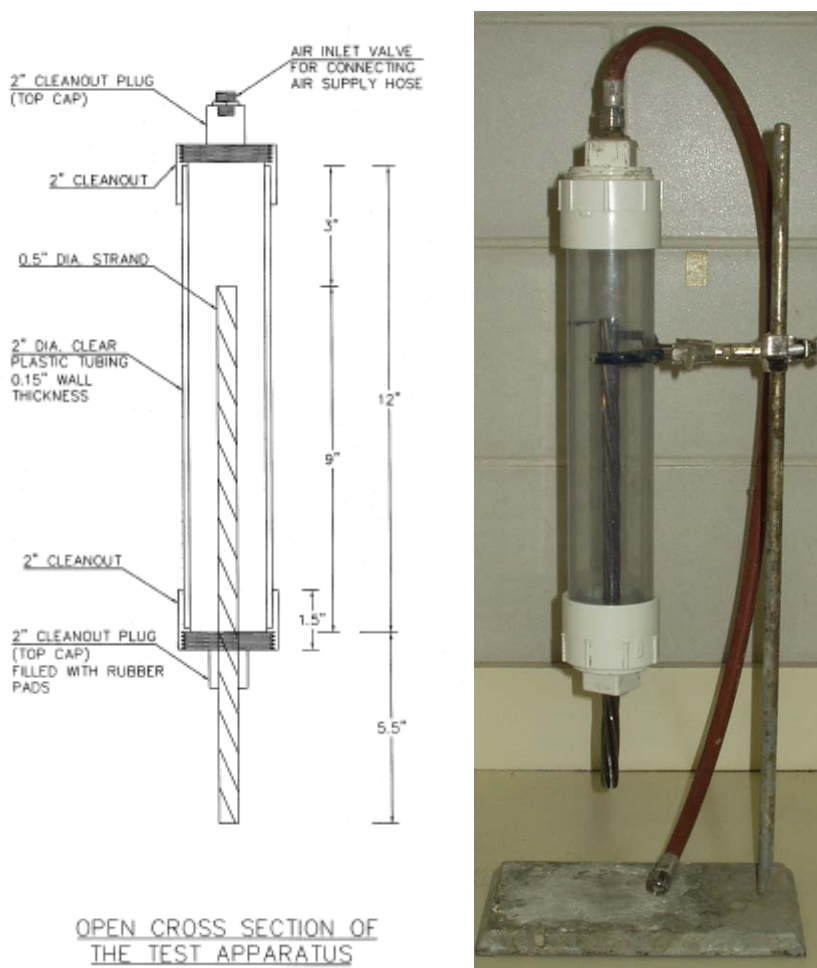


Figure 73 – Assembled Wick Pressure Test apparatus schematic and photograph.

Several alternatives were explored before arriving at the final design. It was desirable to replace the Gelman filtration funnel with a representative clear post-tensioning duct so that the bleed, wicking behavior, and grout level could be seen by the user. A 2-in. internal diameter cylinder was selected to ease access to the interior for cleaning and strand installation. Initial prototypes included multiple strand bundles, but forming an adequate seal around the bundle to prevent the pressurized grout from escaping was not possible. Consistent wicking effects were also difficult with a multi-strand arrangement. A grout column height of 12 in. was used similar to that specified by the standard Wick Test in the PTI specifications (2003)

The selected plastic tube had a safe operating pressure in the range of 150-200 psi. Removable top and bottom caps using 2-in. diameter PVC cleanouts facilitated easy access for cleaning and installation of the strand.

To fix the 14.5-in. long strand in place and provide the necessary seal around its perimeter, a ½-in. diameter hole was drilled through the clean-out cap (see Figure 74). The strand was placed so that a 9-in. length projected into the cylinder. This configuration ensured that water tightness was maintained and that bleed water would only exit the cylinder through the strand interstices. To ensure the water tightness a ½-in. thick rubber membrane was inserted in the cleanout plug with a similar drill hole that fits tight against the strand circumference. It was

found during initial experimentation that the bottom anchor provided sufficient grip to the strand to prevent any downward movement under the action of pressure applied from the top and also was able to keep the strand centralized in the grout column without any additional spacers along the length of the strand.



Figure 74 – Wick pressure test base cap and strand positioning.

Air was supplied to the cylinder through an air fitting installed in the top cleanout plug. To make the cap air-tight a high strength epoxy was applied to ensure bond between the metal valve and PVC end cap. The arrangement was checked for air leakage.

The testing cylinder was clamped to a stand to hold it in a vertically upright position during testing. The stand selected had to be large enough to accommodate the total vertical clearance for the test cylinder, the strands projecting below it and the bleed water collecting container.

An air pressure supply with an in-line regulator and shutoff valve and an air pressure gage were attached to the testing cylinder. The air pressure gage had a capacity of reading pressures up to 200 psi with graduations at 5 psi intervals.

6.4 GENERAL TEST PROCEDURES

The development of the test procedure involved making trial runs with the apparatus and refining the test procedure and test setup until consistent results were obtained. This was done using a plain portland cement and water grout with a constant applied pressure.

It was also necessary to make trial runs to determine if there is a change in the wicking effect under repeated use of a test strand. It was evident within the first two data sets collected that using the same strand repeatedly does affect the bleed. Maximum bleed was observed for the first run with clean strand with bleed water volume decreasing by an average 2-3% for the second use of the strand even after thorough cleaning. Despite cleaning between uses, some cement particles become trapped in the interstices, changing the wicking behavior for subsequent uses. It is therefore recommended that a clean, unused strand be used for each test.

It was also observed that with initial application of pressure, no bleed was expelled. However, grout was expelled out of the strand. After an average interval of 30-50 seconds from the time of application of pressure, bleed was expelled. Thus, the initial discharge of grout is to be collected in a separate container and its volume to be neglected while reporting final bleed volume. Ideally, only bleed water will be present, but the initial grout flow is unavoidable. This effect can be seen in the field at the strand tails at anchorages when ends are left uncapped. There was a clear visual break between the initial grout efflux and the start of filtration during testing.

Several trial pressure tests also resulted in a blowout similar to that seen in the Schupack test for poor grouts. In the case of the WPT, all of the bleed water has been expelled and air begins to escape from the cylinder through the strand interstices. This escape of air is coupled with loss of pressure in the cylinder. The test was terminated at this point and it is considered a failed test. A blowout usually occurs after a large quantity of bleed and grout is expelled and indicates poor bleed resistance from the tested grout.

The Schupack pressure test (PTI 2003) specifies that once the test cylinder is filled with grout it should be conditioned by holding under no external pressure for 10 minutes under air supply at 0 psi and then the desired test pressure be applied on it for the next five minutes. It was found through repeatedly conducting the Schupack test during the course of this research project that during the conditioning time of 10 minutes, poor grouts tend to settle at the bottom of the Gelman filter with water rising to the top. This can form a semi-solid layer at the bottom of the filter. The bleed obtained from testing grout with this layer may not be indicative of the true bleed as the semi-set layer does not allow the bleed from the grout column above it to drain out from the filter at the bottom. This is one aspect of the Schupack test that requires further examination, but indicates that the 10 minute rest period should be eliminated from the standard Schupack test. Thus, for the proposed test the static conditioning time has been eliminated and pressure is applied immediately after connecting the air supply to the test cylinder. For consistency, the pressure is increased from 0 psi to the desired pressure at the rate of 5 psi per second. For both the Schupack and WPT, then grout was held under pressure for 10 minutes.

The initial test trials resulted in the following test procedures:

- Fix a ½-in. dia. unused strand in the bottom cleanout plug with rubber seals.
- Insert the plug into the bottom cleanout.
- Mix the grout as recommended by the manufacturer or applicable specifications.
- Fill the test cylinder to capacity (approximately 20 fl. oz.) of freshly mixed grout. (The grout should be tested within 15 minutes of mixing)
- Screw the top cap on the cylinder hand tight while keeping the cylinder in an upright position.
- Place the cylinder in the stand.
- Connect to air supply at 0 psi.
- Increase the pressure to the desired level gradually at the rate of 5 psi per second.
- Hold at the specified pressure time for 10 minutes and collect the bleed in the bleed collection container.
- Discard the initial grout expelled from the strand.
- Measure the bleed to the nearest to 0.01 fl. oz. at the end of the 10 minute hold time.
- Note the blowout time if any.
- Calculate the bleed volume from the following equation:

$$\% \text{ bleed} = \frac{\text{bleed (fl.oz)}}{20 \text{ fl.oz}} 100 \qquad \text{Equation 6.1}$$

6.5 EXPERIMENTAL PROGRAM

The testing was carried out using plain cement grouts and thixotropic grouts (including pre-packaged grouts) at different water cement ratios to provide an array of bleed conditions. Pressures varying from 20 psi to 50 psi and with water cement ratios varying from 0.25 to 0.45 were used in testing. It was anticipated that the prepackaged grouts would likely show little or no bleed in the test, but varying water contents were used to compare the new method to existing data.

The first phase of testing was directed toward achieving the first objective of developing and refining the test set-up. This was achieved by testing plain cement grouts under various pressures with a water cement ratio of 0.30 until consistent results were obtained. After the apparatus was refined and produced consistent results, multiple water-cement ratios were evaluated for each grout type under varying pressures.

All the initial testing was carried out using plain cement grouts. Plain cement grouts were tested with water cement ratios of 0.25, 0.35 and 0.40 and were subjected to pressures levels ranging from 20 to 50 psi in increments of 10 psi. The results and their respective discussion are detailed in this section. The graphs of comparisons of the Wick Pressure Test (WPT) and the Schupack Test (ST) are presented for each data array. These charts include comparisons of percent bleeds from both tests, and correlations of the two data sets.

6.6 RESULTS

6.6.1 Plain Grout

Results for plain cement grouts with water/cement ratio of 0.35 and 0.40 are shown in Figure 75 and Figure 76, respectively. Further test data are located in Appendix F. Both figures show results for WPT 1 and WPT 2 indicating reuse of the strand. Although there are slight differences in the results they are not as significant as for the results obtained during initial trial batches that indicated variances with strand reuse.

The results from both w/c ratios shows that there is considerable difference between the percent bleed of the WPT and that of the ST. The most interesting aspect of the plots is that in nearly all cases, the ST bleed percentage is less than that of the WPT. If it is assumed that the WPT is more representative of actual tendon wicking conditions, then the ST produces bleed quantities that are less (in some cases 30% less). This suggests that the ST is underestimating the bleed that might form in the strands.

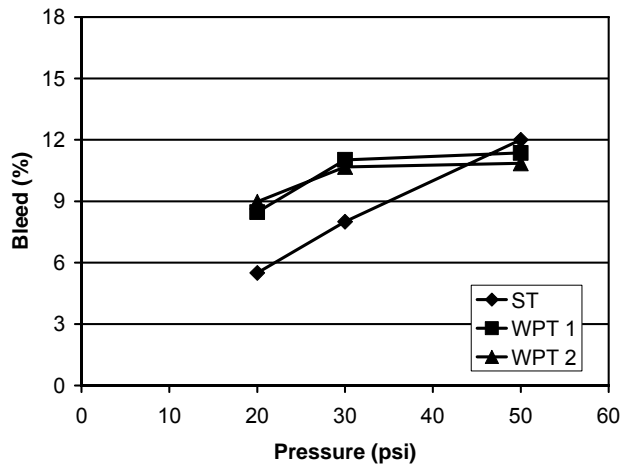


Figure 75 – Comparison of results using plain grout with 0.35 w/c

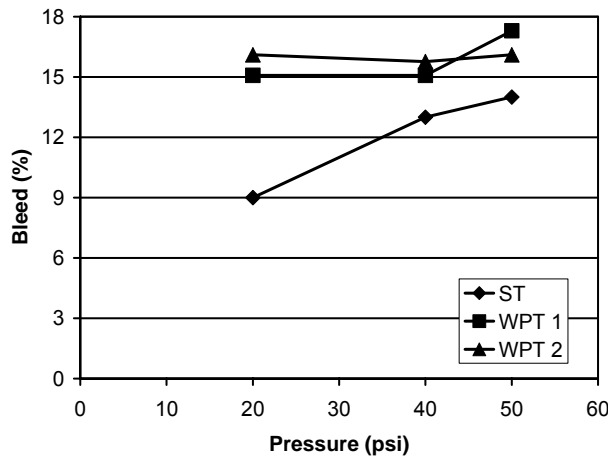


Figure 76 – Comparison of results using plain grout with 0.40 w/c.

6.6.2 Thixotropic Grout

Thixotropic grouts were tested with water cement ratios varying from 0.30 to 0.45 at pressures ranging from 20 psi to 50 psi. A thixotropic admixture (Sikament 300 SC) was added to the plain grout to achieve varying levels of bleed resistance and thixotropy. A dosage rate of 13 to 17 fl.oz per 100 pounds of cement is recommended by the manufacturer. Further recommendations indicate that the dosage should be increased as water content increases. Consequently, for 0.30, 0.35, 0.40, 0.45 water-cement ratios a dosage rate of 12, 14, 16, and 18 fl. oz. per 100 pounds were selected.

Figure 77 shows a comparison of the results of the tests on all for water-cement ratios. The bleed quantities for both ST and WPT have been reduced considerably from that of the plain grouts due to the use of the thixotropic admixture. In nearly all cases, the bleed quantity from WPT was once again greater than that of the ST. This difference can be seen to increase as the w/c ratio increases.

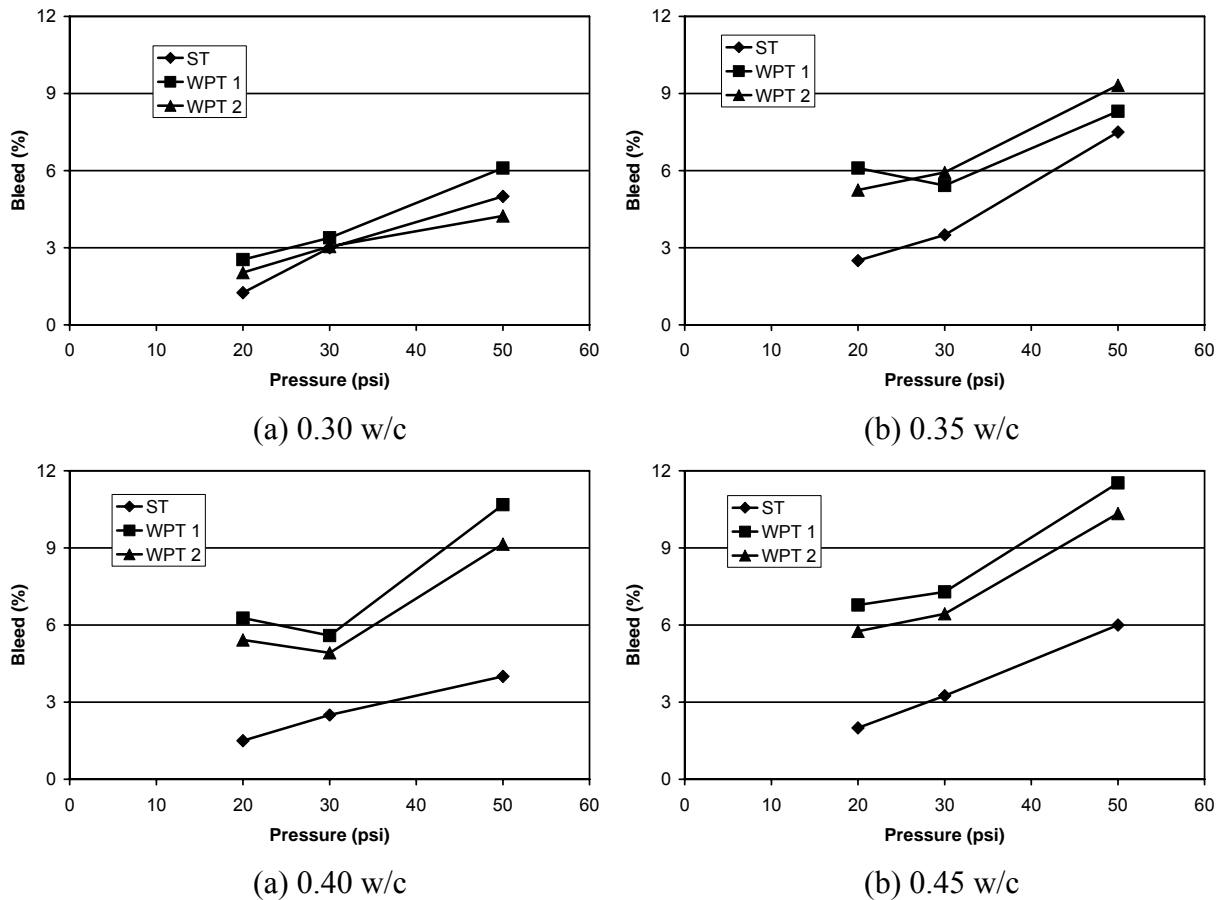


Figure 77 – Comparison of ST and WPT results for plain grout made with thixotropic admixture.

One explanation for this difference is shown in Figure 78. The figure shows a schematic drawing of both WPT and ST. In the ST the excess water must pass through the grout in order to be expelled through the filter. The travel distance in the filter funnel is farther than that in the WPT vessel. In the WPT the moisture travels laterally to the strand and is then expelled through the interstices. In the ST the grout near the filter paper becomes very compacted forming a filter cake and likely inhibits the movement of moisture to and through the filter paper. This would result in a reduced volume of bleed in the ST compared to the WPT. Grouts with lower w/c ratios do not exhibit this behavior (see Figure 77a). This is probably due to the reduced quantity of water in the grout and the associated improvement in the bleed properties. There is simply less moisture available and its movement is inhibited due to the high relative cement content. In conclusion, the tests appear to give similar results for grouts that have good bleed resistant properties, while for grouts more prone to bleed, the WPT probably gives a more realistic picture of the performance in an actual tendon.

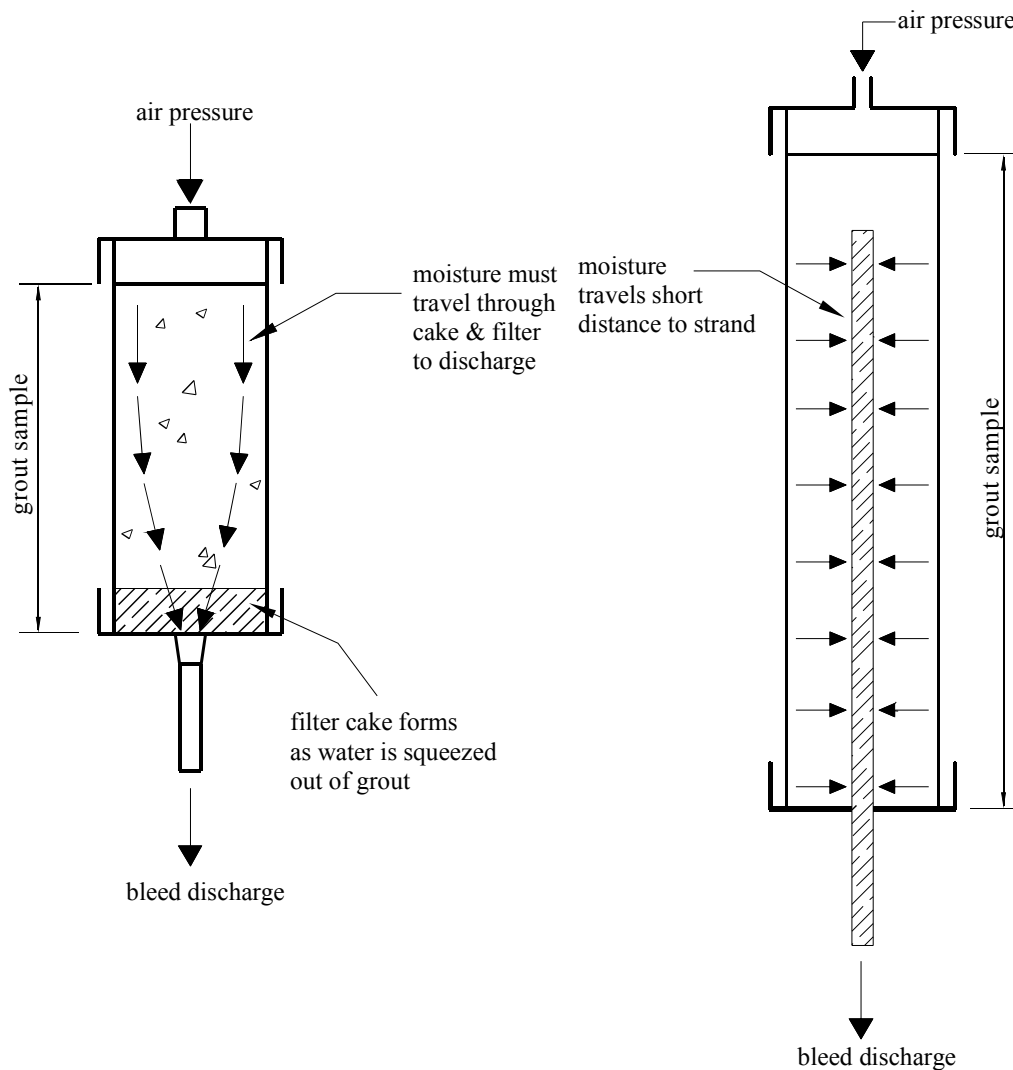


Figure 78 – Proposed explanation for the increase in difference between WPT and ST results

6.6.3 Prepackaged Grout

A prepackaged post-tensioning grout was tested with water to bagged material ratios ratios of 0.25 and 0.30, which are within the recommended values from the manufacturer. No bleed occurred in either ST or WPT for the selected water-cement ratios. This further supports the hypothesis that for high-performance grouts, both test methods give similar results.

6.7 CONCLUSIONS

This phase of the research project involved the development of a new test for evaluating bleed resistance of post-tensioning grouts. The wick pressure test (WPT) is composed of a pressure chamber with a single strand protruding from the base. The grout is placed in the chamber with the strand in place and is pressurized. The water from the grout is forced out of the chamber through the interstices of the strand. This newly developed method was compared to the Schupack Test (ST) that is typically used to measure the bleed properties of high-performance PT grouts. The apparatus was designed and constructed to more closely

approximate the physical conditions encountered in a post-tensioning tendon, including the application of pressure and the use of a prestressing strand to filter the bleed water. Several series of tests were conducted to test the effectiveness of the apparatus in achieving the desired goals. The following conclusions are based on this testing:

- The newly developed WPT is an effective means of evaluating grout bleed resistance of an actual post-tensioning tendon. The configuration of the WPT more closely approximates the situation in a PT tendon than that of the ST.
- In bleed-prone grouts, the WPT results in higher relative volumes of grout than that of the ST. In some cases the difference is near 100%. One explanation for this is that a filter cake is formed at the bottom of the pressure filter in the ST that restricts the passage of water through the filter to discharge. This would occur early in the test forming a seal. The WPT configuration inherently reduces the distance the water must travel, which likely increases the relative amount of water discharged compared to that of the ST. Consequently, the results from the ST may underestimate the actual bleed that one might see in the field with the use of a standard or plain grout mix.
- In high performance grouts, the WPT and ST produce comparable relative bleed quantities.

6.8 RECOMMENDATIONS

The aim of this study was to develop an apparatus and test method that was more representative of actual an actual post-tensioning tendon than that of the Schupack test. The WPT accomplishes these goals. At this time, the WPT shows the most promise as an alternate lab test for grouts under development. The Schupack test is a simpler test due to the absence of strand and gives similar results to the WPT for prepackaged, high-performance grouts. Since FDOT specifications require this type of grout, the Schupack test is an adequate measure of bleed performance for FDOT projects.

7 References

Ahmad, S. (2003). Reinforcement Corrosion in Concrete Structures, Its Monitoring and Service Life Prediction – A Review. *Cement and Concrete Composites*, 25(4-5), 459-471.

Al-Tayyib A. J. & Khan, M. S. (1988). Corrosion Rate Measurements of Reinforcing Steel in Concrete by Electrochemical Techniques. *ACI Materials Journal*, 85, 172-177.

Andrade, C., Macias, A., Feliu, S., Escudero, M. L., & Gonzalez, J. A. (1990). Quantitative Measurement of the Corrosion Rate Using a Small Counter Electrode in the Boundary of Passive and Corroded Zones of a Long Concrete Beam. Corrosion Rates of Steel in Concrete, ASTM STP 1065, N. S. Berke, V. Chaker, and D. Whiting, Eds., American Society for Testing and Materials, Philadelphia, pp. 134-142.

Andrade, J., Dal Molin, D., & Ribeiro, J. L. D. (2003). A Critical Analysis of Chloride Penetration Models in Reinforced Concrete Structures. *SP 207-14 HPC, and Performance and Quality of Concrete Structures*, 217-228.

ASTM C 642 (1997). Standard Test Method for Density, Absorption, and Voids in Hardened Concrete. *American Society of Testing and Materials*, West Conshohocken, PA.

ASTM C 876 (1999). Standard Test Method for Half-Cell Potentials of Uncoated Reinforcing Steel in Concrete. *American Society of Testing and Materials*, West Conshohocken, PA.

ASTM C 939 (2002) – Standard Test Method for Flow of Grout for Pre Placed Aggregate Concrete (Flow Cone Method). *American Society of Testing and Materials*, West Conshohocken, PA.

ASTM C 940 (2002) – Standard Test Method for Expansion and Bleeding of Freshly Mixed Grouts for Preplaced Aggregate Concrete in the Laboratory. *American Society of Testing and Materials*, West Conshohocken, PA.

ASTM G 102 (1999). Standard Practice for Calculation of Corrosion Rates and Related Information from Electrochemical Measurements. *American Society of Testing and Materials*, West Conshohocken, PA.

ASTM G 5 (1999). Standard Reference Test Method for Making Potentiostatic and Potentiodynamic Anodic Polarization Measurements. *American Society of Testing and Materials*, West Conshohocken, PA.

ASTM G 59 (2003). Standard Test Method for Conducting Potentiodynamic Polarization Resistance Measurements. *American Society of Testing and Materials*, West Conshohocken, PA.

Alvarez, G. A. A. and Hamilton III, H. R. (2004). “Grout Bleed Tests in Vertical and Horizontal Post-Tensioning Ducts,” *PTI Journal*, Vol 2, No 1, January 2004, pp. 1-11.

Baweja, D., Roper, H., & Sirivivatnanon, V. (1996). *Corrosion of Steel in Marine Concrete: Long-Term Half-Cell Potential and Resistivity Data*. Performance of Concrete in Marine Environment, Third CANMET/ACI International Conference, Proceedings, St. Andrews by-the-Sea, Canada, SP-163, V. M. Malhotra, Ed., 89-110.

Baweja, D., Roper, H., & Sirivivatnanon, V. (1999). Chloride-Induced Steel Corrosion in Concrete: Part 2 – Gravimetric and Electrochemical Comparisons. *ACI Materials Journal*, 96(3), 306-312.

Berke, N. S. (1991). Corrosion Inhibitors in Concrete. *Concrete International*, 13, 24-27.

Berke, N. S., Shen, D. F., & Sundberg, K. M. (1990). Comparison of Current Interruption and Electrochemical Impedance Techniques in the Determination of Corrosion Rates of Steel in Concrete. The Measurement and Correction of Electrolyte Resistance in Electrochemical Tests, ASTM STP 1056, L. L. Scribner and S. R. Taylor, Eds., American Society for Testing and Materials, Philadelphia, 191-201.

Corven Engineering (2001). Mid-Bay Bridge Post-Tensioning Evaluation, Final Report to the Florida Department of Transportation, October 10, 2001, 67 pp.

Diamond, S. (1997). Alkali Silica Reactions – Some Paradoxes. *Cement and Concrete Composites*, 19, 391-401.

Dickson, T. J., Tabatabai, H., & Whiting, D. A. (1993). Corrosion Assessment of a 34-Year-Old Precast Post Tensioned Concrete Girder. *PCI Journal*, 38(6), 44-51.

Diederichs, U., & Schutt, K. (1989). *Silica Fume Modified Grouts for Corrosion Protection of Post Tensioning Tendons*. SP 114-57, Trondheim Conference, 1173-1195.

Escalante, E. (1990). *Elimination of IR Error in Measurements of Corrosion in Concrete*. The Measurement and Correction of Electrolyte Resistance in Electrochemical Tests, ASTM STP 1056. L. L. Scribner and S. R. Taylor, Eds., American Society for Testing and Materials, Philadelphia, 180-190.

- Gu, P.; Elliot, S.; Hristova, R.; Beaudoin, J. J.; Brousseau, R.; & Baldock, B. (1997). A Study of Corrosion Inhibitor Performance in Chloride Contaminated Concrete by Electrochemical Impedance Spectroscopy. *ACI Materials Journal*, 94(5), 385-395.
- Hamilton, H. R. (1995). *Investigation of Corrosion Protection Systems for Bridge Stay Cables*. PhD Dissertation, The University of Texas at Austin.
- Hamilton, H. R., Breen, J. E., & Frank, K. H. (1998). Bridge Stay Cable Corrosion Protection. I: Grout Injection and Load Testing. *Journal of Bridge Engineering*, 3(2), 64-71.
- Hamilton, H. R., Wheat, H. G., Breen, J. E., & Frank, K. H. (2000). Corrosion Testing of Grout for Posttensioning Ducts and Stay Cables. *Journal of Structural Engineering*, 126(2), 163-170.
- Hornain, H., Marchand, J., Buhot, V., & Moranville-Regourd, M. (1995). Diffusion of Chloride Ions in Limestone Filler Blended Cement Pastes and Mortars. *Cement and Concrete Research*, 25(8), 1667-1678.
- Hussain, S. E., & Rasheeduzzafar (1994). Corrosion Resistance Performance of Fly Ash Blended Cement Concrete. *ACI Materials Journal*, 91(3), 264-272.
- Idriss, A. F., Negi, S. C., Jofriet, J. C., & Hayward, G. L. (2001). Corrosion of Steel Reinforcement in Mortar Specimens Exposed to Hydrogen Sulphide, Part 1: Impressed Voltage and Electrochemical Potential Tests. *Journal of Agricultural Engineering Research*, 79(2), 223-230.
- Jones, D. A. (1996). *Principles and Prevention of Corrosion*. Prentice Hall (Second Edition)
- Kirkpatrick, T. J., Weyers, R. E., Anderson-Cook, C. M., & Sprinkel, M. M. (2002). Probabilistic Model for the Chloride-Induced Corrosion Service Life of Bridge Decks. *Cement and Concrete Research*, 32, 1943-1960.
- Koester, B. D. (1995). Evaluation of Cement Grouts for Strand Protection using Accelerated Corrosion Tests. MSc. Thesis, The University of Texas at Austin.
- Lankard, D. R., Thompson, N., Sprinkel, M. M., & Virmani, Y. P. (1993). Grouts for Bonded Post Tensioned Concrete Construction: Protecting Prestressing Steel from Corrosion. *ACI Materials Journal*, 90(5), 406-414.
- Li, C. Q. (2001). Initiation of Chloride-Induced Reinforced Corrosion in Concrete Structural Members – Experimentation. *ACI Structural Journal*, 98(4), 502-510.
- Liu, W., Hunsperger, R. G., Chajes, M. J., Folliard, K. J., & Kunz, E. (2002). Corrosion Detection of Steel Cables using Time Domain Reflectometry. *Journal of Materials in Civil Engineering*, 14(3), 217-223.
- Loretz, T., & French, C. (1995). Corrosion of Reinforcing Steel in Concrete: Effects of Materials, Mix Composition, and Cracking. *ACI Materials Journal*, 92(2), 181-190.
- Millard S. G., Law, D., Bungey, J. H., & Cairns J. (2001). Environmental Influences on Linear Polarization Corrosion Rate Measurement in Reinforced Concrete. *NDT&E International*, 34, 409-417.
- Montemor, M. F., Simões, A. M. P., & Ferreira, M. G. S. (2003). Chloride-Induced Corrosion on Reinforcing Steel: from the Fundamentals to the Monitoring Techniques. *Cement & Concrete Composites*, 25(4-5), 491-502.
- Montemor, M. F., Simões, A. M. P., & Salta, M. M. (2000). Effect of Fly Ash on Concrete Reinforcement Corrosion Studied by EIS. *Cement & Concrete Composites*, 22, 175-185.

- Peng, J., Li, Z., & Ma, B. (2002). Neural Network Analysis of Chloride Diffusion in Concrete. *Journal of Materials in Civil Engineering*, 14(4), 327-333.
- Post-Tensioning Institute (2003). *Guide Specification for Grouting of Post Tensioned Structures (1st Ed.)*. PTI Committee on Grouting Specifications, Post-Tensioning Institute.
- Powers, R. G., Sagues, A. A., and Virmani, Y. P. (2004). "Corrosion of Post-Tensioned Tendons in Florida Bridges," Florida Department of Transportation, State Materials Office Research Report No. 04-475, August 2004, 17 pp.
- Rasheeduzzafar, Dakhil, F. H., Al-Gahtani, A. S., Al-Saadoun, S. S., & Bader, M. A. (1990). Influence of Cement Composition on the Corrosion of Reinforcement and Sulfate Resistance of Concrete. *ACI Materials Journal*, 87(2), 114-122.
- Rha, C. Y., Kim, W. S., Kim, J. W., & Park, H. H. (2001). Relationship between Microstructure and Electrochemical Characteristics in Steel Corrosion. *Applied Surface Science*, 169-170, 587-592.
- Schokker, A. J. (1999). Improving Corrosion Resistance of Post Tensioned Substructures Emphasizing High Performance Grouts. PhD Dissertation, The University of Texas at Austin.
- Schokker, A. J., Breen, J. E., & Kreger, M. E. (2002). Simulated Field Testing of High Performance Grouts for Post-Tensioning. *Journal of Bridge Engineering*, 7(2), 127-133.
- Schokker, A.J., Koester, B.D., Breen, J.E., and Kreger, M.E. (1999). Development of High Performance Grouts for Bonded Post-Tensioned Structures. *Research Report 1405-2*, Center for Transportation Research.
- Schokker, A.J., Schupack, M., Hamilton III, H.R. (2002). Estimating Post-Tensioning Grout Bleed Resistance Using a Pressure-Filter Test. *PCI Journal*, 47(2), 32-38.
- Schupack, M. (1971). Grouting Tests on Large Post-Tensioning Secondary Nuclear Containment Structures. *PCI Journal*, 16(2), 84-97.
- Schupack, M. (1974). Admixture for Controlling Bleed in Cement Grout Used in Post-Tensioning. *PCI Journal*, 19(6), 28-39.
- Schupack, M. (1994). Studies of the Bissell Bridge: Post Tensioning Tendons after 35 years. *Concrete International*, 16(3), 50-54.
- Stansbury, E. E. & Buchanan, R. A. (2000). *Fundamentals of Electrochemical Corrosion*. ASM International. The Materials Information Society.
- Thompson, N.G., Lankard, D. and Sprinkel, M. (1992). "Improved Grouts for Bonded Tendons in Post-Tensioned Bridge Structures," *Report No. FHWA-RD-91-092, Federal Highway Administration*, Cortest Columbus Technologies.
- Zivica, V. (2001). Possibility of Improvement of Potentiodynamic Method for Monitoring Corrosion Rate of Steel Reinforcement in Concrete. *Bulletin of Material Science*, 24(5), 555-558.

8 APPENDIX A: Proposed ACT Standard

Standard Test Method for Evaluation of the Corrosion Protection Capability of Post-Tensioning Grouts (The Accelerated Corrosion Test for Grouts)

Scope

This test method covers the evaluation of grouts intended to post-tensioning applications with respect to their level of corrosion protection.

This standard does not address safety issues. It is the responsibility of the user to establish appropriate safety and health practices.

Referenced Documents

ASTM Standards:

A 416 Standard Specification for Steel Strand, Uncoated Seven-Wire for Prestressed Concrete

C 938 Standard Practice for Proportioning Grout Mixtures for Preplaced-Aggregate Concrete

C 939 Standard Test Method for Flow of Grout for Pre Placed Aggregate Concrete

G 3 Practice for Conventions Applicable to Electrochemical Measurements in Corrosion Testing

G 5 Standard Reference Test Method for Making Potentiostatic and Potentiodynamic Anodic Polarization Measurements

G 59 Standard Test Method for Conducting Potentiodynamic Polarization Resistance Measurements

Significance and Use

This test method is suitable for quality control and for use in research and development work.

The results obtained by the use of this test method shall not be considered as a means for estimating the structural properties of prestressing steels.

Due to specific testing conditions, the results obtained by the use of this test method shall not be related directly to actual service life of grouts.

Apparatus

The casing assembling apparatus consists of the following:

Auxiliary tubing support, to facilitate the assemblage of the casings (FIG. 1).

The casting apparatus consists of the following:

Balance, sensitive to at least 1 g (0.035 oz).

Container, measuring 30 cm (11.8 in.) in diameter and 40 cm (15.7 in.) in height or large enough to hold the amount of grout to be mixed.

High-shear mixer blade, capable of varying rotation speeds.

Support, to hold the specimens in an upright position during casting and curing (FIG. 2).

Note 1 - During the casting procedure, the user may choose also to run quality control tests, such as the fluidity test given in Test Method C939. In this case, the user shall refer to the proper standard methods for additional equipment requirements.

The testing apparatus consists of the following:
Multiplexer, to electrically connect each sample to a potentiostat.

Potentiostat, to control the voltage difference between the samples and the reference electrode.

Reference electrode, which shall be part of each corrosion cell to provide a voltage baseline for the measurements. A saturated calomel electrode is specified for use (0).

Bulk solution, which shall be composed of distilled or deionized water and a content of 5% of the solution weight of sodium chloride.

Counter electrode, made of an inert metal such as platinum or graphite shall measure 17 cm (6.7 in.) in length, which is enough to pass the exposed grout region of specimens.

Corrosion cell container with support for electrodes (see FIG. 6).

Note 2 - This test method specifies only one type of reference electrode, but others may also be used, such as copper-copper sulfate electrodes. In this case, the potentials measured should be converted to saturated calomel equivalent potentials. The appropriate technique can be found in Practice G3.

Note 3 - Working electrodes, i.e., the samples to be tested, shall compete the corrosion cells.

Test Specimens

Preparing for casting:

Casing segments shall be cut from PVC tubing, following the dimensions given in FIG. 3. Clear PVC shall be used in order to facilitate casting steps and to allow identification of major casting flaws. Additionally, end caps shall also be available for casing assemblage.

Using the auxiliary tubing support, the casings are assembled as illustrated in FIG. 1 and the junctions are caulked with silicone and held in

place with duct tape. After this, the end caps may be cemented to the extremity corresponding to the short plastic segment.

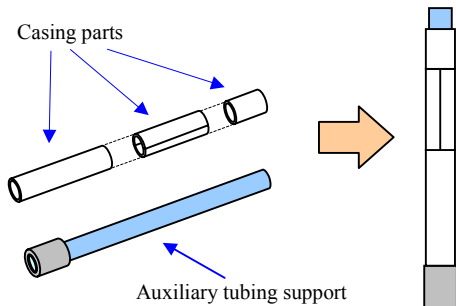


FIG. 1 Auxiliary tubing support is used to keep the casing parts together, allowing caulking and taping of their junctions

Strand segments to be used in the experiments shall be cut from the same reels of Grade 270 prestressing steel (Specification A416). The requirements given in FIG. 3 shall be followed. Previously to casting, they shall be beveled at the ends and thoroughly cleaned with acetone, removing accumulated impurities.

Additional elements that shall be available prior to the casting step are the plastic spacers, which may be cut from larger spacers used in structural concrete construction. These elements are also illustrated in FIG. 3. The spacers should provide a snug fit inside the casing.

After allowing a minimum of one hour for the silicone applied to the casing junctions to vulcanize, the specimens shall be tested for leakages, fixing any apparent defects.

With the casings ready, a spacer should be attached to a strand extremity, and this end inserted inside a casing. The casings then can be put in an upright position with the help of an appropriate support and the casting procedure may start. An example on how to hold a set of specimens in an upright position is shown in FIG. 2.

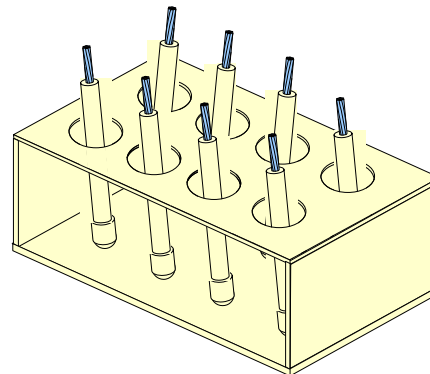


FIG. 2 Set of specimens in a rack

Casting:

A minimum of twelve specimens per grout to be tested shall be cast during this step. Eight specimens shall be used in the potentiostatic test, while four shall be used in LPR measurements (0).

Weigh grout materials. Distilled (or deionized) water shall be used in each mix.

Note 4 - It is recommended, however, that a minimum of three additional specimens be fabricated to assure that twelve visually flawless specimens are available for each grout.

The mixing of grout shall follow Practice C938 with the use of a high shear mixer blade in an appropriate container.

The casings, without removal of their strands, shall be filled with grout in three lifts. Each lift consists of filling with approximately 1/3 of their volume with grout, slowly moving the strand, and, tapping the casing, vibrating them. This procedure should minimize the occurrence of air bubbles and voids in the specimen.

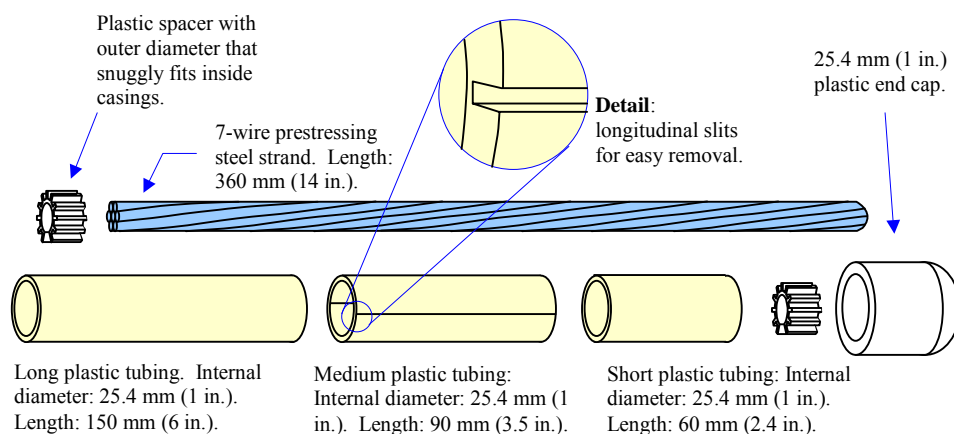


FIG. 3 Casing parts, spacers, and prestressing strand

Then, the second spacer is attached to the top of each specimen and the samples are taken to an environmental chamber for the curing period (28 days or, in the case of mixtures containing fly ash, also at 56 days) (0). Specimens shall remain in a vertical position throughout casting and curing. A schematic of a specimen after casting is shown in FIG. 4.

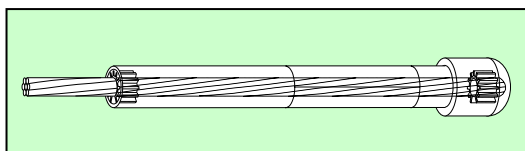


FIG. 4 Schematic of an assembled specimen

Note 5 - It is recommended that a protection be placed on the protruding prestressing strands in order to avoid heavy surface corrosion that may occur on them because of the high humidity level of environmental chambers.

Instrumentation

Corrosion Cell:

Upon finishing the curing period for each grout to be tested, the middle plastic section is easily removed due to the existence of the longitudinal slits diametrically localized in that part of the casings, exposing the testing region of the samples.

Each specimen shall be immediately placed in its respective corrosion cell in order to hinder cracking occurrence.

Once inside their corrosion cells, defects are easily checked with the rotation of the specimens

and careful visual evaluation. A typical defect is shown in FIG. 5. Specimens with obvious defects should be discarded.

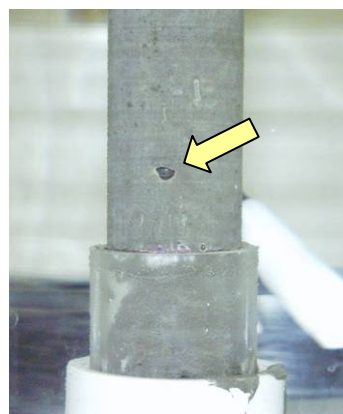


FIG. 5 Typical specimen defect

With the specimens to be tested in place, the connections are made and the corrosion cell shall be placed in the configuration in the schematic presented in FIG. 6.

Test settings:

The settings to be used in the potentiodynamic linear polarization resistance test and in the potentiostatic test shall be the ones given in TABLE 12 (0).

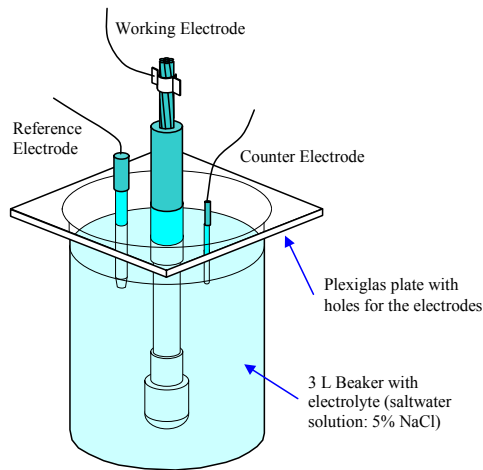


FIG. 6 Corrosion cell

TABLE 12 Test settings	
Test	Value
LPR:	
Analysis region (mV)	5
Initial E (mV) vs. E_{oc}	-20
Final E (mV) vs. E_{oc}	+20
Potentiostatic:	
Sample period (min)	30
Initial E (mV _{SCE})	+200

Note 6 - The analysis region of 5 mV corresponds to the range of potentials about the open circuit voltage of the specimens being measured that is considered approximately linear for determination of R_p . Details for both electrochemical tests are available in Test Methods G59 and G5. Other details regarding electrochemical measurements are found in Practice G3.

Experimental Procedure

Grout approval: With this standard method, a grout with can be approved anytime during a two step testing process as illustrated in

FIG. 7. The multi-layered approval system allows a grout with evident corrosion protection properties to forgo more extensive (and time consuming) testing. A grout containing fly ash, or another additive that may justify additional cure time, may be tested at 56 days instead of 28 days. The engineer may specify a severe environment (coastal or application of deicing salts). The multi-step process is as follows:

The first chance is immediately after the curing period of 28 days of the control grout is satisfied and its R_p is found. The R_p of the grout being tested shall not be lower than 700 kΩ-cm².

The second chance for a grout to be approved for post-tensioning applications is also a verification of its potentiostatic result. The grout t_{corr} shall not be lower than the t_{corr} found for the control grout.

Flow chart: All combinations for grout approval and the conditions for rejection are illustrated in the flowchart presented in FIG. 7.

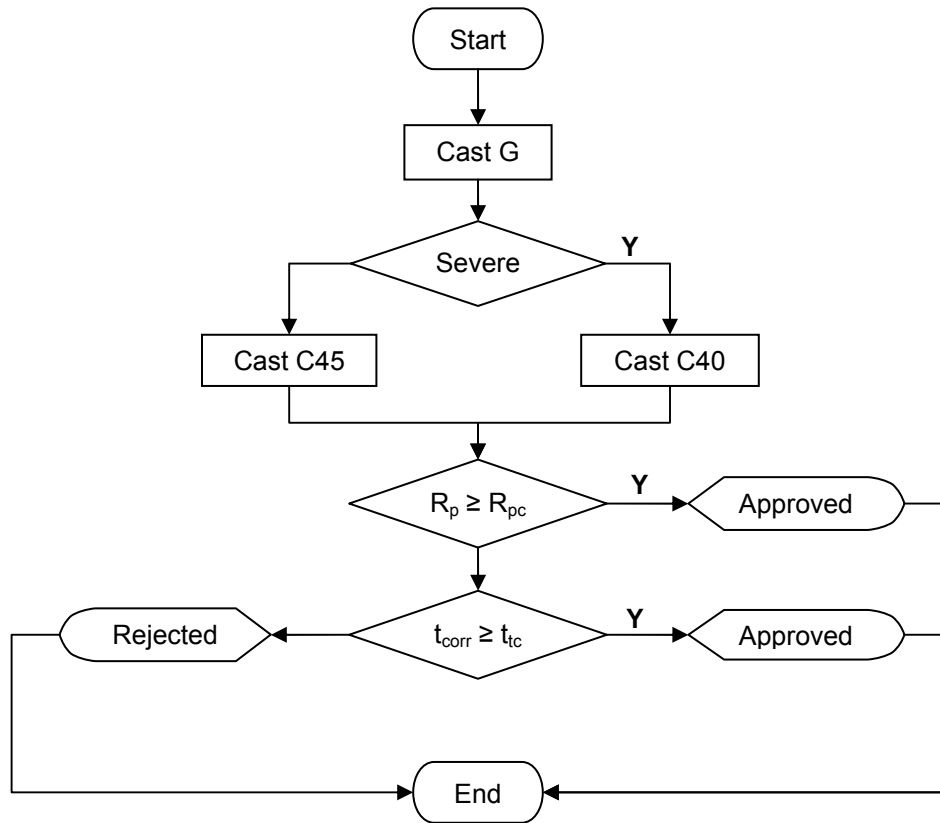
Precision and Bias

The maximum difference between two LPR readings taken on the same grout for the same conditions should be 70 kΩcm².

The maximum difference between determinations of two t_{corr} values in respect to the same grout and taken under the same conditions should be 60 hours.

Keywords

Post-tensioning grout-corrosion activity; corrosion activity; electric half-cell potentials; electrochemical tests; degree of corrosion protection of post-tensioning grouts; degree of corrosion protection; accelerated corrosion test.



LEGEND:

G: Test grout

Severe: severe field conditions are specified

C40: Control grout (w/c = 0.40)

C45: Control grout (w/c = 0.45)

R_p : LPR result for the grout at 28 days (56 days if additional curing justified)

R_{pc} : LPR limit = 700 kΩ-cm²

t_{corr} : Potentiostatic result for the grout at 28 days (56 days if additional curing justified)

t_c : Potentiostatic result for the control

FIG. 7 Experimental procedures for testing of the corrosion protection degree of post-tensioning grouts

9 APPENDIX B: Current ACT Specification (PTI 2003)

9.1 ACCELERATED CORROSION TESTING METHOD (ACTM)

9.1.1 Background and Procedure

The Accelerated Corrosion Testing Method was based on the method developed by Thompson, Lankard, and Sprinkel (1992) in a FHWA sponsored study and refined at the University of Texas at Austin (Hamilton 1995, Schokker et al. 1999). The corrosion test uses anodic polarization to accelerate corrosion by providing a potential gradient, driving negatively charged chloride ions through the grout to the steel. The ACTM is intended to provide a relative comparison of a grout's corrosion resistance. The time to corrosion cannot be directly related to field performance, but can be compared with grouts with known acceptable performance. The ACTM is particularly useful in determining combinations of admixtures that may adversely affect a grout's corrosion performance. A grout which shows a longer average time to corrosion in the ACTM than a neat grout with 0.45 water-cement ratio is considered satisfactory for use in bonded post-tensioning applications covered by this specification.

9.1.2 Specimen Preparation

The test specimens consist of a short length of prestressing strand in a grouted clear PVC mold casing as shown in Figure 1. A minimum of 6 specimens should be used to test a given grout. It may be useful to fabricate additional specimens to ensure that 6 uncracked and undamaged specimens will be available for testing.

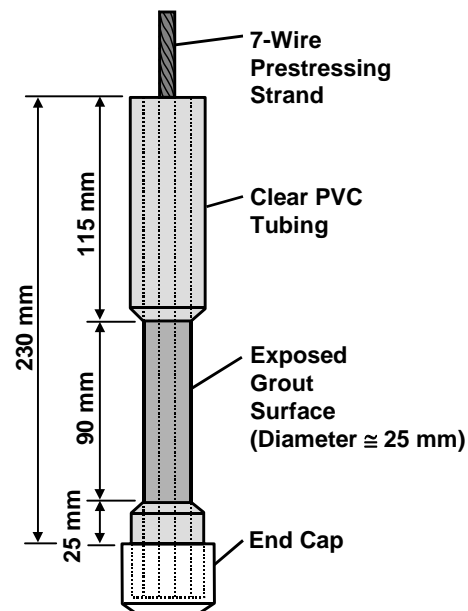


Figure 1: Specimen Dimensions

A plastic spacer is fitted in the bottom of the PVC cap to keep the strand spaced concentrically within the PVC casing. The end cap is then cemented to the PVC casing. The 12.7 mm (0.5 in) diameter strand is beveled at one end for ease of insertion into the spacer, and

the strand is cleaned with acetone to remove surface buildup. The grout mix is prepared using distilled water and is placed into the casing in 3 stages. Before the strand is inserted, the PVC casing is filled to approximately 1/3 with grout. The strand is then inserted into the assembly. The casing is filled in 2 more equal lifts, and the strand is slowly rotated between lifts to allow air bubbles to escape. A spacer is inserted at the top of the casing to hold the strand in place. The specimens are placed in racks and allowed to cure for 7 days in a moist curing room.

After 7 days of curing, a portion of the PVC casing is removed with a rotary wire brush, taking care not to damage the grout. Two radial cuts are made first followed by two longitudinal cuts. The length of casing may be removed using other methods as long as care is taken to avoid damage to the grout. After removal of the casing, the specimen is immediately wrapped in a wet towel to prevent cracking prior to immersion in the NaCl solution.

The specimens are connected to the electrodes and allowed to soak in the NaCl solution for approximately 15 minutes during which time the free corrosion potential is recorded. Testing begins by applying a potential of +200 mV (approximately 400 mV above the free corrosion potential) to each station. The applied potential of +200 mV_{SCE} is within the passive region of the polarization curve for the strand.

9.1.3 Instrumentation

During testing, the specimens are immersed in a 5% NaCl solution in a 3000 ml beaker. The beaker is covered with a Plexiglas cap with holes for the electrodes. A gel-filled saturated calomel electrode is used as a reference electrode. A potentiostat is used to apply the +200 mV_{SCE} through the counter electrode in each station. A multiplexer sends data back to a PC one station at a time. Corrosion potential (E_{corr}) is measured from the reference electrode relative to the working electrode, and the corrosion current (i_{corr}) is found by measuring the voltage across the 100 Ω resistor in-line with the lead on the counter electrode. A diagram and picture of one of the experimental stations is shown in Figure 2.

Chemical and mineral admixtures will change the ohmic resistance (or IR drop) of the grout. Grouts with different ohmic resistances will have different polarized potentials at the steel/grout interface. The polarization read by the potentiostat cannot be read directly at the steel/grout interface, so differences in the ohmic resistance of the grout will affect the actual polarization potential. For this reason, a potentiostat that includes IR compensation is preferable.

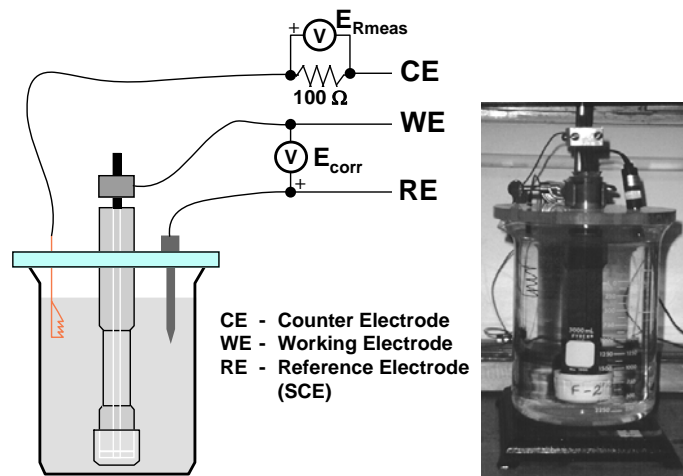


Figure 2: (a) schematic of experimental station (b) test setup

9.1.4 Behavior

Typical initial behavior after potential is applied is shown in Figure 3. This initial high corrosion current followed by a rapid reduction is helpful in isolating and correcting a faulty station early in testing. Once a specimen corrodes, the corrosion current typically increases by orders of magnitude very rapidly as shown in Figure 4. The spike in corrosion current is immediate in many specimens, but in some cases the rise begins gradually. The time to corrosion is estimated as the time where the sharp rise in corrosion current begins on the plot.

9.1.5 Corrosion Resistance

The Accelerated Corrosion Testing Method provides relative comparison of the corrosion protection provided by different grouts. For each grout tested, the average time to corrosion should be found from the average of a minimum of 6 specimens. If 8 or more specimens are tested, the high and low values may be removed before computing the average. For the grout under investigation, a comparison test should be run with a 0.45 water-cement ratio neat grout. This comparison grout should be tested by the same technician using the same equipment and the same number of specimens should be tested. The samples should be fabricated using cement and strand from the same batch. Strand condition should be as close as possible to the strand used in the test grout (strand that is noticeably more corroded should be discarded). The grout is considered satisfactory for bonded post-tensioned applications as outlined in this specification if the average time to corrosion from the test grout is longer than the average time to corrosion of the 0.45 water-cement ratio comparison grout.

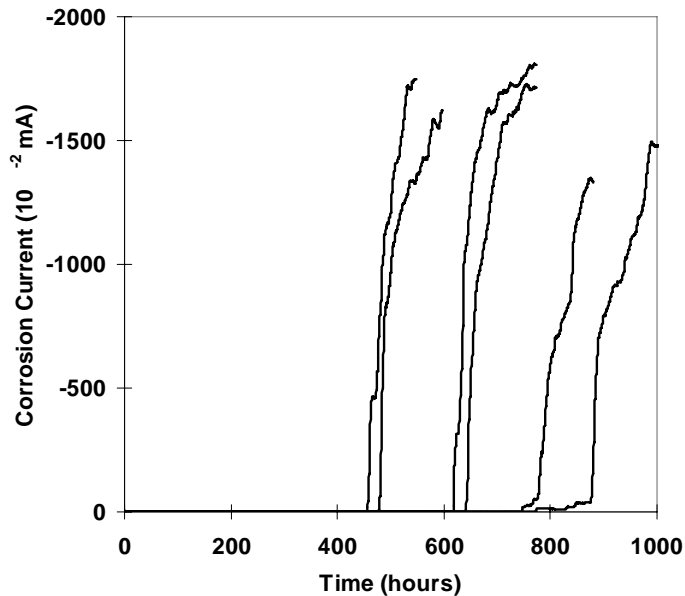


Figure 3: Initial Behavior of Corrosion Current with Time³

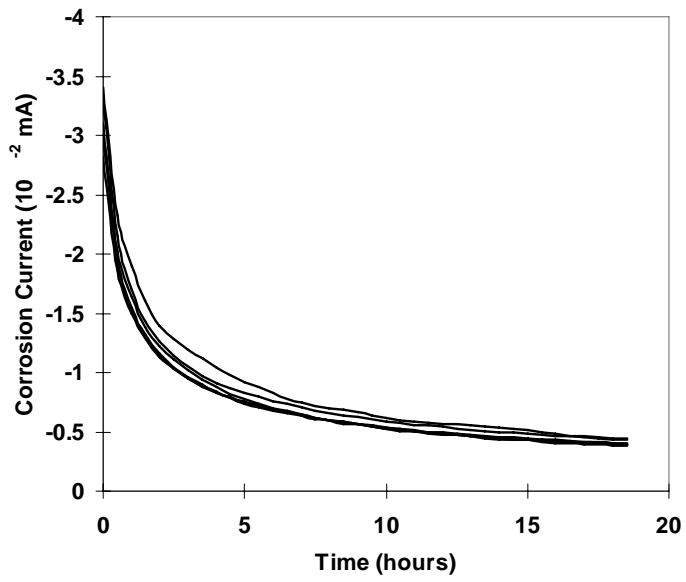


Figure 4: Behavior of Corrosion Current with Time³

10 APPENDIX C: Prestressing Strand Report

Issued: 06/16/98
Supersedes: New

Confidential
WQS X-XXX-XXX
Page 1 of 1

Insteel Industries Inc. Carbon Steel Wire Rod Specification

Parameter	Quality Characteristics	
1. Steel Description	1/2", 3/8", & 5/16 1080	
2. Quality	For C Strand application, ASTM A616 requirements Acid Cleaning Quality	
3. Preferred Refining Route	No Aluminum Additions Control Grain Practice Mandatory	
4. Chemical Composition (% by weight)	<u>Range</u>	<u>Target</u>
a. Carbon	0.78 - 0.82	0.80
b. Manganese	0.60 - 0.80	0.70
c. Phosphorus	0.015 Max	0
d. Sulfur	0.015 Max	0
e. Silicon	0.15 - 0.30	0.2
f. Copper	0.15 Max	0
g. Nickel	0.08 Max	0
h. Chromium	0.12 Max	0
i. Molybdenum	0.03 Max	0
j. Tin	0.010 Max	0
k. Aluminum	trace	0
l. Nitrogen	0.006 Max	0
5. Rod Diameter	+0.016" or -0.016"	
6. Ovality	0.012" Max	0
7. Surface Quality	a. Decarburization: 0.003" Max (Partial) / 0 (Carbon Free) b. Laps / Seams: 0.004" Max (Ind) 0.008" Max (Cum.) c. Fins, Rolled-in Defects, Roll Marks: Restricted (No Surf. Damage Breaks up to 90% Red.) d. Abrasions, Snags, Burrs, Cut Ends: Restricted (No Surf. Damage Breaks up to 90% Red.) e. Rust: Light Rust Acceptable, No Pitting Allowed	
8. Non-Metallic Inclusions / Center Segregation	Restricted (No Center Bursting up to 95% Reduction)	
9. Metallurgical Structure	a. % Proeutectoid Ferrite: Minimum Allowed b. % Proeutectoid Cementite: Not Allowed c. % Martensite: Not Allowed	
10. Physical and Mechanical Properties	<u>Range</u>	<u>Target</u>
a. Recommended Scale Oxide Weight	0.7% Max	0.4%
b. UTS (Individual)	165 - 175 ksi	168 ksi
c. UTS (Heat Average)	165 - 172 ksi	168 ksi
d. UTS Range Within Heat		4 ksi Max
e. Reduction of Area		40%
11. Coil Packaging	a. Rod Coil Weight: 4000 lb Min, 6000 lb Max b. Tag Identification: P.O.#, Size, Grade, Heat #, Coil #, Weight c. Tag Location: Bands: only—One (1) on Coil ID, One (1) on Coil OD	
12. Certification	Each heat certified for chemistry, Min, Max, Ave., and number tested UTS, ROA, diameter and ovality. The certification should be sent or faxed prior to shipment, and accompany the shipment. Deviations must be approved prior to shipment by the Insteel Technical Manager.	

11 APPENDIX D: Cement Mill Test Report

CEMENT MILL TEST REPORT Whitehall Plant Silo: B-1 Type: II

Date: October 2001

Chemical Analysis (%)		Physical Tests	
Total Alkalies.....	0.81	Fineness: blaine, m ² /kg.....	391
Loss on ignition.....	1.1	% Passing (325 mesh).....	97.9
Insoluble residue.....	0.24	Soundness:	
		% Autoclave Expansion.....	0.00
Silicon dioxide (SiO ₂).....	20.8	Setting Time: Gillmore	
Aluminum oxide (Al ₂ O ₃).....	4.6	Initial (minutes).....	220
Ferric oxide (Fe ₂ O ₃).....	3.9	Final (minutes).....	330
Calcium oxide (CaO).....	62.5	Vicat: Initial (minutes).....	180
Magnesium oxide (MgO).....	2.2	% Air Content.....	7.8
Sulfur trioxide (SO ₃).....	2.8		
	ASTM AASHTO		
Mineralogical Composition:	<u>C-150-97</u> <u>M-85</u>	Compressive Strength:	<u>Mpa</u> <u>psi</u>
Tricalcium silicate (C ₃ S).....	52 49	3 day.....	26.5 3850
Dicalcium silicate (C ₂ S).....	21 23	7 day.....	31.6 4580
Tricalcium aluminate (C ₃ A).....	6 6		
Tetracalcium aluminoferrite (C ₄ AF).....	12 12		

The test results given above were made on a cement composite from a Denver/Wezin sampler grinding into the silo listed above. The Bogue Compounds are calculated using the ASTM and AASHTO formulas. This cement complies with the specifications listed below.

Specifications: ASTM C-150-97
AASHTO M-85

This report is in compliance with your request.

Approved by


 Lorraine E. Faccenda
 Supervisory Chemist

CEMENT GROUP/WHITEHALL PLANT
5160 Main Street, Whitehall, PA 18052
Office: (610) 262-7831 Fax: (610) 261-9020 (800) 523-9211

12 APPENDIX E: Phase I Experimental Data Summary

Grout	Undamaged Condition										Damaged Condition									
	V (%)	-E _c (mV)	i _c (A/cm ²)	β _a (mV)	-β _c (mV)	R _p (Ωcm ²)	B (mV)	E _{oc} (mV)	t _{corr} (h)	Q(C)	-E _c (mV)	i _c (A/cm ²)	β _a (mV)	-β _c (mV)	R _p (Ωcm ²)	B(mV)				
PG 07Y	33						198	282	179	658	1.5E-06	1020	280	40000	95					
PG 07N	33						198	315	166	658	1.5E-06	1020	280	40000	95					
PG 14Y	32	258					196	277	136											
PG 21Y	28		1.1E-07	435	146	436690	180	403	504											
PG 28Y	35	284	2.2E-07	531	240	325370	232	401	355	884	1.0E-05	2296	254	12566	99					
PG 28N	35	284	2.2E-07	531	240	325370	232	474	294	884	1.0E-05	2296	254	12566	99					
PG 56Y	37	293	1.1E-07	689	157	396825	261	479	319											
PG 56N	37	293	1.1E-07	689	157	396825	261	630	307											
PP A 28Y							253	1087												
PP B 28Y	29						162	1500		394	1.1E-07	2415	462	1010714	168					
PP C 28Y	31	248	4.0E-08	862	106	710877	144	793	2327	616	5.3E-07	566	177	50300	58					
PP D 28Y	33	267	5.0E-08	807	116	641403	184	712	717	607	1.4E-06	757	234	31480	78					
PP E 28Y	28	276	6.5E-08	763	130	617584	232	909		581	9.0E-07	861	174	58580	63					
Cl A 28Y	35	921	2.3E-06		213	192697	194	295	215	601	2.3E-06	1098	163	66942	62					
Cl A 28N	35	921	2.3E-06		213	192697	194	617	225	601	2.3E-06	1098	163	66942	62					
Cl B 28Y	38	900	3.0E-07		114	137670	250	163	232	671	2.0E-06	736	149	72117	54					
Cl B 28N	38	900	3.0E-07		114	137670	250	177	268	671	2.0E-06	736	149	72117	54					
Cl C 28Y	39	601	7.0E-07	421	165	148233	253	265	226	783	6.4E-06	928	257	54670	87					
Cl C 28N	39	601	7.0E-07	421	165	148233	253	329	227	783	6.4E-06	928	257	54670	87					
SF3 07Y	38	651	2.1E-06		287	78756	195	187	137					20278						
SF3 28Y	38	839	1.2E-07	750	106	248967	234	349	282	730	9.0E-06	931	250	33693	85					
SF3 28N	38	839	1.2E-07	750	106	248967	234	329	267	730	9.0E-06	931	250	33693	85					
SF3 56Y	37	1070	8.9E-07		104	172290	216	268	125	859	3.7E-05		374	9877						
SF5 07Y	37	739	3.4E-06	1055	284		203	124	125					17458						
SF5 28Y	36	755	3.6E-07	513	91	211337	264	240	124	768	1.0E-05		289	25707						
SF5 28N	36	755	3.6E-07	513	91	211337	264	307	180	768	1.0E-05		289	25707						
SF5 56Y	37	854	2.4E-07		127	182757	212	267	98	770	5.2E-06		249	42911						
SF7 07Y	38						247	155	84	799	9.4E-06	1140	223	24620	81					
SF7 28Y	38	1101	3.6E-06		140	250583	280	200	96	781	2.4E-05	885	313	13090	100					
SF7 28N	38	1101	3.6E-06		140	250583	280	266	368	781	2.4E-05	885	313	13090	100					
SF7 56Y	38	992	6.6E-07		120	136178	286	223	125	849	2.5E-05		294	6905						
FA 07Y	39	546	1.3E-07	399	150	163292	316	74	21	923	5.4E-05	1000	292	11406	98					
FA 07N	39	546	1.3E-07	399	150	163292	316	62	18	923	5.4E-05	1000	292	11406	98					
FA 28Y	41	1016	1.1E-06		120	168599	334	162	132	883	2.0E-05	998	345	26895	111					
FA 28N	41	1016	1.1E-06		120	168599	334	183	323	883	2.0E-05	998	345	26895	111					
FA 56Y	41	841	8.3E-07	703	230	246086	268	435	441	865	7.9E-06	2011	365	20336	134					
FA 56N	41	841	8.3E-07	703	230	246086	268	552	994	865	7.9E-06	2011	365	20336	134					

13 APPENDIX F: Bleed Test Data

Table 13 - Bleed Test Results for Plain Grout: 0.35 W/C Ratio

Applied Pressure	Schupack Pressure Test			Wick Pressure Test - 1				Wick Pressure Test - 2				Average Wick Test Bleed	Difference From Schupack
	Bleed		Blowout time	Bleed		Blowout time	Strand	Bleed		Blowout time	Strand		
	Volume	Percent		Volume	Percent			Volume	Percent				
psi.	fl. Oz	%	sec	fl. Oz	%	sec		fl. Oz	%	sec		Percent	Percent
20	0.37	5.5	-	1.69	8.47	200	5th Use	1.79	8.98	480	6th Use	8.73	3.23
30	0.54	8	-	2.2	11.02	95	3rd Use	2.13	10.68	275	4th Use	10.85	2.85
50	0.81	12	-	2.27	11.36	60	1st Use	2.16	10.85	185	2nd Use	11.11	-0.90

Table 14 - Bleed Test Results for Plain Grout: Variability Testing - 0.40 W/C Ratio

Applied Pressure	Schupack Pressure Test			Wick Pressure Test - 1				Wick Pressure Test - 2				Wick Pressure Test - 3				Average Wick Test Bleed	Difference From Schupack
	Bleed		Blowout time	Bleed		Blowout time	Strand	Bleed		Blowout time	Strand	Bleed		Blowout time	Strand		
	Volume	Percent		Volume	Percent			Volume	Percent			Volume	Percent			Volume	Percent
psi.	fl. Oz	%	sec	fl. Oz	%	sec		fl. Oz	%	sec		fl. Oz	%	sec		Percent	Percent
30	0.71	10.5	-	2.74	13.73	65	1st Use	3.58	17.97	115	2nd Use	3.21	16.10	125	3rd Use	15.85	5.35
30	0.81	12	-	3.11	15.59	71	1st Use	3.55	17.80	140	2nd Use	3.25	16.27	151	3rd Use	16.70	4.70
30	0.78	11.5	-	2.71	13.56	73	1st Use	3.45	17.29	130	2nd Use	3.31	16.61	156	3rd Use	15.43	3.93

Table 15 - Bleed Test Results for Plain Grout: 0.40 W/C Ratio

Applied Pressure	Schupack Pressure Test			Wick Pressure Test - 1				Wick Pressure Test - 2				Average Wick Test Bleed	Difference From Schupack
	Bleed		Blowout time	Bleed		Blowout time	Strand	Bleed		Blowout time	Strand		
	Volume	Percent		Volume	Percent			Volume	Percent				
psi.	fl. Oz	%	sec	fl. Oz	%	sec		fl. Oz	%	sec		Percent	Percent
20	0.61	9.00	-	3.01	15.08	155	1st Use	3.21	16.10	210	2nd Use	15.59	6.59
40	0.88	13.00	-	3.01	15.08	180	1st Use	3.14	15.76	220	2nd Use	15.42	2.42
50	0.95	14.00	-	3.45	17.29	290	1st Use	3.21	16.10	280	2nd Use	16.69	2.69

Table 16 - Bleed Test Results for Thixotropic Grout: 0.30 W/C Ratio

Applied Pressure	Schupack Pressure Test			Wick Pressure Test - 1				Wick Pressure Test - 2				Average Wick Test Bleed	Difference From Schupack
	Bleed		Blowout time	Bleed		Blowout time	Strand	Bleed		Blowout time	Strand		
	Volume	Percent		Volume	Percent			Volume	Percent				
psi.	fl. Oz	%	sec	fl. Oz	%	sec		fl. Oz	%	sec		Percent	Percent
20	0.08	1.25	-	0.51	2.54	420	1st Use	0.41	2.03	-	2nd Use	2.29	1.04
30	0.20	3.00	-	0.68	3.39	162	1st Use	0.61	3.05	-	2nd Use	3.22	0.22
50	0.34	5.00	-	1.22	6.10	135	1st Use	0.85	4.24	-	2nd Use	5.17	0.17

Table 17 - Bleed Test Results for Thixotropic Grout: 0.35 W/C Ratio

Applied Pressure	Schupack Pressure Test			Wick Pressure Test - 1				Wick Pressure Test - 2				Average Wick Test Bleed	Difference From Schupack
	Bleed		Blowout time	Bleed		Blowout time	Strand	Bleed		Blowout time	Strand		
	Volume	Percent		Volume	Percent			Volume	Percent				
psi.	fl. Oz	%	sec	fl. Oz	%	sec		fl. Oz	%	sec		Percent	Percent
20	0.17	2.50	-	1.22	6.10	-	1st Use	1.05	5.25	-	2nd Use	5.68	3.18
30	0.24	3.50	-	1.08	5.42	-	1st Use	1.18	5.93	-	2nd Use	5.68	2.18
50	0.51	7.50	-	1.66	8.31	-	1st Use	1.86	9.32	-	2nd Use	8.81	1.31

Table 18 - Bleed Test Results for Thixotropic Grout: 0.40 W/C Ratio

Applied Pressure	Schupack Pressure Test			Wick Pressure Test - 1				Wick Pressure Test - 2				Average Wick Test Bleed	Difference From Schupack
	Bleed		Blowout time	Bleed		Blowout time	Strand	Bleed		Blowout time	Strand		
	Volume	Percent		Volume	Percent			Volume	Percent				
psi.	fl. Oz	%	sec	fl. Oz	%	sec		fl. Oz	%	sec		Percent	Percent
20	0.10	1.50	-	1.25	6.27	-	1st Use	1.08	5.42	-	2nd Use	5.85	4.35
30	0.17	2.50	-	1.12	5.59	-	1st Use	0.98	4.92	-	2nd Use	5.25	2.75
50	0.27	4.00	-	2.13	10.68	-	1st Use	1.83	9.15	-	2nd Use	9.92	5.92

Table 19 - Bleed Test Results for Thixotropic Grout: 0.45 W/C Ratio

Applied Pressure	Schupack Pressure Test			Wick Pressure Test - 1				Wick Pressure Test - 2				Average Wick Test Bleed	Difference From Schupack
	Bleed		Blowout time	Bleed		Blowout time	Strand	Bleed		Blowout time	Strand		
	Volume	Percent		Volume	Percent			Volume	Percent				
	fl. Oz	%	fl. Oz	%	fl. Oz	%							
psi.													
20	0.14	2.00	-	1.35	6.78	-	1st Use	1.15	5.76	-	2nd Use	6.27	4.27
30	0.22	3.25	-	1.45	7.29	-	1st Use	1.28	6.44	-	2nd Use	6.86	3.61
50	0.41	6.00	-	2.30	11.53	-	1st Use	2.06	10.34	-	2nd Use	10.93	4.93